Coherent Control of Atomic Quantum States using Frequency-chirped Laser Pulses

UNIVERSITY OF PÉCS
Doctoral School in Physics
Quantumoptics and Quantuminformation Programme

Coherent Control of Atomic Quantum States using Frequency-chirped Laser Pulses

PhD Thesis

Nóra Sándor

Supervisor:
Dr. Gagik Djotyan
scientific advisor

PÉCS, 2013.

To my brother, Áron

Contents

Introduction

Understanding the interaction of matter and light was the problem which led to the birth of quantum mechanics a hundred year ago. One of the most important discoveries which burst the frames of classical physics was the discovery of spectral lines of the atoms. The first model suitable to explain this observation was by Niels Bohr in 1913: according to his model, only specific orbits of electron can exist inside an atom with well-defined energies. When jumping between the orbits, the electron would absorb or emit light corresponding to the energy difference of the orbits. In 1917, as an extension to Bohr's model, Einstein introduced the concept of spontenous and stimulated emission and absorption, with which he created the foundation for the discovery of the laser. However, more than 40 years was needed for the first realization of this important tool in 1960.

The appearance of lasers, besides having an enormous amount of useful applications in everyday life, created new directions for the investigations of matter-light interactions, by providing an intense, monochromatic and coherent light source. One of the important tasks that one may achieve is a better and better coherent control of quantum states of atoms or atomic ensembles. By now, this area has become an important and rapidly developing field of quantum optics. On one hand, atoms are relatively simple systems which are suitable to demonstrate the basic concepts of quantum mechanics. The significance of such investigations was recently highlighted by the Nobel-prize. On the other hand, the coherent control of atomic states opens a way for numerous important applications in various fields of modern physics, including quantum chemistry [1–4], magnetometry [5–9], trapping and cooling atoms and molecules [10–13], or quantum computation [14–20] and processing of optical information [17, 21–23]. By coherently preparing the atoms, one can modify the optical (refractive and absorption) properties of the medium composed of such atoms. As a result, several interesting and important nonlinear optical effects may occur or be enhanced, including high harmonic generation[24–27], multiphoton ionization[28–30], nonlinear frequency conversion[31–34],

electromagnetically induced transparency[35–38], and many others.

There is a large variety of techniques for the coherent preparation of the atomic states. In the simplest case of a two-level model atom interacting with a resonant laser pulse, Rabi-oscillation occurs between the populations of the atomic states. The proportion of the populations in each state after the interaction depends on the area of the Rabi frequency (integral of the Rabi frequency over time). For example, if this area equals an odd integer multiple of π, complete population inversion can be established. However, the process is sensitive even to relatively small variations of the pulse area and to the resonance conditions between the interacting laser field and atomic transition [39]. This may result in additional difficulties in experiment, especially in the case of multilevel atoms.

More robust control of atomic quantum states (against small-to-medium variations in the parameters of the laser fields) can be achieved by coherent control schemes based on adiabatic following(see [40–42] and references therein). In these cases the control is achieved by adiabatically tuning one of the parameters of the atom-laser interaction in time, which drives the atomic populations along the adiabatic states of the system [43, 44]. The most-used schemes of the adiabatic following include stimulated Raman adiabatic passage (STIRAP) and adiabatic rapid passage (ARP).

In the STIRAP-scheme [40, 41, 45–52] two time-shifted laser pulses having constant carrier frequencies are applied to a Λ-atom, in order to adiabatically change the coupling between the laser fields and the atomic transitions. As a result, the population of one of the ground states can be transferred to the other ground state without excitation of the atom, if the pulses arrive in the proper (counterintuitive) order. With extensions to the STIRAP scheme [53–59], coherence creation among metastable states of the atom is also possible. The STIRAP-based schemes are advantageous in those situations where minimizing the excitation of the atom is a top priority to avoid the decoherence effects caused by spontaneous decay from the excited states. When applying these schemes one needs to take into account that they are generally sensitive to the two-photon resonance conditions.

In the schemes based on ARP, the detuning between the frequency of the interacting laser fields and the atomic transitions is changed in time [60]. In case of the Stark chirped rapid adiabatic passage (SCRAP) schemes[61–66] a far detuned strong laser field is applied to shift the energy level of the excited state in time via the Stark-effect. These schemes are not sensitive to the resonance conditions, but the population redistribution process is accompanied by temporary excitation of the atom.

Frequency modulated (chirped) laser pulses applied in the atom-laser interaction represents another possibility for performing ARP [67–80]. In this case, it is the frequency of the driving electromagnetic field(s) that is a key parameter governing the rearrangement of the atomic population among its quantum states. The investigation of this kind of atomic control has been the main focus of the group of "Cold plasma and atomic physics" in the Wigner Research Center of Hungarian Academy of Sciences, both by experimental [81, 82] and theoretical [12, 70, 73–78, 83–85] methods. Arrangements using frequency-chirped (FC) pulses have been shown to be suitable for solving several coherent control problems. A scheme for complete population transfer between metastable states of a Λ-atom was proposed in [74, 77], and was generalized for creating coherent superposition in the metastable states of a tripod-atom [78]. It was demonstrated for both cases that by using a single FC pulse, adiabatic control can be achieved with negligible atomic excitation, although perfect population trapping cannot be achieved (like in STIRAP-based schemes). The main advantage of these schemes is that due to the frequency chirp, they are less sensitive to resonance conditions and may be successfully utilized in media with both homogeneously and inhomogenously broadened transition lines. In Λ-atoms another interesting control scheme was demonstrated [73, 75]. Namely, being initially prepared in a superpositional state, the atoms are transferred into such a population distribution by two FC laser pulses, that depends strongly on the difference between the initial phases of the pulses. It was proposed to use this property for mapping the optical phase information into populations of the atomic states. However, this scheme has the drawback that the process results in excitation of the atom, inevitably leading to limitation of the information writing and storage times by the decay time of the excited state.

Being motivated by the above described schemes using FC pulses, one of our goals in our work was to create a generalized control scheme which may be applied to optical information writing and storage. In order to broaden the possibilities of controlling the created superpositions, we used three FC pulses interacting with a tripod-atom instead of one like in [78]. We wished to find arrangements suitable for, on one hand, on-demand coherence creation in metastable states of the tripod atom and on the other hand optical information mapping in the population of the metastable states. In order to avoid the decoherence caused by spontaneous decay and thus to extend the storage time of the mapped information, we considered the elimination of the atomic excitation as a top priority.

We also investigated control schemes in Λ-atoms including the application of a pulse having

constant carrier frequency simultanously with a FC pulse which frequency is swept through the two-photon resonance. We analyzed the schemes of the coherent control of the atomic population in two cases regarding the one-photon detuning of the constant frequency pulse. We have shown that, for resonant coupling, a robust coherence-creation is possible between one of the metastable states and the excited state, which may be applied for high-order harmonic generation or multi-photon ionization [24, 28, 29, 86–89]. For the far-detuned case, a population transfer occurs between the ground states in a Λ-atom. However, if the scheme is applied to the Zeeman-sublevels of the D2-line in ^{87}Rb, coherent superposition between the ground states is also possible due to nonadiabatic effects. We also proposed the presented scheme for application in an experiment based on Faraday-rotation.

In the above mentioned interaction schemes the coherent control is considered in single atoms and the back-action of the atoms on the laser fields is neglected, along with propagation effects such as interaction of the laser pulses with each other. This may be a good approximation in optically dilute media, but these effects have to be taken into account when we wish to perform a coherent control in an optically thick medium [90–93]. In this case, preparation of the atoms of a medium in coherent superposition of the quantum states may significantly modify its optical properties leading to very interesting and important propagation effects, like electromagnetically induced transparency (EIT). In the EIT-based schemes (see [35–37, 94] and references therein), an intense laser pulse (of constant carrier frequency) renders the whole medium transparent for a weak probe pulse in Raman resonance with the intense one. A nearly lossless propagation was also demonstrated for a single FC laser pulse in optically thick media consisting of Λ-atoms[91]. The two above mentioned schemes agree in the point that for even significant propagation distances, basically the same population-control mechanism is established in the atoms of the extended media, as for a single atom. The explanation is that the initial preparation of the atoms in the medium in both cases corresponds to a dark superposition of the ground states. This means that no excitation occurs in the atoms during the interaction, which significantly reduces the back-action of the atoms on the laser field. On the other hand, it has been shown that for a sufficiently intense laser pulse pair having constant frequencies in Raman resonance with Λ-atoms, it is not indispensable that the atoms of the medium are initially prepared in the dark state: the pulse-pair by itself renders a dark state through the interaction with the atoms after propagation of some distance in the medium when the envelopes of the interacting laser pulses become matched to each other [95–99]. In our work we analyzed the propagation of a FC

pulse pair in an optically thick medium consisting of Λ-atoms in case of Raman-resonant coupling. We addressed the question whether there is a matching effect for frequency-modulated laser-pulse pairs? We were interested in investigating the physical mechanism of population dynamics in the atoms of the optically thick media in the field of the pair of strong FC laser pulses.

This dissertation is organized as follows. In Chapter 1 we briefly summarize those elements of quantum mechanics and quantum optics which will be applied throughout the work. In Section 1.1, we overview the models and approximations which is used for describing the time evolution of the inner quantum state of atoms interacting with quasi-resonant classical laser pulses. In Section 1.2 we introduce a semiclassical approach for describing the propagation of classical laser pulses in an optically thick medium consisting of few-state atoms. In Section 1.3 we describe the adiabatic approximation which we use for understanding the underlying physics of the proposed coherent control schemes. Our results are presented in Chapters 2, 3 and 4.

In Chapter 2, we investigate the interaction of a tripod-atom with three FC laser pulses, two of them in Raman resonance and the third one out of it. We propose to use this arrangement for, on one hand, creating a coherent superposition of the ground states of the tripod-atom (Section 2.3) and, on the other hand for writing and storage of classical phase information in the populations of the ground states (Section 2.4). The effect of longitudinal and transverse decay processes are analyzed for both schemes.

The coherent control of atoms using a combination of a FC and a constant-frequency pulse is analyzed in Chapter 3. We consider two limiting cases. In Section 3.2, we present our numerical results for the time evolution of the state of an atom interacting with a resonant constant-frequency pulse and an FC pulse which frequency is swept through both one-photon and two photon resonance. We show that this scheme is suitable for very robust creation of coherent superposition between one of the ground states and the excited state of a Λ-atom. In the scheme presented in Section 3.3, the frequency of the pulses are far detuned from the atomic transition frequencies. We show numerically that by applying this scheme for ^{87}Rb, a coherent superposition can established between two of its Zeeman-sublevels.

We analyze the propagation of two Raman-resonant FC pulses in optically thick medium in Chapter 4. We show by numerically integrating the Maxwell-Bloch equation that the pulse pair become matched to each other in such a way that they can propagate in the medium without getting

absorbed and they prepare the majority of the atoms in a certain superposition of the ground states.

Part I

Theoretical Background

Chapter 1

Interaction of atoms and quasi-resonant laser fields

In this thesis, we study the interaction of atoms or atomic ensembles with electromagnetic fields. We put the emphasis on the effect of the interaction on the inner states of the atoms and do not take into consideration other degrees of freedom (e.g. mechanical motion). The atoms are coupled to a limited number (one to three) of laser pulses. We assume that the frequency of the regarded laser pulses are quasi-resonant with some selected atomic transition frequencies and are monotonicly modulated in a small range (compared to the atomic transition frequency).

It is consistent with the quasi-resonant coupling to describe the atoms by simple quantum systems of a few dimensions. The interaction of the atoms with the laser pulses are taken into account in a semiclassical approach regarding the lasers as classical electric fields coupled to the atomic dipoles. The time duration of the laser pulses is in the order of magnitude of the lifetime of the excited state of the atoms, or smaller. However, the Fourier spectrum of the pulse envelope is narrow enough to allow the application of the rotating wave approximation (RWA).

If the atoms form a spatially extended, optically thick ensemble, their back-action on the controlling electromagnetic field also have to be considered. The dynamics of the classical field is described by the Maxwell equations, where the effect of the atoms can be included through the macroscopic polarization. Consistently with the RWA, we use the slowly varying envelope approximation (SVEA) to reduce the second-order wave equation to a first order differential equation.

The coupling of atoms by frequency-modulated lasers is a possible method for performing adia-

batic control if proper parameters are used, which allows a relatively robust control of the atomic states. These processes are suitable to be analyzed by the adiabatic approximation. In this frame the physical mechanism can be understood based on the analysis of the eigenvalues and eigenvectors of the interaction Hamiltonian, without solving the Schrödinger or the master equation for the atomic state.

In this chapter, we present a short review of the above mentioned methods and approximations. We also give a brief introduction to the methods of experimental generation of such frequency-modulated laser pulses for which the assumptions of the theoretical investigations are true.

1.1 Interaction of an atom with quasi-resonant classical electromagnetic fields

1.1.1 Few-state atom models

The atom-field interaction schemes analyzed in this dissertation are best applicable to alkali atoms, which possess only one valency electron. The interaction of these atoms with an electromagnetic field having frequency in the optical range changes the state of this valency electron by transferring it among the energy-eigenstates. We do not take the mechanical effects of the laser field into consideration, so henceforth we identify the *state of the atom* by the state of the valency electron inside the atom. The effect of the laser field on the atom is taken into account through the coupling of its electric field to the atomic dipole moment operator $\hat{\mathbf{d}}$:

$$\hat{H}_S = \hat{H}_A + \hat{H}_{\text{dipole}} = \hat{H}_A - \hat{\mathbf{d}} \cdot \mathbf{E}\left(\mathbf{r_0}\right), \tag{1.1}$$

where $\hat{H}_A$ is the Hamiltonian of the non-interacting atom and $\mathbf{E}\left(\mathbf{r_0}\right)$ is the coupling electric field at the position $\mathbf{r}_0$ of the dipole. Note that this is a good approximation for coupling lasers in the optical frequency range, since the typical atomic radius $(0.3 - 3\mathring{A})$ is less than 1/1000 of the wavelength of visible light (400-700 nm), so the atom can be regarded pointlike. [100].

The atomic Hamiltonian $\hat{H}_A$ has a discrete spectrum known for the real atoms from spectroscopic experiments, which give a rather complicated level structure. However, for quasi-resonant coupling, a

radical simplification can be made. Let us consider two energy levels $|0\rangle$ and $|1\rangle$ with energies of e_0 and e_1, respectively, interacting with a quasi-monochromatic field having carrier frequency ω coincident with the transition frequency connecting the two levels $\omega_{01} = (e_0 - e_1)/\hbar$ and moderate power. With high probability [101], the transition process induced by the interaction takes place between these two levels, provided that resonant frequencies of other transitions in the atom differ significantly from the laser frequency. Thus, the interaction can be described in the 2-dimensional subspace[39], spanned by $\{|0\rangle, |1\rangle\}$, of the many dimensional Hilbert-space of atomic levels. Accordingly, from the aspect of the interaction, the atom can be modeled as a "*two-state atom*", which is shown in Fig. 1.1.

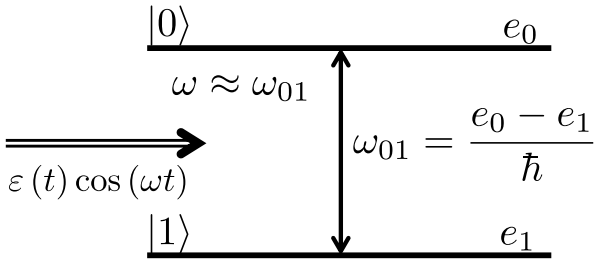

Figure 1.1: Level structure of a two-state atom model. The atomic transition is coupled by a laser pulse with a frequency ω nearly coincident with the transition frequency ω_{01} connecting the excited state $|0\rangle$ and ground state $|1\rangle$

If the interacting electromagnetic field may induce transitions among several atomic levels with finite probability, then the two-state atom has to be generalized to more complicated level structures. In this work, we mostly consider atom models with one *excited state* (with finite lifetime) and two or three *ground states* (metastable states with substantially longer lifetimes compared to the upper state, thus regarded stable). Electric dipole transitions are only allowed between the excited state and the ground states and forbidden among the ground states. Motivated by the shape of the coupling schemes, these atom models are commonly called lambda (1.2(a)) and tripod (1.2(b)) atoms.

Therefore, the atomic state in the analyzed cases are described in a three or four dimensional Hilbert-space as:

$$|\psi_S(t)\rangle = \sum_{k=0}^{N} a_k(t)\,|k\rangle, \tag{1.2}$$

where N is the number of the ground states of the model atom. $a_k(t)$ is the probability amplitude of state $|k\rangle$, whose time evolution is determined by the Hamiltonian $\hat{H}_S$ given in Eq. (1.1) via the

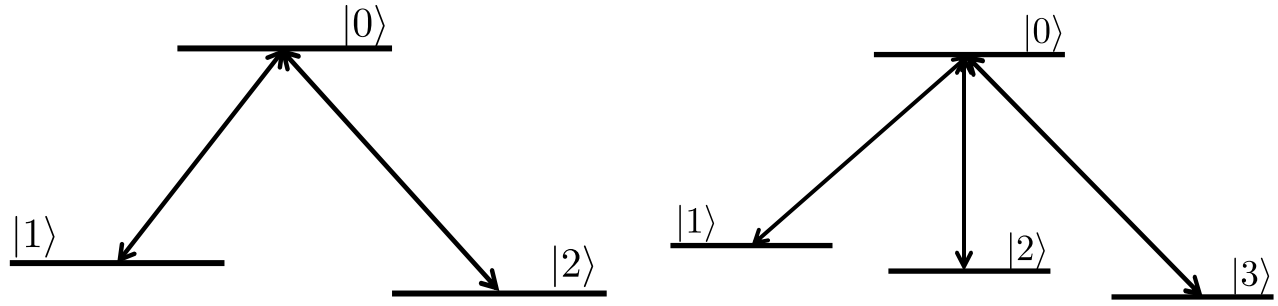

(a) Lambda-atom (b) Tripod-atom

Figure 1.2: Level schemes of the atom models generally used in this dissertation. The dipole-allowed transitions are signed by arrows, which occurs between the excited state $|0\rangle$ and the ground states $|k\rangle$, a.) $k \in \{1, 2\}$ and b.) $k \in \{1, 2, 3\}$. The upper state has a finite lifetime, while the lifetime of the lower states are approximated to be infinite.

Schrödinger-equation

$$i\hbar\partial_t|\psi_S(t)\rangle = \hat{H}_S|\psi_S(t)\rangle. \tag{1.3}$$

The Hamiltonian and dipole moment operators for these model atoms reads as

$$\hat{H}_A = \sum_{k=0}^{N} \hbar\nu_k|k\rangle\langle k|, \qquad \hat{\mathbf{d}} = \sum_{k=1}^{N} \left(d_{0k}|0\rangle\langle k| + H.c.\right), \tag{1.4}$$

where N has the value of 1 for a two-state atom, 2 for lambda- and 3 for tripod-atoms. Note that $\hat{H}_A$ is trivially diagonal in the basis of $|k\rangle$, $k \in \{0...N\}$ since these are energy eigenstates of the atom, while $\hat{\mathbf{d}}$ has only off-diagonal elements, as it has an odd parity being a vector-operator.

In the most of the discussed cases we analyze interaction between atoms and a limited number of laser pulses in such a way that each atomic transition is coupled by a separate laser pulse. This gives us more freedom to control the interaction since we are able to manipulate the coupling of each transition independently by manipulating the parameters of the corresponding laser pulse. This assumption is valid, on one hand, when the frequency difference of the transitions is large enough that the probability that one laser pulse couples the other transition is negligible. For example, in a ^{85}Rb atom, a lambda-atom can be formed by the $F = 2$ and $F = 3$ hyperfine levels of the $5^2S_{1/2}$ orbit as ground states and the $F' = 4$ hyperfine level of the $5^2P_{3/2}$ as excited state (for the level structure see [102]). On the other hand, the separate coupling can be ensured via selection rules: a

lambda-atom may be realized by an $F = 1 \rightarrow F' = 0$ transition in an atom interacting with two laser pulses having circular σ^+ and σ^- polarizations. For realizing a tripod structure, one have to include an additional pulse with π polarization.

Consistently with these assumptions, the interacting radiation field can be described by the following formula:

$$\vec{E}\left(x,t\right) = \sum_{k=1}^{N} \vec{\epsilon}_k \mathcal{E}_k\left(\vec{x},t\right) \cos\left(\vec{k}_k\vec{x} - \omega_k t - \phi_k\left(\vec{x},t\right)\right). \tag{1.5}$$

The interacting field is given by the sum of N modes, each of them is characterized by the $\vec{\epsilon}_k$ polarization vector, ω_k carrier frequency and $\vec{k}_k$ wave vector. However, we do not consider perfectly monochromatic planar waves, but laser pulses with possible frequency modulation. These properties can be taken into account an envelope $\mathcal{E}_k\left(\vec{x},t\right)$ and phase $\phi_k\left(\vec{x},t\right)$ that change slowly in time and space, on the timescale of the inverse carrier frequency ω_k^{-1} and the magnitude of the wavelength $\left|\vec{k}_k\right|^{-1}$. We use the exponential representation of the cosine function and, in parallel, we introduce complex envelopes which incorporate the slowly varying terms

$$\mathcal{E}_k^{(\pm)}\left(\vec{x},t\right) = \mathcal{E}_k\left(\vec{x},t\right) \exp\left[\mp i\phi_k\left(\vec{x},t\right)\right]. \tag{1.6}$$

Using these complex envelopes, the electric field of the laser radiation reads as

$$\vec{E}\left(x,t\right) = \frac{1}{2}\sum_{k=1}^{n} \vec{\epsilon}_k \left(\mathcal{E}_k^{(+)}\left(\vec{x},t\right) \exp\left\{i\left(\vec{k}_k\vec{x} - \omega_k t\right)\right\} + c.c.\right). \tag{1.7}$$

1.1.2 Interaction picture

For the analysis of the impact of the laser pulses on the atom, the values of the energies of the atomic eigenstates are not needed. Therefore, it is convenient to transform to the interaction picture using the

$$\hat{U} = e^{-i\hat{H}_A t/\hbar} = \sum_{j=0}^{N} e^{-i\cdot e_j t/\hbar} |j\rangle\langle j| \tag{1.8}$$

time-evolution operator, which transforms the state vector as

$$|\psi_I\rangle = \hat{U}^\dagger |\psi_S\rangle = \sum_{k=0}^{N} A_k(t)\,|k\rangle, \tag{1.9}$$

where $A_k(t) = a_k(t)\, e^{ie_k t/\hbar}$ is slowly varying for $\forall k \in \{0 \dots N\}$ and is determined by the Schwinger-Tomonaga equation

$$i\hbar\partial_t |\psi_I(t)\rangle = \hat{H}_I |\psi_I(t)\rangle. \tag{1.10}$$

Here $\hat{H}_I$ is the interaction Hamiltonian

$$\hat{H}_I = \hat{U}^\dagger \hat{H}_{\text{dipole}} \hat{U} = -\sum_{k=1}^{N} \Big(d_{0k}\, e^{i\omega_{0k}t} \vec{E} |0\rangle\langle k| + H.c. \Big), \tag{1.11}$$

where the transition frequency between states $|0\rangle \leftrightarrow |k\rangle$ has been introduced as

$$\omega_{0k} = (e_0 - e_k)/\hbar, \;\; k \in \{1, \dots N\}, \tag{1.12}$$

and we used the following expression for the dipole moment operator in interaction picture:

$$\hat{d}_I = \hat{U}^\dagger \hat{\mathbf{d}} \hat{U} = \sum_{k=1}^{N} \left[d_{0k}\, e^{i\omega_{0k}t} |0\rangle\langle k| + H.c. \right]. \tag{1.13}$$

We substitute the formula given in (1.7) for the electric field into the Hamiltonian given in Eq. (1.11) and we take into account the assumption that each of the allowed transitions are coupled by a separate laser pulse, to obtain the following form for the interaction Hamiltonian:

$$\hat{H}_I = -\frac{1}{2} \sum_{k=1}^{N} \Big[d_{0k} \Big(\mathcal{E}_k^{(+)}(\vec{x}, t) \exp\{-i(\omega_k - \omega_{0k})t\} e^{i\vec{k}_k \vec{x}} + \mathcal{E}_k^{(-)}(\vec{x}, t) \exp\{i(\omega_k + \omega_{0k})t\} e^{-i\vec{k}_k \vec{x}} \Big) |0\rangle\langle k| + H.c. \Big]. \tag{1.14}$$

Using this Hamiltonian (Eq 1.14), the following equation of motion is derived for the probability amplitudes of the state vector $|\psi_I\rangle$ in interaction picture:

$$\partial_t A_0(t) = \frac{i}{2}\sum_{k=1}^{N}\left(\Omega_k^{(+)}(\vec{x},t)\, e^{-i\delta_k t} e^{i\vec{k}_k\vec{x}} + \Omega_k^{(-)}(\vec{x},t)\, e^{i(\omega_k+\omega_{0k})t} e^{-i\vec{k}_k\vec{x}}\right) A_k(t) \tag{1.15a}$$

$$\partial_t A_k(t) = \frac{i}{2}\left(\Omega_k^{(+)}(\vec{x},t)\, e^{-i(\omega_k+\omega_{0k})t} e^{i\vec{k}_k\vec{x}} + \Omega_k^{(-)}(\vec{x},t)\, e^{i\delta_k t} e^{-i\vec{k}_k\vec{x}}\right) A_0(t),$$

$$k \in \{1\dots N\}, \tag{1.15b}$$

where the detuning between the ω_{0k} frequency of the transition $|0\rangle \to |k\rangle$ and the ω_k carrier frequency of the corresponding laser pulse has been defined as

$$\delta_k = \omega_k - \omega_{0k}, \tag{1.16}$$

and Rabi frequencies for each dipole-allowed transition were introduced as

$$\Omega_k^{(+)} = \frac{d_{0k}\mathcal{E}_k^{(+)}(x,t)}{\hbar} \equiv \vartheta_k(\vec{x},t)\, e^{-i\phi_k(\vec{x},t)} \text{ and } \Omega_k^{(-)} = \left(\Omega_k^{(+)}\right)^{\dagger}, \tag{1.17}$$

which characterize the strength of the coupling. Here d_{0k} denotes the matrix element of the atomic dipole moment operator for the $|0\rangle \to |k\rangle$ transition, $\vartheta_k(\vec{x},t)$ is the absolute value, $\phi_k(\vec{x},t)$ is the phase of the k$^{\text{th}}$ Rabi frequency.

1.1.3 The rotating wave approximation

As it was already mentioned, in our model we consider quasi-monochromatic laser pulses with carrier frequencies quasi-resonant with the frequency of the transition coupled by them, having slowly varying envelope functions and moderate intensity. These properties are equivalent with the following inequalities:

$$|\delta_k| \ll \omega_{0k} \Leftrightarrow \omega_k \approx \omega_{0k} \tag{1.18a}$$

$$\left|\partial_t \Omega_k^{(\pm)}\right| \ll \left|\omega_{0k}\Omega_k^{\pm}\right| \tag{1.18b}$$

$$\left|\Omega_k^{(\pm)}\right| \ll \omega_{0k}, \quad \forall k \in \{1\dots N\}. \tag{1.18c}$$

If we take a closer look at Eq. (1.15) taking into account the inequalities (1.18) we can observe that the time dependence of the probability amplitudes are determined by two terms changing in sharply separable timescales. This allows us to neglect the terms containing the terms oscillating by the sum frequencies $\omega_k + \omega_{0k}$, as they average out on the timescale of the other, slowly varying term. This approximation, i.e. neglecting the terms oscillating with the sum-frequencies $\omega_{0k} + \omega_k$ is called the *rotating wave approximation* (RWA) [39].

In the frame of RWA, the interaction is characterized by the Hamiltonian

$$\hat{H}_{\mathrm{RWA}} = -\hbar \sum_{k=1}^{N} \left\{ \frac{1}{2} \Omega_k \left(t \right) e^{-i(\delta_k t - k_k x)} |0\rangle\langle k| + H.c. \right\}. \tag{1.19}$$

1.1.4 Phase transformations

It makes further calculations more convenient if we introduce a new basis on the atomic states using the following transformation:

$$\hat{\mathcal{V}} = \sum_{k=1}^{N} \left[e^{i(\delta_k t - k_k x)} |k\rangle\langle k| \right] + |0\rangle\langle 0|. \tag{1.20}$$

The operator $\hat{\mathcal{V}}$ defines basis vectors that follow the rotation of the coupling electric fields:

$$\left\{ |0\rangle_{\mathcal{V}} \equiv |0\rangle, |k\rangle_{\mathcal{V}} \equiv e^{i(\delta_k t - k_k x)} |k\rangle \mid k \in \{1, 2, \ldots n\} \right\}. \tag{1.21}$$

The Hamiltonian in the new basis is given by (see A.1)

$$\hat{H}_{\mathcal{V}} = -\hbar \sum_{k=1}^{N} \left[-\delta_k |k\rangle_{\mathcal{V}}\langle k|_{\mathcal{V}} + \left(\frac{1}{2} \Omega_k |0\rangle\langle k|_{\mathcal{V}} + \mathrm{H.c.} \right) \right]. \tag{1.22}$$

In the Hamiltonian (1.22) the frequency modulation of the interacting laser pulses is taken into account through the time-dependent complex phase $\phi_k \left(\vec{x}, t \right)$ of the Rabi frequencies (c.f. (1.17)). In some investigations, it is advantageous to perform another basis transformation by introducing the

operator

$$\hat{\mathcal{R}} = \sum_{k=1}^{N} \left[e^{i\,\varphi_k(\vec{x},t)} |k\rangle_{\mathcal{V}} \langle k|_{\mathcal{V}} \right] + |0\rangle\langle 0|. \tag{1.23}$$

This transformation incorporates the time-dependent part of the complex phase

$$\phi_k\left(\vec{x},t\right) = \varphi_k\left(\vec{x},t\right) + \varphi_k^{(0)}\left(\vec{x}\right) \tag{1.24}$$

into the rotation of the basis vectors, that now reads as

$$\left\{ |0\rangle, |\tilde{k}\rangle \equiv e^{i\varphi_k(\vec{x},t)} |k\rangle_{\mathcal{V}} \mid k \in \{1 \dots N\} \right\}. \tag{1.25}$$

The advantage of using this basis for describing the interaction is that the Hamiltonian only contains time dependence in the real part of its elements, which is going to be beneficial when using the adiabatic approximation (see 1.3). With introducing the time- (and, in general, space-) dependent detuning

$$\Delta_k\left(\vec{x},t\right) \equiv \delta_k + \partial_t \phi_k\left(\vec{x},t\right) = \delta_k + \partial_t \varphi_k\left(\vec{x},t\right), \tag{1.26}$$

we obtain the following formula for the Hamiltonian:

$$\hat{H}_{\mathcal{R}} = -\hbar \sum_{k=1}^{N} \left[-\Delta_k\left(\vec{x},t\right) |\tilde{k}\rangle\langle\tilde{k}| + \left(\frac{1}{2} \tilde{\Omega}_k\left(\vec{x},t\right) |0\rangle\langle\tilde{k}| + \text{H.c.} \right) \right], \tag{1.27}$$

$$\text{with } \tilde{\Omega}_k\left(\vec{x},t\right) = \Omega_k\left(\vec{x},t\right) e^{i\varphi(\vec{x},t)} \equiv \vartheta\left(\vec{x},t\right) e^{-i\varphi^{(0)}(\vec{x})} \tag{1.28}$$

being the Rabi frequency (see Eq. (1.17)), with the phase modulation in time *excluded* (since it is already incorporated in the rotating basis vectors). Note that the Hamiltonians given in Eqs. (1.22) and (1.27) equivalently describe the same interaction. Which one should be used, depends on the problem at hand.

1.1.5 The classical Rabi-problem

An important example for the quasi-resonant atom-laser interaction consists of only a two-state atom and one monochromatic laser pulse. This model, which is analytically solvable in RWA, is called Rabi-model because it is analogous to the problem of a spin in an oscillating magnetic field analyzed by Rabi [103]. We regard the atom in a fixed location $\vec{x} = \vec{x}_0$ thus we do not need to deal with the spatial dependence of the electric field.

The Hamiltonian (1.22) applied to this case (suppressing the subscript $\mathcal{V}$) is given by the formula

$$\hat{\mathcal{H}}_2 = -\hbar \left[-\delta |1\rangle\langle 1| + \left(\frac{1}{2}\Omega(t) |0\rangle\langle 1| + \text{H.c.} \right) \right]. \tag{1.29}$$

Here $\Omega = \mathcal{E}(t)\, d_{0k}/\hbar$ is the coupling strength. It slowly varies in the absolute value and has a constant complex phase, which can always be set to zero in case of one transition. δ is the detuning between the atomic transition frequency and the laser's carrier frequency.

We can describe the state of the atom as

$$|\psi(t)\rangle = A_0(t) |0\rangle + A_1(t) |1\rangle. \tag{1.30}$$

The time evolution of the probability amplitudes is determined by the Schrödinger equation (c.f. (1.10)):

$$\partial_t A_0(t) = \frac{i}{2}\Omega(t) A_1(t) \tag{1.31a}$$

$$\partial_t A_1(t) = i \left[\frac{1}{2}\Omega(t) A_0(t) - \delta A_1(t) \right]. \tag{1.31b}$$

As an initial condition we take all the population to be in the ground state: $A_0(0) = 0$ and $A_1(0) = 1$. Eliminating $A_1(t)$ from Eq. (1.31), we obtain the following second-order differential

equation with initial conditions:

$$\partial_t^2 A_0(t) + i\,\delta\,\partial_t A_0(t) + \frac{1}{4}\Omega^2(t)\,A_0(t) = 0 \tag{1.32a}$$

$$A_0(0) = 0 \tag{1.32b}$$

$$\partial_t A_0(0) = \frac{i}{2}\Omega(0)\,. \tag{1.32c}$$

For time-independent coupling ($\Omega(t) = \Omega$), the differential equation in (1.32) is easy to solve. Taking the initial conditions also into account, the solution is (see e.g. [104])

$$A_0(t) = i\frac{\Omega}{\Omega_R}e^{-i\delta t/2}\sin(\Omega_R t/2) \tag{1.33a}$$

$$A_1(t) = e^{-i\delta t/2}\left[\cos(\Omega_R t/2) + i\frac{\delta}{\Omega_R}\sin(\Omega_R t/2)\right], \tag{1.33b}$$

where $\Omega_R = \sqrt{\delta^2 + \Omega^2}$. It is customary to refer to this quantity as "the generalized Rabi frequency". Note that at resonance, it coincides with the Rabi frequency defined in Eq. (1.17). The probabilitiy that the atom is in the excited state $|0\rangle$ or in the ground state $|1\rangle$ are given by

$$P_0(t) = |A_0(t)|^2 = \frac{\Omega^2}{2\Omega_R^2}\left[1 - \cos(\Omega_R t)\right] \tag{1.34a}$$

$$P_1(t) = |A_1(t)|^2 = \frac{\Omega_R^2 + \delta^2}{2\Omega_R^2} + \frac{\Omega^2}{2\Omega_R^2}\cos(\Omega_R t)\,, \tag{1.34b}$$

thus there is an oscillation between the ground and the excited state with a frequency of Ω_R, see Fig. 1.3. For a resonant case, namely $\delta = 0$, a complete population inversion occurs for $\Omega t = (2l+1)\pi,\ l \in \mathbb{Z}$. This means that a resonant laser "pulse" which has a steady Rabi frequency Ω_0 between t_1 and t_2 induces a population inversion if $\theta = \Omega_0(t_2 - t_1) = (2l+1)\pi$. Notice that in case of such a pulse, it is the pulse area that determines the transition induced by the pulse. Motivated by this, let us introduce the pulse envelope area for pulses with time-dependent Rabi frequencies as

$$\theta(t) = \int_{-\infty}^{t} \Omega(t')\ \mathrm{d}t'. \tag{1.35}$$

Based on Eq. (1.33), we can guess the solution for the differential equations (1.31) for resonant

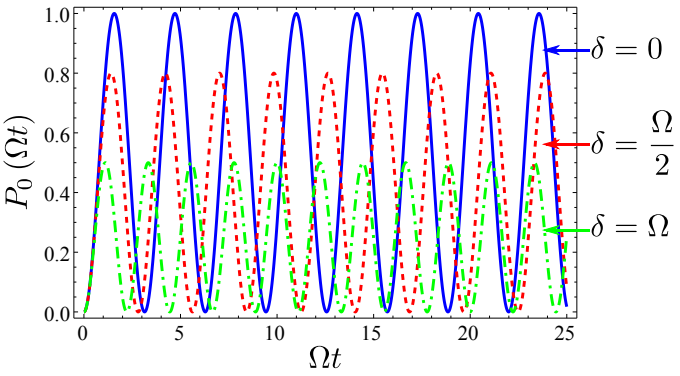

Figure 1.3: The population of the excited state $|0\rangle$ as a function of Ωt for different detunings. The probability that the atom is in the excited state oscillates in Ωt. The frequency and the amplitude of this oscillation changes with the detuning according to Eq. (1.34a).

coupling (i.e. $\delta = 0$). By substituting this pulse envelope area function in the place of Ωt, we obtain

$$A_0(t) = a_0 \sin\left[\frac{1}{2}\theta(t)\right] + a_1 \cos\left[\frac{1}{2}\theta(t)\right] \tag{1.36a}$$

$$A_1(t) = -a_1 \sin\left[\frac{1}{2}\theta(t)\right] + a_0 \cos\left[\frac{1}{2}\theta(t)\right], \tag{1.36b}$$

which can be easily proved to be a solution by substituting into Eq. (1.31).

1.1.6 Interaction with the environment: master equation

So far, we have considered the interaction of the laser pulses with a motionless atom as a closed system. In this frame we regarded atomic levels with an infinite lifetime. This approach may be a good approximation if the interaction of the atom with the resonant laser field occurs in a shorter timescale than any other interactions with the environment. These interactions manifest themselves as relaxation processes. On one hand, there is spontaneous decay from the excited state of the atom (longitudinal relaxation). On the other hand, interactions such as collisions in a gas or phonon scattering in a solid can disturb the dipole oscillations of the resonant atom without disturbing its energy, but causing a decay of the coherences (transverse relaxations). Let us consider for example a cold atomic gas of Rb atoms. The spontaneous decay time is of the order of 27ns, while the transverse relaxation time may change in wide range of values depending on experimental parameters such as the atomic density or the temperature of the atomic cloud.

In this work, these mechanisms are taken into account in a phenomenological way. Namely, we

use the master equation for describing the atom-laser interaction in which the relaxation processes are represented by decay rates. The time evolution of the atomic state, described by the density matrix operator $\hat{\rho}$, is given by

$$\partial_t \hat{\rho} = -\frac{i}{\hbar}\left[\hat{H}_{\mathcal{V}}, \hat{\rho}\right] + \hat{\mathcal{U}}_\Gamma\left(\hat{\rho}\right), \tag{1.37}$$

where [105]

$$\hat{\mathcal{U}_\Gamma}\left(\hat{\rho}\right) = -\left(\sum_{k=1}^{N}\Gamma_k\right)\rho_{00}|0\rangle\langle 0| + \sum_{k=1}^{N}\left[\Gamma_k\rho_{00}|k\rangle\langle k| - \left(\gamma_{0k}\rho_{0k}|0\rangle\langle k| + \text{H.c.}\right)\right] + \sum_{k\neq l}\left(\gamma_{kl}\rho_{kl}|k\rangle\langle l| + \text{H.c.}\right). \tag{1.38}$$

Here ($\rho_{kl} = \langle k|\hat{\rho}|l\rangle$) is the matrix element of the density operator in the basis defined in Eq. (1.21). We have neglected the spontaneous decay from the excited state out of the considered $N+1$ dimensional Hilbert space. The longitudinal decay rate from the excited state $|0\rangle$ towards state $|k\rangle$, $k \in \{1 \dots N\}$ is given by Γ_k, the relaxation rates of the coherences is denoted by γ_{ij}, $i, j \in \{0, \dots N\}$, where

$$\gamma_{ij} = \frac{1}{2}\sum_{k=1}^{N}\Gamma_{ik} + \frac{1}{2}\sum_{l=1}^{N}\Gamma_{jl} + \gamma'_{ij}, \tag{1.39}$$

γ'_{ij} being the relaxation rate due to dephasing processes. Substituting the formula for the Hamiltonian given in Eq. (1.22) into the expression in (1.37), the following set of differential equations is obtained:

$$\partial_t\rho_{00} = \frac{i}{2}\sum_{k=1}^{N}\left(\Omega_k\rho_{k0} - \Omega_k^*\rho_{0k}\right) - \left(\sum_{k=1}^{N}\Gamma_k\right)\rho_{00} \tag{1.40a}$$

$$\partial_t\rho_{kk} = \frac{i}{2}\left(\Omega_k^*\rho_{0k} - \Omega_k\rho_{k0}\right) + \Gamma_k\rho_{00} \quad \forall k \in \{1, 2, \dots n\} \tag{1.40b}$$

$$\partial_t\rho_{0k} = i\left[\sum_{l=1}^{n}\frac{1}{2}\Omega_l\rho_{lk} + \delta_k\rho_{0k} - \frac{1}{2}\Omega_k\rho_{00}\right] - \gamma_{0k}\rho_{0k} \tag{1.40c}$$

$$\partial_t\rho_{kl} = i\left[-\left(\delta_k - \delta_l\right)\rho_{kl} + \frac{1}{2}\left(\Omega_k^*\rho_{0l} - \Omega_l\rho_{k0}\right)\right] - \gamma_{kl}\rho_{kl}, \tag{1.40d}$$

where $\forall k, l \in \{1, \dots N\}$.

1.1.7 Scope of the model

In this section we have presented the mathematical formalism to describe the interaction between a limited number of laser pulses with atoms at a certain fixed location. Let us overview the conditions upon which the formalism is valid.

- The wavelength of the electromagnetic field is much longer than the atomic size.
- The interacting electromagnetic field consists of laser pulses. These pulses have a carrier frequency quasi-resonant with the transition frequencies of the atomic transitions coupled by them and an envelope function which may change slowly in space and time.
- The coupling strengths, expressed by the Rabi frequencies, are small compared to the atomic transition frequency.
- Each atomic transition is separately coupled by one laser pulse.

If the timescale of the interaction is shorter than the relaxation processes in the system, they can be neglected. In this case, the atomic state can be described by the wave function and the Schrödinger equation (1.15) determines its time dependence. If the interaction time is comparable or longer than the relaxation times (both longitudinal and transverse), the time evolution of the atomic state, represented by the density matrix operator, follows the master equation (1.40).

1.2 Interaction of laser pulses with optically thick medium

So far, we considered the atom-laser interaction from the point of view of the atoms. The Hamiltonian (1.22) gives the impact of the electromagnetic field on an atom in a fixed $\vec{x}$ space location. In this approach the laser fields can be regarded as externally given. However, when our aim is to describe the atom-laser interaction in a spatially extended ensemble of atoms, the dynamics of the fields also have to be taken into account. That is, the propagation of the laser pulses is needed to be described along with the possible back-action of the atoms on them.

1.2.1 Evolution of the classical laser field in the medium of atoms

We consider the propagation of N laser pulses, given by the electric field in (1.7), in an ensemble of identical $(N+1)$-level atoms, presented in Sec. 1.1. We assume that all the pulses propagate in the same direction, for example, along the x-axis. We also suppose that the conditions of using the Hamiltonian (1.22), summarized in subsec. 1.1.7, are fulfilled.

Continuing the semiclassical approach that we followed in the description of the atomic state, we use the classical Maxwell-equation for determining the evolution of the electromagnetic field:

$$\left(\nabla^2 - \frac{\partial^2}{\partial\left(ct\right)^2}\right)\vec{E}\left(x,t\right) = \mu_0 \frac{\partial^2}{\partial t^2}\vec{P}\left(x,t\right). \tag{1.41}$$

Here $\vec{P}$ denotes the macroscopic polarization, which represents the impact of the atoms on the laser field

$$\vec{P}\left(x,t\right) = \mathcal{N}\mathrm{Tr}\Big\{\hat{\rho}\left(x,t\right)\hat{\mathbf{d}}\Big\}. \tag{1.42}$$

Here $\hat{\mathbf{d}}$ is dipole moment operator. $\hat{\rho}\left(x,t\right)$ is defined as the average of the density operators of the atoms located in a small segment $[x, x+\delta x]$ of the medium:

$$\hat{\rho}\left(x,t\right) = \frac{1}{\mathcal{N}}\sum_{i=1}^{\mathcal{N}}\hat{\rho}^{(i)}\left(t\right), \tag{1.43}$$

with $\mathcal{N}$ atoms in a segment. We have previously assumed that each dipole-allowed transition is separately coupled by one corresponding pulse. Consequently, an independent differential equation describes the evolution of the electric field

$$\vec{E}_k\left(x,t\right) = \frac{1}{2}\left[\mathcal{E}_k^{(+)}\left(x,t\right)e^{-i(\omega_k t - k_k x)} + \text{c.c.}\right] \tag{1.44}$$

of each pulse, with the following macroscopic polarization as a source:

$$\begin{aligned}\vec{P}_k\left(x,t\right) &= \mathcal{N}\left(\rho_{k0}e^{i(\omega_k t-k_k x)}e^{-i\omega_{0k}t}\cdot d_{0k}e^{i\omega_{0k}t} + \rho_{0k}e^{-i(\omega_k t-k_k x)}e^{i\omega_{0k}t}\cdot d_{0k}e^{-i\omega_{0k}t}\right)\\ &\equiv \frac{1}{2}\left(\mathcal{P}_k^{(+)}\left(x,t\right)e^{-i(\omega_k t-k_k x)} + \mathcal{P}_k^{(-)}\left(x,t\right)e^{i(\omega_k t-k_k x)}\right),\end{aligned} \tag{1.45}$$

where $\rho_{ij} = {}_{\mathcal{V}}\langle i|\hat{\rho}\,(x,t)\,|j\rangle_{\mathcal{V}}$ is the matrix element of the density operator in the basis (1.21).

1.2.2 Slowly varying envelope approximation (SVEA)

When describing the electric field with the formula given in Eq. (1.5), we have already made the assumption that the envelope $\mathcal{E}_k^{\pm}(x,t)$ changes slowly in time and space compared to the inverse laser frequency ω_k^{-1} and the inverse of absolute value of the wave vector $|k|_k^{-1}$, that is

$$\left|\nabla^2 \mathcal{E}_k^{\pm}\right| \ll \left|k_k \nabla \mathcal{E}_k^{\pm}\right| \tag{1.46a}$$

$$\left|\partial_t^2 \mathcal{E}_k^{\pm}\right| \ll \left|\omega_k \partial_t \mathcal{E}_k^{\pm}\right|, \;\; \forall k \in \{1 \dots N\}\,. \tag{1.46b}$$

On the other hand, the condition for using RWA is the characteristic time of the interaction being significantly longer than ω_k^{-1}. Consequently, the density matrix elements ρ_{ij} and thus the envelope of the macroscopic polarization $\mathcal{P}_k^{(\pm)}$ vary also slowly in time, namely

$$\left|\partial_t^2 \mathcal{P}_k^{\pm}\right| \ll \left|\omega_{0k} \partial_t \mathcal{P}_k^{\pm}\right|, \;\; \forall k \in \{1 \dots N\}\,. \tag{1.47}$$

It follows from these assumptions, that the terms of the laser field (1.44) and the polarization vector (1.42) oscillating with ω_k and $-\omega_k$ have to satisfy separately the Maxwell equation (1.41). Substituting the expressions in Eqs. (1.44) and (1.42) into Eq. (1.41), we obtain the following expressions for the terms oscillating with positive frequency ($E_k^{(+)}$ and $P_k^{(+)}$) in the left (1.48a) and right (1.48b) side, respectively:

$$\left(\nabla^2 - \partial_{(ct)}^2\right) \vec{E}_k^{(+)} = \left\{ \left[\left(\nabla^2 + 2ik_k\nabla - |k_k|^2\right) - c^{-2}\left(\partial_t^2 - 2i\omega_k\partial_t - \omega_k^2\right)\right] \mathcal{E}_k^{(+)} \right\} e^{-i(\omega_k t - k_k x)} \tag{1.48a}$$

$$\frac{\partial^2}{\partial t^2}\vec{P}_k^{(+)} = \left\{ \left(\partial_t^2 - 2i\omega_k\partial_t - \omega_k^2\right) \vec{\mathcal{P}}_k^{(+)} \right\} e^{-i(\omega_k t - k_k x)}. \tag{1.48b}$$

The second order Maxwell equation (1.48) can be reduced to a first order differential equation if we take into account the conditions given in (1.46b) and (1.47) and only keep the leading terms:

$$\left(\nabla + \partial_{(ct)}\right) \mathcal{E}_k^{(+)} = \frac{i\mu_0\omega_k^2}{2\,|k_k|}\mathcal{P}_k^{(+)}. \tag{1.49}$$

Using the definitions for the Rabi frequency (1.17) and the macroscopic polarization (1.42) we can get an equation analogous with Eq. (1.49) for the quantities which appear in the master equation (1.40):

$$\left(\nabla + \frac{\partial}{\partial (ct)}\right)\Omega_k (x,t) = i\frac{\mu_0 \omega_k c \left|d_{0k}\right|^2}{2\hbar}\mathcal{N}\rho_{0k} (x,t), \quad k \in \{1,2,\dots n\}. \tag{1.50}$$

Here $\rho_{k0} (x,t)$ is determined by averaging the results of the master equations (1.40) which describe the state of the atoms in the space segment $[x, x+\delta x]$ interacting with laser pulses having $\Omega_k (x,t), \ k \in \{1 \dots N\}$ as Rabi frequencies.

1.3 Adiabatic control of atoms

The simplest case of quasi-resonant interaction of an atom with a laser field was presented in 1.1.5. We have seen that the population transfer process in the atom induced by the laser field is mostly determined by two parameters of the interaction. On one hand, complete population transfer is only possible in resonance. On the other hand, the amount of the population transferred between the states depends on the pulse area (integral of the pulse's Rabi frequency over time). These properties of the process represent serious limitations in experimental situations, when the goal is to control the inner states of the atoms by the laser pulse. However, if the parameters of the interaction are changed very slowly (adiabatically), a more robust control can be achieved (see for example [40–42] and references therein).

In this section we overview the theory of adiabatic processes based on [106] and present the most common examples of coherent control based on adiabatic passage.

1.3.1 The adiabatic approximation

The essence of an adiabatic process is that a gradual change occurs in the external conditions of the system. In atom-laser interaction this may be realized by very slowly changing the parameters of the interacting laser field(s) in time. Therefore the $\mathcal{H}(R(t))$ Hamiltonian which describes the interaction will change very slowly in time through the parameter $R(t)$. The state vector $|\psi(t)\rangle$ of the system

satisfies the Schrödinger equation

$$i\hbar\partial_t|\psi\left(t\right)\rangle = \mathcal{H}\left(R\left(t\right)\right)|\psi\left(t\right)\rangle, \tag{1.51}$$

The Hamiltonian has instantaneous eigenvectors $|v_j\left(R\right)\rangle$, which satisfy the characteristic equation

$$\mathcal{H}\left(R\right)|v_j\left(R\right)\rangle = \lambda_j\left(R\right)|v_j\left(R\right)\rangle. \tag{1.52}$$

We can represent the general solution of Eq. (1.51) in the basis of the instantaneous eigenvectors as

$$|\psi\left(t\right)\rangle = \sum_j r_j\left(t\right)e^{i\alpha_j(t)}|v_j\left(R\left(t\right)\right)\rangle, \tag{1.53}$$

where the so-called dynamic phase has been introduced:

$$\alpha_j\left(t\right) = -\frac{1}{\hbar}\int_{-\infty}^{t}\lambda_j\left(R\left(\tau\right)\right)\,\mathrm{d}\tau. \tag{1.54}$$

The *adiabatic theorem* states that if $R\left(t\right)$ varies sufficiently slowly and the system is prepared in the initial state $|v_j\left(R\left(0\right)\right)\rangle$, then the time-dependent state vector remains in $|v_j\left(R\left(t\right)\right)\rangle$, apart from a phase factor. Namely, in the adiabatic regime of the interaction $r_j\left(t\right) = r_j\left(-\infty\right)$ in the representation of the state vector in (1.53).

Let us give a deeper insight to this statement which refers to the scope of this approximation as well. Using the representation given in Eq. (1.53), the Schrödinger equation (1.51) leads to

$$\sum_j\left[\dot{r_j}e^{i\alpha_j}|v_j\rangle + r_j e^{i\alpha_j}|\dot{v}_j\rangle\right] = 0, \tag{1.55}$$

where the indication of the time dependence is suppressed and dot denotes derivation with respect to time. With the differentiation of the characteristic equation follows that

$$\dot{\mathcal{H}}|v_j\rangle + \mathcal{H}|\dot{v}_j\rangle = \dot{\lambda}_j|v_j\rangle + \lambda_j|\dot{v}_j\rangle. \tag{1.56}$$

Taking the inner product of (1.55) and (1.56) with another instantaneous eigenvector, $\langle v_k| =$

$\langle v_k(R(t))|$, and substituting the result of the latter operation into the former one, we obtain

$$\dot{r}_k = \sum_j r_j e^{i(\alpha_j - \alpha_k)} \langle v_k|\dot{\mathcal{H}}|v_j\rangle \left(\lambda_k - \lambda_j\right)^{-1}, \quad (k \neq j)\,. \tag{1.57}$$

Now let us suppose that the initial state coincides with one of the instantaneous eigenvectors, $|\psi(0)\rangle = |v_j(R(0))\rangle$, so that $r_j(0) = 1$ and $r_k(0) = 0$ for $k \neq j$. Then, from Eq. (1.57) follows that

$$\dot{r}_k \approx e^{i(\alpha_j - \alpha_k)} \langle v_k|\dot{\mathcal{H}}|v_j\rangle \left(\lambda_k - \lambda_j\right)^{-1}. \tag{1.58}$$

For an adiabatic process, the time dependences of $\langle v_k|\dot{\mathcal{H}}|v_j\rangle$ and $(\lambda_k - \lambda_j)$ are slow, thus we can have the following estimation for the probability amplitude of an eigenstate $|v_k\rangle$ where the system was *not* prepared initially, by using $\exp\{i(\alpha_j - \alpha_k)\} \approx \exp\{i(\lambda_k - \lambda_j)\,t/\hbar\}$:

$$r_k(t) \approx -i\hbar \frac{\langle v_k|\dot{\mathcal{H}}|v_j\rangle}{\lambda_k - \lambda_j} \left[e^{i(\lambda_k - \lambda_j)} - 1\right], \tag{1.59}$$

which is small provided that the rate of variation of $H(R(t))$ is slow compared to the difference of the eigenenergies in any t points:

$$\left|\langle v_k|\dot{\mathcal{H}}|v_j\rangle\right| \ll \frac{|\lambda_k - \lambda_j|}{\hbar}, \tag{1.60}$$

which can be regarded the applicability condition of the adiabatic approximation. An analogous, more easily applicable form of this requirement only contains the eigenvectors and eigenvalues [107]:

$$|\langle \dot{v}_k|v_j\rangle| \ll |\lambda_k - \lambda_j|\,. \tag{1.61}$$

1.3.2 Stimulated Raman adiabatic passage (STIRAP)

Stimulated Raman adiabatic passage is an adiabatic process commonly used in coherent control of atomic inner states (see e.g. the review papers [40–42] and the other references mentioned in the Introduction). Generally, the aim of the control in case of STIRAP is to achieve complete population transfer among the ground states, avoiding excitation of the atom. The transfer process is achieved by adiabatically tuning the coupling strengths of the dipole-allowed transitions.

The classical arrangement of STIRAP is presented in Fig. 1.4(a), a Λ-atom (see 1.2(a)) interacts with two laser pulses. The two coupling pulses (usually called Stokes and pump pulses) have constant frequencies which are equally detuned from the corresponding transition frequencies, that is they are in Raman resonance (this is an essential condition). The atom is initially prepared in one of the ground states, for example, in state $|1\rangle$, which is coupled to the excited state $|0\rangle$ by the pump pulse (Ω_p). The initially empty ground state (state $|2\rangle$ in our case) is coupled by the Stokes pulse Ω_S. The coupling laser pulses are time-shifted with respect to each other in a so-called counter-intuitive order, which means that atom is exposed first to the Stokes-pulse and, after a while, to the pump pulse (see Fig. 1.4(b)). It is important, however, that the two pulses have a significant overlap. Applying

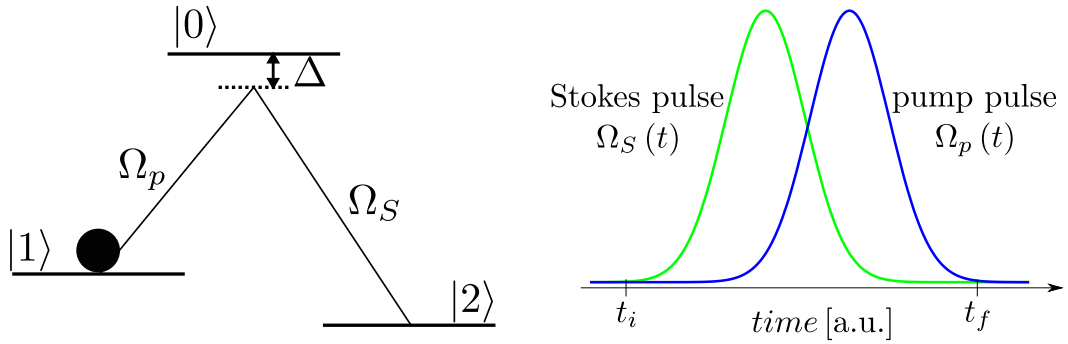

(a) (b)

Figure 1.4: a.) Classical arrangement of stimulated Raman adiabatic passage. The two ground states $|1\rangle$ and $|2\rangle$ are separately coupled by the pump and Stokes pulses, which are in Raman resonance. b.) Counter-intuitive order of the overlapping Stokes and pump pulses. The Stokes pulse Ω_S, which couples the initially unpopulated ground state to the excited state $|0\rangle$ comes first, followed by the pump pulse Ω_p.

the Hamiltonian given in Eq. (1.22) for our case, we obtain the following expression:

$$\hat{\mathcal{H}}_{\text{STIRAP}} = -\hbar \left[-\Delta \left(|1\rangle\langle 1| + |2\rangle\langle 2| \right) + \frac{\Omega_p}{2} \left(|0\rangle\langle 1| + \text{H.c.} \right) + \frac{\Omega_S}{2} \left(|0\rangle\langle 2| + \text{H.c.} \right) \right], \tag{1.62}$$

where $\Delta = \omega_p - \omega_{01} = \omega_S - \omega_{02}$ (cf. Eq. (1.16)).

The eigenvectors (often referred to as "dressed states") of Hamiltonian (1.62) are

$$|a^+\rangle = \cos\Phi|0\rangle + \sin\Theta\sin\Phi|1\rangle + \cos\Theta\sin\Phi|2\rangle \tag{1.63a}$$

$$|a^-\rangle = -\sin\Phi|0\rangle + \sin\Theta\cos\Phi|1\rangle + \cos\Theta\cos\Phi|2\rangle \tag{1.63b}$$

$$|a^0\rangle = \cos\Theta|1\rangle + \sin\Theta|2\rangle, \tag{1.63c}$$

where Φ is some function of the Rabi frequencies and detunings which is not relevant in this discussion and the mixing angle $\Theta(t)$ is defined by

$$\tan\Theta(t) = \frac{\Omega_p(t)}{\Omega_S(t)}. \tag{1.64}$$

The dressed state $|a^0\rangle$ evolves in a subspace which is perpendicular to the excited state $|0\rangle$, thus it can be applied for transferring the population from the ground state $|1\rangle$ to $|2\rangle$. Eqs. (1.63c) and (1.64) reveal how this is possible. For counter-intuitive order of the pulses (see Fig. 1.4(a)), the mixing angle, which is the adiabatic parameter here, slowly changes between $\Theta(t_i) = 0$ to $\Theta(t_f) = \pi/2$. Consequently, $|a_0\rangle$ coincides with $|1\rangle$ in the beginning, and with $|2\rangle$ at the end of the interaction. Thus, the required population transfer is achieved provided that the process is adiabatic, for which the criterion (based on Eq. (1.61)) is formulated as

$$\left|\frac{\dot{\Omega}_p\Omega_S - \Omega_p\dot{\Omega}_S}{\Omega_p^2 + \Omega_S^2}\right| \ll \left|\lambda^{\pm} - \lambda^0\right|, \tag{1.65}$$

where

$$\lambda^{\pm} = \frac{1}{2}\left(-\Delta \pm \sqrt{\Delta^2 + \Omega_p^2 + \Omega_S^2}\right) \tag{1.66a}$$

$$\lambda^0 = -\Delta \tag{1.66b}$$

are the eigenenergies corresponding to the eigenvectors (1.63).

The expression in Eq. (1.63c) gives a recipe for creating coherent superposition between the ground state, too. If the two coupling pulses vanish simultaneously, in such a way that

$$\lim_{t\to\infty}\frac{\Omega_p(t)}{\Omega_S(t)} = \tan\alpha, \tag{1.67}$$

then the system evolves along the adiabatic state $|a^0\rangle$ into $\cos\alpha|1\rangle + \sin\alpha|2\rangle$ (fractional STIRAP, [55]). That is, the created superposition is determined by the proportion of the trailing edges.

1.3.3 Frequency-chirped (FC) laser pulses

In this dissertation, we concentrate on the interaction of atoms with laser pulses having monotonic modulation in their frequencies (see Fig. 1.5). This represents another possibility for performing adiabatic control. In this case, the adiabatic process is governed by the slowly changing detunings between the frequencies of the coupling laser(s) and the corresponding atomic transition(s).

In order to demonstrate the main population control mechanism which is made possible by using frequency-chirped laser pulses, we analyze here the simplest case of a two-state atom coupled by one chirped laser pulse. This interaction can be described by the Hamiltonian (c.f. Eq (1.27))

$$\mathcal{H}_2^{\text{chirp}}(t) = -\hbar\left[\tfrac{1}{2}\Omega(t)\left(|1\rangle\langle 0| + |0\rangle\langle 1|\right) - \Delta(t)\,|1\rangle\langle 1|\right] \equiv -\hbar\begin{pmatrix} 0 & \frac{1}{2}\Omega(t) \\ \frac{1}{2}\Omega(t) & -\Delta(t) \end{pmatrix}, \tag{1.68}$$

where $(1\ \ 0)^T$ was assigned to the excited state $|0\rangle$ whose energy is used as reference energy level and $(0\ \ 1)^T$ to the ground state $|1\rangle$ dressed with the time-varying detuning $\Delta(t)$ (Eq. (1.26)) which incorporates the frequency-modulation. $\Omega(t)$ here denotes the Rabi frequency[1], which can be here assumed to be real without loss of generality. Note that only time dependences are need to be indicated since we regard the interaction in a fixed location. We assume that the system changes adiabatically and thus we use the adiabatic states for the analysis. The eigenstates of the Hamiltonian $\mathcal{H}_2^{\text{chirp}}$ are given by

$$\begin{aligned} |v_\pm\rangle &= \begin{pmatrix} -\frac{p(t)\pm\sqrt{1+p^2(t)}}{N_\pm} & \frac{1}{N_\pm} \end{pmatrix}^T \\ N_\pm &= \sqrt{2\sqrt{1+p^2(t)}\left[\sqrt{1+p^2(t)} \pm p(t)\right]}, \end{aligned} \tag{1.69}$$

where the parameter $p(t) = \Delta(t)/\Omega(t)$ was used. The energies of these adiabatic states are the eigenvalues of the Hamiltonian:

$$\lambda_\pm(t) = \frac{1}{2}\left[\Delta(t) \pm \sqrt{\Delta(t)^2 + \Omega(t)^2}\right]. \tag{1.70}$$

[1] To be more precise, it is the real part of the Rabi frequency defined in Eq. (1.17). However, in this context we will refer to it as Rabi frequency, as the time evolution of the complex part ϕ has been taken care of by the time-changing detuning.

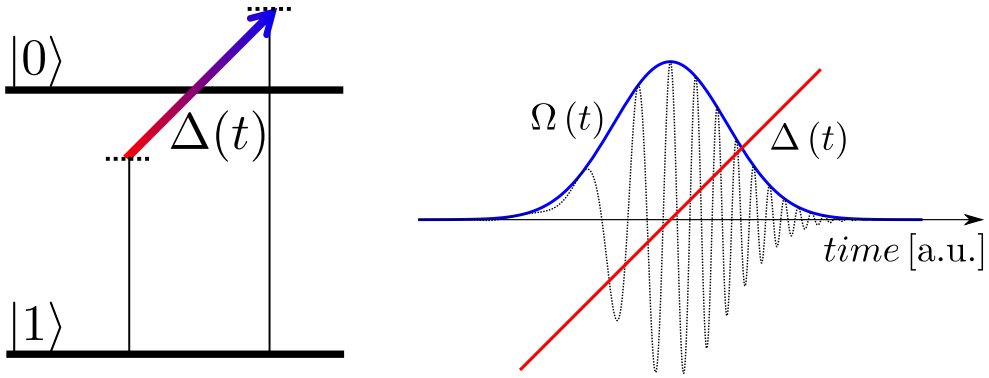

(a) (b)

Figure 1.5: a.) Schematic of the two-state atom. The detuning $\Delta(t)$ of the interacting laser pulse from the transition frequency monotonicly changes in time b.) Time dependence of the Rabi frequency $\Omega(t)$ and the detuning $\Delta(t)$. The frequency of the field starts below and ends up above resonance during the interaction. The strength of the electric field of the laser pulse is plotted with a black dotted line.

The specific form of the frequency modulation is not important so long as it varies slowly and the frequency is monotonicly swept through resonance with a large negative to a large positive value of detuning. (In this context, "large" is meant compared to the Rabi frequency, we still remain in the closely resonant regime so the detuning is significantly smaller than the atomic transition frequency.) This behavior implies that $\lim_{t\to\pm\infty} p(t) = \pm\infty$, which gives the following asymptotic behavior of the adiabatic states:

$$\lim_{t\to-\infty} |v_+\rangle = |1\rangle \qquad \lim_{t\to\infty} |v_+\rangle = -|0\rangle \tag{1.71a}$$

$$\lim_{t\to-\infty} |v_-\rangle = |0\rangle \qquad \lim_{t\to\infty} |v_-\rangle = |1\rangle, \tag{1.71b}$$

that is, the adiabatic states coincide with the diabatic states in the beginning and at the end of the interaction with the laser pulses, where we refer to the eigenstates of the non-interaction Hamiltonian as *"diabatic states"*. Naturally this is also true for the eigenenergies (see Fig. 1.6(a)). The adiabatic energies approach the diabatic energies (which are the eigenvalues of the non-interaction Hamiltonian and therefor given by the diagonal elements of the Hamiltonian $\mathcal{H}_2^{\text{chirp}}$) at early and later times, but the presence of the coupling $\Omega(t)$ prevents their intersection. Namely, the adiabatic energies have an *avoided crossing*.

In consequence, if the system is prepared in, for example, the ground state $|1\rangle$, it evolves along

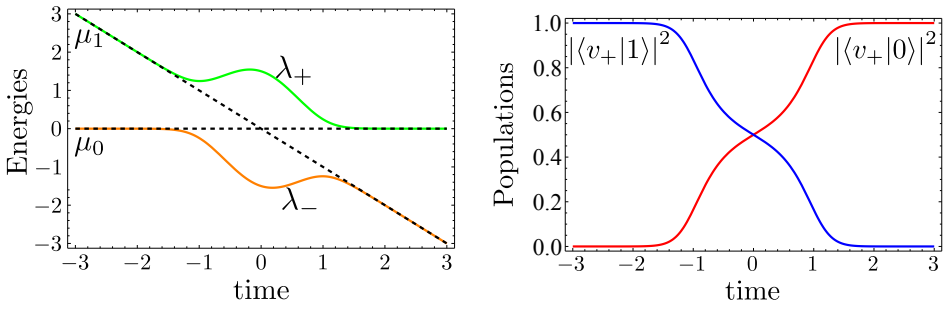

(a) (b)

Figure 1.6: a.) Eigenvalues of the Hamiltonian $\mathcal{H}_2^{\text{chirp}}$. The μ_0 and μ_1 energies of the diabatic states $|0\rangle$ and $|1\rangle$ are plotted with black dashed lines, the adiabatic eigenenergies are indicated with solid lines. Because of the interaction, the energies of the adiabatic states have an avoided crossing. b.) Time evolution of the populations of the states $|0\rangle$ (red) and $|1\rangle$ (blue) when the system follows the adiabatic state $|v_+\rangle$. A complete transfer is induced between the ground and the excited state. The functions $\Omega(t) = 3\exp(-t^2)$ and $\Delta(t) = t$ were used for calculation.

the adiabatic eigenstate $|v_+\rangle$, end eventually ends up in the excited state $|0\rangle$. Thus, the frequency modulated laser pulse has induced complete population transfer (see Fig. 1.6(b)). Note that this mechanism does not depend on the direction of the chirp, adiabatic passage takes place for both $\partial_t\Delta(t) > 0$ and $\partial_t\Delta(t) < 0$. Furthermore, the population transfer process is not too sensitive to the resonance conditions: the detuning between the carrier frequency of the laser and the atomic transition frequency may vary in a range which is swept through by the frequency-chirp. Thus, the control by a FC pulse can be established in the presence of inhomogeneous broadening, which represents and advantage compared with the other control schemes.

Adiabaticity condition for linearly chirped laser pulses

The analysis of the system in the frame of adiabatic following is a good approximation only if the condition of adiabaticity is fulfilled. In our case this condition can be formulated as follows (after substituting into the expression given in Eq. (1.61)):

$$\frac{1}{2}\left|\partial_t\Omega(t)\,\Delta(t) - \Omega(t)\,\partial_t\Delta(t)\right| \ll \left[\Omega^2(t) + \Delta^2(t)\right]^{3/2}. \tag{1.72}$$

In the dissertation, we deal with the laser pulses which have Gaussian time dependence in their envelopes and linear chirp in their frequencies, namely

$$\Omega(t) = \vartheta \exp\left(-\frac{t^2}{2t_\sigma^2}\right) \text{ and } \Delta(t) = \beta t. \tag{1.73}$$

Here ϑ is the peak amplitude of the Rabi frequency, t_σ indicates the length of the interaction time and β is the rate of the frequency-modulation, often referred to as the "speed of chirp". Substituting these formulas into Eq. (1.72) we obtain

$$\frac{1}{2} e^{-\frac{t^2}{2t_\sigma^2}} \left(\frac{t^2}{t_\sigma^2} + 1\right) |\vartheta\beta| \ll \left(\beta^2 t^2 + \vartheta^2 e^{-\frac{t^2}{t_\sigma^2}}\right)^{3/2} \tag{1.74}$$

The left side of the inequality has the maximum value of $\beta\,\vartheta/\sqrt{e}$ at $t = \pm t_\sigma$. If $|\theta| < |t_\sigma\beta|$, then the expression in the right side has a global minimum at $t = 0$ with a value of ϑ^3. Thus, we can say that the process is adiabatic if the following requirements are fulfilled[2]:

$$\left|\frac{\beta}{\vartheta^2}\right| \ll 1 \tag{1.76a}$$

$$t_\sigma > \left|\frac{\vartheta}{\beta}\right|. \tag{1.76b}$$

1.4 Experimental generation of FC pulses

The theoretical work presented in this thesis is motivated by the experiments on the interaction between FC pulses and cold atoms conducted in our group [81, 82, 108]. In this section we give a few

[2]The condition (1.76b) is not strict. If $|\theta| > |t_\sigma\beta|$, the expression $\left(\beta^2 t^2 + \vartheta^2 e^{-\frac{t^2}{t_\sigma^2}}\right)^{3/2}$ has two global minima at $t = \pm t_\sigma \sqrt{\ln\left[\vartheta^2/\left(t_\sigma^2\beta^2\right)\right]}$, with the value of $\vartheta^3 \left[\mu^{-1}(1 + \ln\mu)\right]^{3/2}$, where $\mu = \vartheta^2/\left(t_\sigma^2\beta^2\right) > 1$ parameter has been introduced. That is, if $\mu \approx 1$, the global minima of the difference of the eigenvalues are still in the order of θ^3 and consequently the inequality in (1.76a) is still a good condition for adiabaticity. In the context of this investigation, the expression $\mu \approx 1$ may be interpreted as $\mu < 1 + |\beta|/\vartheta^2$, which gives a condition for the interaction length (which is slightly weaker than the one in (1.76b)):

$$t_\sigma > \left|\frac{\vartheta}{\beta}\right| \sqrt{\frac{1}{1 + |\beta|/\vartheta^2}}. \tag{1.75}$$

examples of the experimental techniques which are capable of creating FC pulses with the required intensity, chirp and pulse length to fulfill the adiabaticity conditions given by Eq. (1.76).

Unlike femtosecond pulses, where the chirp can be generated using passive elements such as gratings or a prism pair [72, 109], an active optical element is needed for creating chirped pulses with a length of at least a few nanoseconds. In the following we outline two, principally different methods, used to create chirped pulses relevant to this work [81, 82, 108].

1.4.1 FC pulse generation by current modulation and subsequent pulse shaping

Figure 1.7 is a schematic of a method first proposed by Nebenzahl and Szőke [110], in which frequency modulated light is generated by mixing a sinusoidal modulation of a few tens of MHz on the drive current of a free-running semiconductor laser diode. The modulated laser diode current produces continuous laser radiation with sinusoidal modulation both in the frequency and intensity. To form a pulse the modulated light is injected into a Fabri-Perot (FP) cavity.

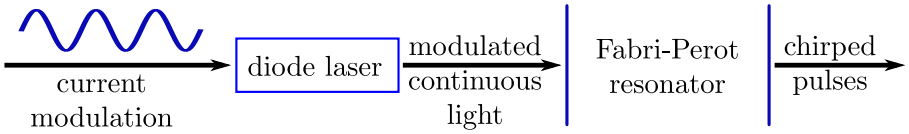

Figure 1.7: Schematic of the generation of chirped pulses using frequency modulated continuous light that is pulse shaped with a Fabri-Perot resonator.

In the case of a frequency modulation which exceeds the linewidth of the resonator, pulses are cut from the continuous laser radiation since only the light which is within the linewidth of the cavity will be transmitted. Fig. 1.8 is a plot of the intensity and frequency of a CP created by the FP method. As the sinusoidally modulated frequency sweeps through the transmission window of the cavity within one period, two light pulses are produced in one cycle. However, due to the fact that the intensity modulation of the light introduced by the current modulation of the laser diode has a π phase delay with respect to the frequency modulation, the second pulse coming out of the FP cavity is significantly weaker.

For the particular pulses used in [81], the cavity was tuned to resonance with the $|5^2S_{1/2}, F = 3\rangle$ to $|5^2P_{3/2}, F = 4\rangle$ transition in ^{85}Rb. The finesse and the pass-band of the resonator were 10 and 500 MHz, respectively.

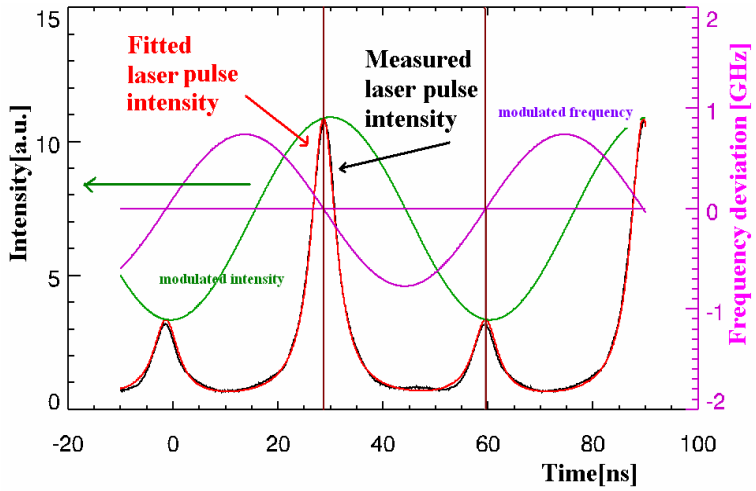

Figure 1.8: Chirped pulses generated by the Fabry-Perot resonator [108]. The frequency and intensity of the continuous light emitted from the diode laser are plotted in purple and green, respectively. The black dots visualize measurement data of the radiation after the FP cavity, while the red line is a fitting function calculated from the Airy transmission function of the cavity.

By using a current modulation of 16.6MHz, laser pulses with a duration of approximately $t_\sigma = 5$ns were tailored with an average chirp rate of $\beta = 30$MHz/ns, where the center frequency of the laser was set to the same frequency as the resonator. The peak power transmitted by the resonator was $I = 20mW$ over a pulse cross-section area $A = 0.5\text{mm}^2$, corresponding to an estimated peak Rabi-frequency of $\theta \approx 1.32$GHz [111].

Substituting these parameters in the inequalities imposing the restriction on adiabaticity, we get:

$$\frac{\beta}{\theta^2} = \frac{30\text{MHz/ns}}{(1320\text{MHz})^2} = 0.17 < 1 \tag{1.77}$$

$$\frac{\theta}{\beta} = \frac{1320\text{MHz}}{30\text{MHz/ns}} = 4.4\text{ns} < t_\sigma. \tag{1.78}$$

Consequently, the pulses with these parameters may be used for inducing an adiabatic passage.

Note that the above described method, suitable for creating FC pulses that fulfill the conditions of adiabaticity, suffers however from drawbacks following from the characteristics of the pulse tailoring. First, two pulses are created instead of one, which may cause complications in the analysis of experimental data. Second, the time function of the frequency modulation is determined by the relation of the center frequency of the laser radiation and the resonance frequency of the FP resonator. If there is difference between the two, the pulse is created from a part of the sinusoidal cycle. Therefore it is complicated to change the central frequency of the incoming laser field. It may therefore be

advantageous to use a different method for the pulse tailoring, such as a Mach-Zehnder type intensity modulator described in the following section.

1.4.2 Creation of FC pulses by a Mach-Zehnder-type intensity modulator

Using a Mach-Zehnder based intensity modulator is a possible alternative for chirped pulse generation [108, 112]. The schematic of the principle of the device is presented in Fig. 1.9. The continuous laser radiation enters a Mach-Zehnder interferometer in which a nonlinear crystal (Lithium-Niobate for example) is placed in each arm of the interferometer.

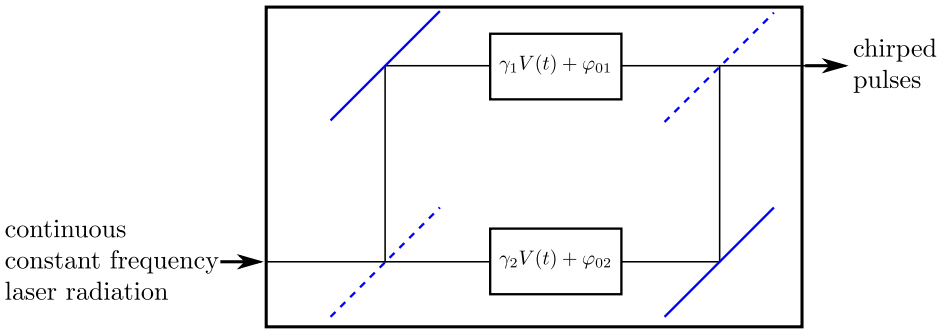

Figure 1.9: Schematic of the principle of the Mach-Zehnder-type intensity modulator. Two nonlinear crystals are placed in the two arms of a Mach-Zehnder interferometer, which are driven by an outer voltage $V(t)$.

Each crystal can be interdependently driven by an external voltage, which causes a change in the optical path length according to the voltage $V(t)$. As a result, assuming that the input field is split without loss between the two arms, the output field is given by [112]:

$$E(t) = \frac{1}{2} E_0 \left[e^{i(\omega_0 t + \gamma_1 \cdot V(t) + \varphi_{01})} + e^{i(\omega_0 t + \gamma_2 \cdot V(t) + \varphi_{02})} \right], \tag{1.79}$$

where γ_1 and γ_2 are the voltage-to-phase coefficients for the two arms, and ω_0 is the frequency of the ingoing laser light. φ_{01} and φ_{02} are the static phases of each arm of which the difference can be controlled by a bias dc voltage. The ratio of the output power to the input power is determined by the phase difference of the two arms according to

$$P(t)/P_0 = \cos\left(\Delta\varphi(t)\right), \text{ with } \Delta\varphi(t) = \left[(\gamma_1 V(t) + \varphi_{01}) - (\gamma_2 V(t) + \varphi_{02})\right]. \tag{1.80}$$

The time-dependent frequency is given by the derivative of the output phase:

$$\omega(t) = \partial_t \left[(\gamma_1 V(t) + \varphi_{01}) - (\gamma_2 V(t) + \varphi_{02}) \right] = \frac{1}{2} (\gamma_1 + \gamma_2) \, \partial_t V(t). \tag{1.81}$$

It follows from the above formulae that the time-characteristic of both the intensity and the frequency of the output light is controlled by the time shape of the controlling voltage $V(t)$. Using this peculiarity, laser pulses of a few nanosecond duration and almost monotonic frequency modulation have been generated [108]. Fig. 1.10 is a plot of the intensity and frequency of a CP pulse created with the Mach-Zehnder method. The main restraint of this method is clearly seen in this figure.

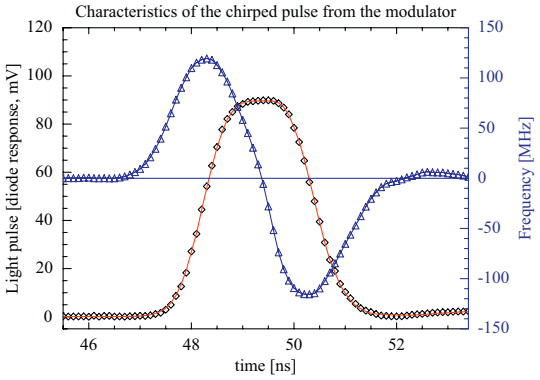

Figure 1.10: Time evolution of the intensity (rhombuses) and frequency (triangle) of the pulses generated by a Mach-Zehnder intensity modulator [108]

Namely, as the time function of the frequency of the pulse is given by the derivative of the pulse shape, it is challenging to guarantee the monotony of the chirp during the whole pulse duration.

Part II

Results

Chapter 2

Adiabatic control of tripod-atoms by three FC pulses

Selective population transfer is an important problem of quantum optics which has been widely investigated and applied in the last two decades. The main goal is to begin with an atom (or any quantum system can be modelled by a discrete, few dimensional level structure) prepared in a specified inner quantum state and, using a certain combination of external laser pulses, force its internal state into a desired target state.

Among these, interaction schemes based on adiabatic passage (see Sec. 1.3) represent a considerable group. The reason is that they allow efficient control along with relative robustness against small-to-moderate variations in certain parameters of the coupling field, which is advantageous in experimental situations. Adiabatic control (AC) can be achieved by very slowly tuning a certain parameter of the interaction. As we have already seen through some simple examples (in subsecs 1.3.2 and 1.3.3), there are different kinds of AC schemes depending on which parameter is changed in time.

One of the possibilities of performing AC is to apply FC pulses in the atom-laser interaction. The simplest case of a two-state atom controlled by one FC pulse (see in subsec. 1.3.3) has already been generalized to solve different population-control problems.

Two, substantially different schemes were investigated in Λ-atoms. In [73, 75] both transitions of the atom are coupled by separate FC pulses in Raman resonance, that is, the detunings between the pulses' frequencies and the corresponding transition frequencies are the same. As a result of the interaction a coherent superposition of the three (i.e. ground and *excited*) states is created. The

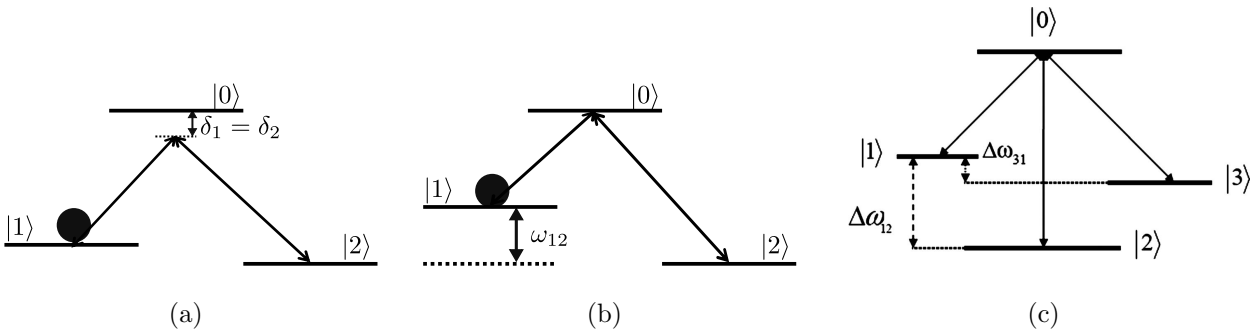

Figure 2.1: Coherent control schemes using one or two FC laser pulses to couple the allowed transition of an atom having Λ (a. and b.) and tripod (c.) structure. a.) Two Raman-resonant pulses separately interact with the atomic transitions, [73, 75]. b.) Both transitions, having different frequencies, are driven by a single FC pulse, [74, 77]. c.) All the transitions interact with the same FC pulse. States $|1\rangle$ and $|3\rangle$ are quasi-degenerate levels, whereas the energy difference $\Delta\omega_{12}$ is large compared to the frequency width of the light pulse (without chirp), [78].

proportion of the probabity amplitudes is shown to be controlled by the difference of the initial phases of the pulses (referred to as "relative phase"). This property can be understood based on the fact that a "bright" and "dark" superposition of the ground states are created by the Raman-resonant pulse pair. The composition of the superpositions depends on the relative phase. Now the "dark" superposition is uncoupled from the light so remains unaffected by the interaction, while the bright superposition if transferred into the excited state, like in a two-state atom. However, because of the sponaneous decay, the lifetime of the created superposition is restricted by the lifetime of the excited state which may restrain the applicability of the scheme.

On the other hand, in the schemes presented in [74, 77] both ground states of different energies are coupled by a single FC pulse. Thus, in contrast with the previous scheme, the detuning of the pulse from the frequency of the separate transitions is different. Note that this scheme is analogous of a Λ-atom whose transitions are separately coupled by two FC-pulses out of Raman resonance. In this case, as it was shown, the population initially trapped in one ground state is driven into the other ground state by the interaction. Although complete population trapping in the ground states does not occur like in the STIRAP-scheme (see 1.3.2), the excitation of the atom may be suppressed to be almost negligible via quantum interference. It is worth noting that, contrary to the two-state case, the result of the population transfer depends strongly on the direction of the frequency-modulation.

The latter scheme in the Λ-atom was further generalized to a tripod-structured atom interacting with a single FC-pulse, which couples all the ground states to the excited state. The atom was

assumed to have a special level-structure with two near-degenerate ground states and the third ground state with a large energy difference from the energy of the former ones. Here, two dipole-allowed atomic transitions are coupled in a Raman-resonant and the third one in a Raman-detuned way. As a result, a dark and bright superposition is formed from the former two states, similarly to the case of the Λ-scheme mentioned first. The population of the bright state is transferred into the third, Raman-detuned ground states, likewise in the second Λ-scheme. As a result, coherent superposition is established among the ground states of the tripod-atom without significant excitation of the atom. The drawback of the scheme is that the superposition is also determined by properties of the atom before the interaction.

One possible application of the coherent control of atoms is the storage and processing of optical (classical and quantum) information. There are numerous methods which are based on electromagnetically induced transparency (EIT), see [38, 42, 113] and references therein. These kind of schemes were proposed for storing and studying transverse images in hot atomic vapors [17, 21, 22, 114, 115]. Because the information is being written (mapped) in the coherences of the atomic states, the EIT-based methods are sensitive to the transverse relaxation processes during the writing and storage of the information [15, 17, 21–23, 38, 113–119]. In case of *classical information* , the information storage times may be substantially increased if the optical information is written into the populations of the metastable states instead of the atomic spin coherences.

The interaction scheme of the Λ-atom coupled by a pair of Raman-resonant FC pulses (Fig. 2.1(a)) was proposed to be applied for classical information writing. The information was coded into the relative phase of the coupling pulse pair, which was proven to control the population distribution created by the pulses. However, the storage time was restricted by the spontaneous decay rate.

In this chapter, we analyze the interaction of a tripod-atom with three FC pulses, two in Raman resonance and one out of it, with several initial preparations of the atom. Our aim is to unify the advantages of the three above mentioned schemes. We examine the possibilities of creating coherent superpositional states among the ground states of atoms. In doing so, we have two priorities. First, we require that the created superposition is controllable by external parameters such us the intensity or relative phase of the coupling light pulses. Second, we search for such mechanisms that are accompanied by only negligible excitation of the atom, in order to avoid spontaneous emission from the excited state.

An interaction scheme which fulfills these requirements is suitable for optical information mapping, similarly to the Λ-scheme ([73, 75]). However, if it can be guaranteed that the excitation of the atom remains negligible, the storage time becomes significantly extended. That is, it is limited by the lifetime of the ground states instead of the lifetime of the excited state, which means an increase of several orders of magnitude.

From the point of view of practical applications of coherent control schemes, it is important to investigate their applicability in real media with inhomogeneously broadened transition lines typical for atomic gases. Another important question to be addressed is the effect of longitudinal and transverse relaxations on the efficiency of the schemes. For example, the effect of dephasing was investigated in [51, 52, 59] in case of STIRAP, and the influence of inhomogeneous broadening was also investigated in schemes applying FC pulses [74]. Here, we analyze in detail the effect of the Doppler broadening of transition lines on the efficiency of the transfer mechanism by considering an atomic gas of tripod-atoms at different temperatures. We also study the possible impact of relaxation processes on the population control.

2.1 Mathematical formalism for describing the interaction between a tripod atom and three FC pulses

We consider the interaction of three laser pulses with a tripod-atom (see Fig. 1.2(b)). Each laser field is acting on the corresponding allowed electric-dipole transition in the atom (between a ground state $|k\rangle$ ($k \in \{1,2,3\}$) and the excited state $|0\rangle$). Here, we focus on the effect of the field on the atomic state and we neglect propagation effects of the lasers. The physical process which we are interested in takes place in a certain point in space (defined by the location of the atom), thus we further suppress the space-dependence in the description of the interacting laser fields:

$$E(t) = \sum_{k=1}^{3} \mathcal{E}_k(t) \cos\left(\omega_k t + \int_{-\infty}^{t} \beta\hat{t}\,\mathrm{d}\hat{t} + \varphi_k^{(0)}\right), \tag{2.1}$$

where we have assumed an identical linear time variation of the frequencies of all the interacting laser pulses with a rate of β (c.f. Eq. 1.73). $\mathcal{E}_k(t)$ and ω_k denote the slowly varying amplitude and the central frequency of the k$^{\text{th}}$ laser pulse, φ_k^0 is a constant phase term.

We analyze the atomic dynamics in the rotating basis introduced in Eq. (1.21). The interaction is described in the frame of rotating wave approximation (see 1.1.3) by the the Hamiltonian (c.f. (1.22))

$$\hat{\mathcal{H}}_{\text{tripod}} = -\frac{1}{2}\hbar \sum_{k=1}^{3} \left(\Omega_k |0\rangle\langle k| + \text{H.c.}\right) - \hbar \left[\Delta \left(|1\rangle\langle 1| + |2\rangle\langle 2|\right) + \left(\Delta + \delta_R\right)|3\rangle\langle 3|\right]. \tag{2.2}$$

Here $\Omega_k(t) \equiv W_k f\,(t) \exp\left(i\beta t^2/2\right)$ is the time-dependent Rabi frequency (1.17) of the laser pulse which drives the transition $|0\rangle \leftrightarrow |k\rangle$, which includes the modulation of the phase in time. The envelope function $f\,(t)$ is supposed to be the same for the three laser pulses, with (in general, different) complex amplitudes $W_k = |W_k| \exp(i\varphi_k^{(0)})$, $k \in \{1, 2, 3\}$. We regard laser pulses having Gaussian shape $f\,(t) = \exp\left(-t^2/2\right)$, where the time is measured in the unit of $\tau_p = \tau_L/(2\sqrt{\ln 2})$, τ_L being the full width at half-maximum of the pulse (intensity) envelope.

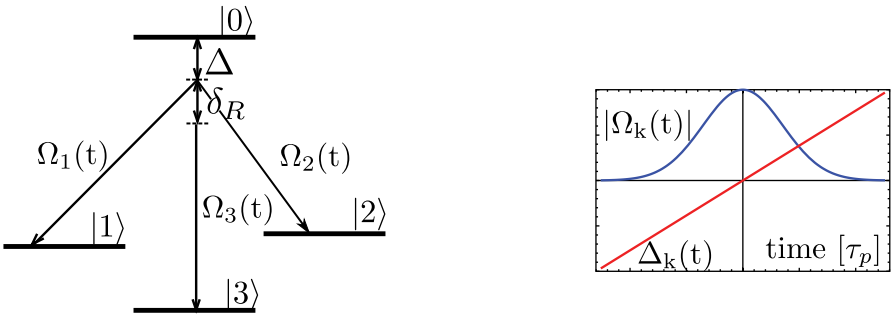

Figure 2.2: Interaction of three FC pulses with a tripod atom. The pulses having Rabi frequencies Ω_1 and Ω_2 are in Raman resonance with a common detuning of Δ and the third pulse is Raman-detuned from the other two pulses with δ_R. The interacting pulses have Gaussian envelopes and linear frequency chirp.

We also assume that the transitions $|0\rangle \leftrightarrow |1\rangle$ and $|0\rangle \leftrightarrow |2\rangle$ are coupled by pulses in Raman resonance with a common one-photon detuning Δ. In contrast, the third transition is supposed to be out of Raman resonance, with a two-photon detuning large compared with the transform-limited bandwidth of the laser pulses: $\delta_R \gg 1/\tau_p$.

2.1.1 Equations of motion

The dynamics of the atomic populations and coherences is given by the master equation (1.37), which gives the following set of differential equations:

$$\partial_t \rho_{00} = -\frac{i}{2} \sum_{i=1}^{3} \left(\Omega_i \rho_{0i}^* - \Omega_i^* \rho_{0i} \right) - \Gamma \rho_{00} \tag{2.3a}$$

$$\partial_t \rho_{kk} = \frac{i}{2} \left(\Omega_k \rho_{01}^* - \Omega_k^* \rho_{01} \right) + \frac{\Gamma}{3} \rho_{kk}, \quad k \in \{1, 2, 3\} \tag{2.3b}$$

$$\partial_t \rho_{01} = -\frac{i}{2} \left[\Omega_2 \rho_{12}^* + \Omega_3 \rho_{13} + \Omega_1 \left(\rho_{11} - \rho_{00} \right) + 2\Delta \rho_{01} \right] - \left(\Gamma/2 + \gamma \right) \rho_{01} \tag{2.3c}$$

$$\partial_t \rho_{02} = -\frac{i}{2} \left[\Omega_1 \rho_{12} + \Omega_3 \rho_{23}^* + \Omega_2 \left(\rho_{22} - \rho_{00} \right) + 2\Delta \rho_{02} \right] - \left(\Gamma/2 + \gamma \right) \rho_{02} \tag{2.3d}$$

$$\partial_t \rho_{03} = -\frac{i}{2} \left[\Omega_1 \rho_{13} + \Omega_2 \rho_{23} + \Omega_3 \left(\rho_{33} - \rho_{00} \right) + 2 \left(\Delta + \delta_R \right) \rho_{03} \right] - \left(\Gamma/2 + \gamma \right) \rho_{03} \tag{2.3e}$$

$$\partial_t \rho_{12} = \frac{i}{2} \left[\Omega_2 \rho_{01}^* - \Omega_1^* \rho_{02} \right] - \gamma \rho_{12} \tag{2.3f}$$

$$\partial_t \rho_{13} = \frac{i}{2} \left[\Omega_3 \rho_{01}^* - \Omega_1^* \rho_{03} + 2\delta_R \rho_{13} \right] - \gamma \rho_{13} \tag{2.3g}$$

$$\partial_t \rho_{23} = \frac{i}{2} \left[\Omega_3 \rho_{02}^* - \Omega_2^* \rho_{03} + 2\delta_R \rho_{23} \right] - \gamma \rho_{23}. \tag{2.3h}$$

Here we assumed, on one hand, that the longitudinal decay rate from the excited state is the same ($\Gamma/3$) towards all three ground states, and, on the other hand, that the transverse relaxation, caused by other effects than the spontaneous emission, can also be expressed by the same rate γ. The diagonal elements $\rho_{jj}, \quad j \in \{0, 1, 2, 3\}$ of the density matrix are the populations of the corresponding states; the nondiagonal elements $\rho_{kj}, \quad k \neq j$ are the complex coherences between the corresponding states.

2.1.2 Coordinate transformation: introducing dark and bright superpositional states

For further analysis, it is convenient to introduce a new basis using the complex amplitudes of the interacting pulses as

$$|b_1\rangle = e^{-i\Delta t}\frac{W_2^*|1\rangle - W_1^*|2\rangle}{W_{12}} \qquad |b_2\rangle = e^{-i\Delta t}\frac{W_1|1\rangle + W_2|2\rangle}{W_{12}}$$
$$|b_3\rangle = e^{-i\Delta t}\frac{W_3|3\rangle}{|W_3|} \qquad |b_0\rangle = |0\rangle\, e^{-i\left(\beta t^2/2+\Delta t\right)}, \tag{2.4}$$

which can be obtained from the original rotating basis defined in (1.21) by the transformation

$$\mathcal{S} = e^{-i\Delta t}\left[\frac{\left(W_2^*|1\rangle - W_1^*|2\rangle\right)\langle 1| + \left(W_1|1\rangle + W_2|2\rangle\right)\langle 2|}{W_{12}} + \frac{W_3}{|W_3|}|3\rangle\langle 3| + e^{-i\beta t^2/2}|0\rangle\langle 0|\right], \tag{2.5}$$

where $W_{12} = \sqrt{|W_1|^2 + |W_2|^2}$. The phase factor $\exp\{-i\Delta t\}$ only shifts the reference energy by $\hbar\Delta$ and is introduced in order to simplify the formulas.

The interaction Hamiltonian in the basis (2.4) is given by

$$\hat{\mathcal{H}}_{\mathrm{db}} = \hbar f(t)\left[W_{12}\left(|0\rangle\langle b_2| + |b_2\rangle\langle 0|\right) + |W_3|\left(|0\rangle\langle b_3| + |b_3\rangle\langle 0|\right)\right]$$
$$+ \hbar\left[(\beta t + \Delta)|b_0\rangle\langle b_0| - \delta_R|b_3\rangle\langle b_3|\right], \tag{2.6}$$

where the transformation rule given in Eq. (A.1) was used.

2.2 Analysis of the adiabatic states

First, we analyze the effect of the three FC pulses on the inner state of the tripod-atom by using the adiabatic theorem (see 1.3). Note that this method gives an approximation for the Hamiltonian evolution of the system (for parameters that suit to the constraints given in Eqs. (1.76a) and (1.76b)) and it cannot describe the relaxation processes. The deviations caused by the decay processes from the results of this approximation are discussed in 2.3.4. As we have seen in Sec. 1.3, the adiabatic approximation allows us to describe the dynamics of the system by the eigenstates and eigenvalues of the Hamiltonian. Substituting the Hamiltonian given in Eq. (2.6), the following equation follows

from Eq. (1.52) for the eigenvalues $\lambda = \lambda_j$:

$$\lambda \left\{ \lambda \left(\lambda + \hbar\delta_R \right) \left[\lambda - \hbar \left(\beta t + \Delta \right) \right] - \hbar^2 f(t)^2 \left[\lambda \left(W_{12}^2 + |W_3|^2 \right) + \hbar\delta_R W_{12}^2 \right] \right\} = 0, \tag{2.7}$$

and the following expressions are obtained for the corresponding eigenvectors $|a_k\rangle$:

$$|a_1\rangle = |b_1\rangle \tag{2.8a}$$

$$|a_j\rangle = \frac{\hbar f\left(t\right) W_{12}}{\sqrt{N_j}} |b_2\rangle + \frac{\lambda_j \left[\lambda_j - \hbar \left(\Delta + \beta t \right) \right] - \hbar^2 f(t)^2 W_{12}^2}{\hbar f\left(t\right) |W_3| \sqrt{N_j}} |b_3\rangle \tag{2.8b}$$

$$+ \frac{\lambda_j}{\sqrt{N_j}} |b_0\rangle, \;\; j \in \{2,3,4\}\,.$$

Here the normalization factor for $|a_j\rangle$ is

$$N_j = \sqrt{\hbar^2 f(t)^2 W_{12}^2 + \left| \frac{\lambda_j \left[\lambda_j - \hbar \left(\Delta + \beta t \right) \right] - \hbar^2 f(t)^2 W_{12}^2}{\hbar f(t) |W_3|} \right|^2 + \lambda_j^2}. \tag{2.9}$$

As it follows from Eq. (2.8), the following relations take place between the components of the dressed state vector $|b_j\rangle$, $\;j \in \{2,3,4\}$:

$$\frac{\langle a_j | b_3 \rangle}{\langle a_j | b_2 \rangle} = \frac{\lambda_j \left[\lambda_j - \hbar \left(\Delta + \beta t \right) \right] - \hbar^2 f(t)^2 W_{12}^2}{\hbar^2 f\left(t\right)^2 W_{12} |W_3|}, \qquad \frac{\langle a_j | b_0 \rangle}{\langle a_j | b_2 \rangle} = \frac{\lambda_j}{\hbar f(t) W_{12}}. \tag{2.10}$$

2.2.1 Adiabatic paths for positive and negative chirp

The dynamics of the four eigenvalues (quasi-energies) of $\hat{\mathcal{H}}_{db}$ is shown in Fig 2.3 for positive (from below to above resonce) linear chirp both for positive and negative values of Raman detuning. In the former case ($\delta_R > 0$), the laser pulse out of Raman resonance (Ω_3) reaches the single-photon resonance with the corresponding transition earlier than the pulses in Raman resonance (Ω_1 and Ω_2), while, in the latter case ($\delta_R < 0$), the resonances occur in the reversed order. As can be seen in Fig. 2.3, in both cases of negative and positive chirp, the eigenenergies λ_2 and λ_3 coincide with the energy μ_0 of the (diabatic) excited state $|b_0\rangle$ in the end and beginning of the interaction, respectively. In this chapter, however, we wish to find such ways of coherent population control in the tripod atom by the FC pulses which are accompanied with only negligible excitation of the atom. Thus, we only

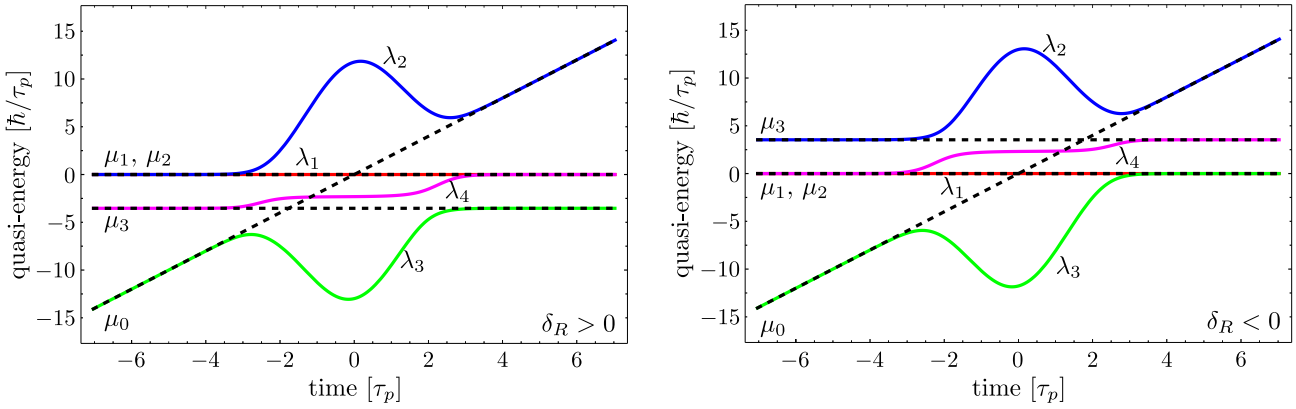

(a) (b)

Figure 2.3: Eigenvalues of the Hamiltonian $\hat{\mathcal{H}}_{db}$ in case of a.) positive and b.) negative values of Raman detuning δ_R. The energies μ_k of the diabatic states $|b_k\rangle$, $k \in \{0,1,2,3\}$ are plotted in dashed lines, while the eigenvalues λ_j, $j \in \{1,2,3,4\}$ are indicated with solid lines. The parameters used for calculation are $W_1 = W_2 = W_3 = 5\sqrt{2}\,[1/\tau_p]$, $\beta = 2\sqrt{2}\,[1/\tau_p^2]$, $\Delta = 0\,[1/\tau_p]$, $|\delta_R| = 5/\sqrt{2}\,[1/\tau_p]$.

consider initial preparations of the atom which ensure that the dynamics takes place on the subspace spanned by the dressed states $\{|a_1\rangle, |a_4\rangle\}$.

Note that this preparation is different for the cases of positive and negative Raman detuning (see Fig. 2.4). In both cases, the dark (diabatic) state $|b_1\rangle$ is also an adiabatic state, since it is uncoupled from the interaction with the three FC pulses (this is also obvious from the expression for the interaction Hamiltonian $\hat{\mathcal{H}}_{db}$ in Eq. (2.6)). Thus, if the atom is initially prepared in $|b_1\rangle$, it remains unexcited during the interaction, since this state is perpendicular to the excited state (cf. with the definition in Eq. (2.4)). On the other hand, for different signs of the Raman detuning, substantially different behavior follows from the preparation of the atom in the states $|b_2\rangle$ and $|b_3\rangle$.

For $\delta_R > 0$, see Fig. 2.3(a) and 2.4(a), the eigenvalue μ_2 coincides with λ_2, which means that the population initially set in the corresponding (diabatic) bright state $|b_2\rangle$ is adiabatically driven into the excited state. In the same time, the energy μ_3, belonging to state $|b_3\rangle$ coincides with the eigenvalue λ_4, which tends to the energy μ_2, which belongs to the bright superposition $|b_2\rangle$ of the atomic ground states. Namely, the population, placed in $|b_3\rangle$ at the beginning of the interaction, is transferred into state $|b_2\rangle$.

However, for $\delta_R < 0$ (Fig. 2.3(b)and 2.4(b)) the role of the states $|b_2\rangle$ and $|b_3\rangle$ is inverted. That is, it is state $|b_3\rangle$ in which the preparation leads to excitation of the atom, while the population prepared in state $|b_2\rangle$ gets into state $|b_3\rangle$ as a result of the interaction.

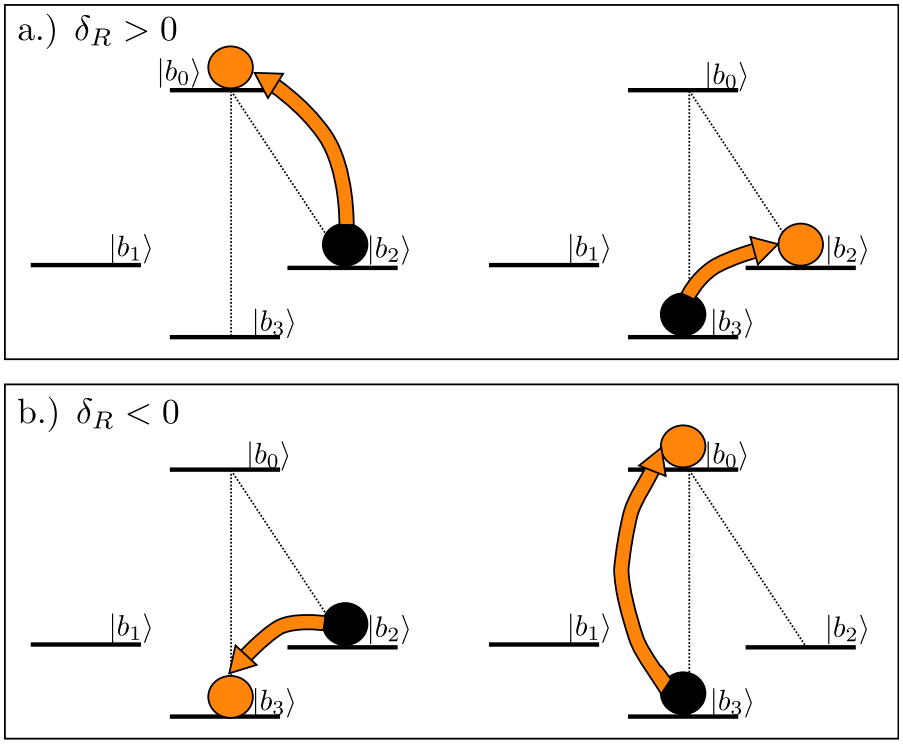

Figure 2.4: Adiabatic transfer in the tripod atom induced by the three FC pulses in the arrangement shown in Fig. 2.2 in case of a.) positive and b.) negative Raman detuning. The initial and the final states of the atom are indicated with black and orange desks, respectively. $|b_k\rangle$ $k \in \{0 \dots 3\}$ are the elements of the "dark-bright" basis defined in Eq. (2.4).

All in all, in order that the atom evolve in the required subspace, we need to prepare it in

$$c_1|b_1\rangle + c_2|b_3\rangle \text{ for } \delta_R > 0 \tag{2.11a}$$

$$d_1|b_1\rangle + d_2|b_2\rangle \text{ for } \delta_R < 0, \tag{2.11b}$$

respectively, with positive chirp in both cases. Here, c_j and d_j, $j \in \{1, 2\}$ are arbitrary complex numbers fulfilling the normalization condition of the quantum states.

2.2.2 Suppression of the excitation of the atom

Now let us assume that the atom is prepared according to (2.11), thus, it evolves in the subspace spanned by the adiabatic states $|a_1\rangle$ and $|a_4\rangle$ to end up in some superposition of the atomic ground states. However, as it follows from Eqs. (2.9) and (2.10), the excited state has a nonzero contribution in the dressed state $|a_4\rangle$, which depends on the corresponding eigenvalue λ_4. Notice that this quasi-energy does not depend strongly on the Rabi frequencies and is restricted by the value of the Raman

detuning δ_R for both positive and negative values (see Fig. 2.3):

$$0 \leq |\lambda_4| \leq |\delta_R| \,. \tag{2.12}$$

Using Eq. (2.12), the relative contribution of the excited state may be estimated as

$$\left| \frac{\langle a_4 | b_0 \rangle}{\langle a_4 | b_2 \rangle} \right| \leq \left| \frac{\delta_R}{W_{12}} \right| . \tag{2.13}$$

Consequently, the population of the excited state may be suppressed by increasing the amplitudes W_1 or/and W_2 of the Rabi frequencies of the laser pulses in Raman resonance.

2.3 Creation of coherent superposition states

In this section we discuss creation of coherent superposition of ground states in the tripod atom, which is initially optically pumped into one of the ground states, in accordance with (2.11). Namely, we assume that the atom is initially prepared in state $|3\rangle$ for positive ($\delta_R > 0$) and in state $|1\rangle$ for negative ($\delta_R < 0$) Raman detuning, respectively. In both cases, positive frequency chirp ($\beta > 0$) is assumed.

2.3.1 Adiabatic following

First, let us describe the transition process in the tripod-atom induced by the three positively frequency chirped ($\beta > 0$) pulses for the initial conditions

$$|\psi\,(t \to -\infty)\rangle = |3\rangle = W_3^* e^{+i\Delta t} / \,|W_3|\,|b_3\rangle \qquad \text{for } \delta_R > 0 \tag{2.14a}$$

$$|\psi\,(t \to -\infty)\rangle = |1\rangle = \left(W_2 |b_1\rangle + W_1^* |b_2\rangle\right) e^{+i\Delta t} / W_{12} \qquad \text{for } \delta_R < 0. \tag{2.14b}$$

Note that, due to Raman resonance between states $|1\rangle$ and $|2\rangle$ (see Fig. **??**), the initial condition $|\psi\,(t \to -\infty)\rangle = |2\rangle$ would lead to the same result that the conditions given in Eq. (2.14b) do. For

the preparation given in (2.14a) and (2.14b), the coefficients

$$r_1 = r_2 = r_3 = 0, \;\; r_4 = W_3^* / |W_3| \;\; \text{and} \tag{2.15a}$$

$$r_1 = W_2/W_{12}, \qquad r_2 = W_1^*/W_{12}, \qquad r_3 = 0, \qquad r_4 = 0, \tag{2.15b}$$

describe the statistical weights of the eigenstates in the dressed states representation of the atomic wave function (cf. Eq. (1.53)):

$$|\psi(t)\rangle = \sum_{k=1}^{4} r_k |a_k\rangle \exp\left(\int_{-\infty}^{t} \lambda_k\left(\hat{t}\right) \mathrm{d}\hat{t}\right). \tag{2.16}$$

In the case of positive Raman detuning ($\delta_R > 0$), as it was discussed above, the dressed state $|a_4\rangle$ evolves from state $|b_3\rangle$ to state $|b_2\rangle$ with an additional π phase-factor, so the final state vector becomes

$$|\psi(t \to +\infty)\rangle = -\frac{W_3^* e^{-i\Delta t}}{|W_3|}|b_2\rangle = -\frac{W_3^*\left(W_1|1\rangle + W_2|2\rangle\right)}{|W_3|\, W_{12}}. \tag{2.17}$$

As it follows from Eq. (2.17), a coherent superposition of two ground states connected by the two laser pulses in Raman resonance is created. The contribution of different ground states into the obtained admixture is governed by the Rabi frequencies (intensities) of the two laser pulses in Raman resonance. It is worth noting that if $W_1 = W_2$, a maximum coherence of 0.5 is achieved in this scheme.

A slightly more complicated consideration may be provided for the case of negative Raman detuning ($\delta_R < 0$). The dressed state $|a_1\rangle$, corresponding to the eigenvalue λ_1 coincides with the "dark" state and does not change during the interaction. In the same time, as a result of the interaction, the dressed state $|a_4\rangle$ evolves from the "bright" state $|b_2\rangle$ to the state $|b_3\rangle$, with an additional π phase-factor. The resulting state vector will have the following form in the "dark-bright" basis (defined in Eq. (2.4)) and the bare basis respectively:

$$|\psi(t \to +\infty)\rangle = \frac{W_2|b_1\rangle - W_1^*|b_3\rangle}{W_{12}} e^{-i\Delta t} = \frac{|W_2|^2|1\rangle - W_1^* W_2|2\rangle}{W_{12}^2} - \frac{W_1^* W_3|3\rangle}{W_{12}|W_3|}. \tag{2.18}$$

As it follows from the obtained equation, the final atomic wave function is a coherent superposition of the three ground states of the tripod-atom. As in the previous case, the intensities of the pulses

in Raman resonance govern the contribution of the two ground states in the coherent superposition. Note that the excited state is absent in the final atomic wave function. During the interaction process there may be some temporary excitation of the atom, which however may be successfully suppressed by increasing the intensity of the pulses in Raman resonance, (see Eq. (2.13)).

2.3.2 Results of numerical simulations for negligible relaxation

In the present subsection, we analyze the above considered scheme of creation of coherent superposition states by numerical simulation of the system of Eqs. (2.3) for the density matrix elements. At this point, we take the duration of the pulses shorter than longitudinal and transverse relaxation times of the atomic system to confirm the conclusions based on the dressed state analysis of the previous subsections.

The results of the numerical simulations are presented in Figs. 2.5 and 2.6 for the cases of positive and negative Raman detuning, with initial conditions given by Eqs. (2.14a) and (2.14b), respectively. As it follows from the numerical solutions, the dynamics of the states' populations and coherences confirm the results of subsection 2.3.1 based on the adiabatic consideration of the problem. Accordingly, in the case of positive Raman detuning, population of the initially populated state $|3\rangle$ is transferred into the "bright" superposition $|b_2\rangle$ of the states $|1\rangle$ and $|2\rangle$. The time evolution of the populations in this case is connected with the single dressed state $|a_4\rangle$. As a result, no oscillations occur in the dynamics of the populations, (see Fig. 2.5(a)).

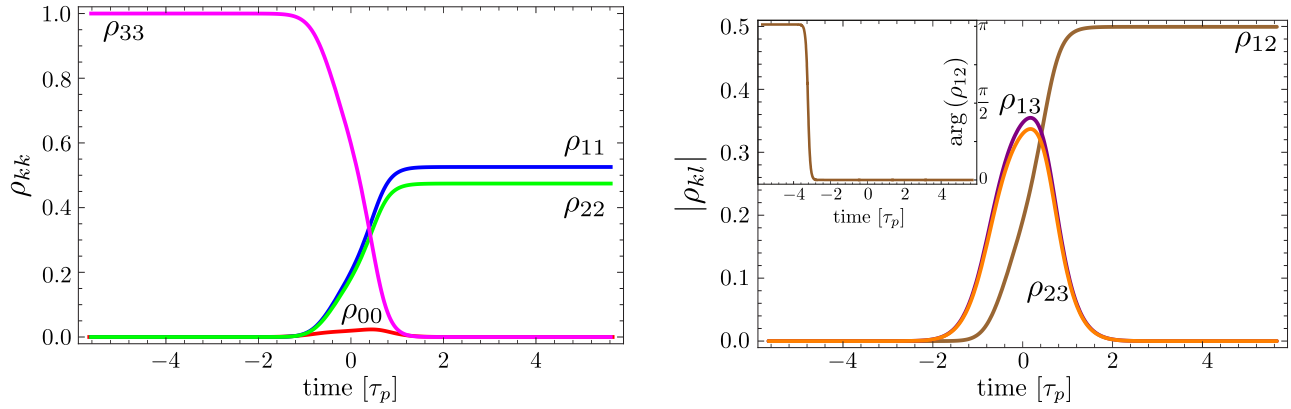

(a) Populations

(b) Coherences

Figure 2.5: Time evolution of the populations and coherenceces in case of positive Raman detuning (and positive chirp). Inset: the phase of the coherence ρ_{12}. The parameters used for calculation are $W_1 = 250\sqrt{2}\ [1/\tau_p]$, $W_2 = 237.5\sqrt{2}\ [1/\tau_p]$, $W_3 = 262.5\sqrt{2}\ [1/\tau_p]$, $\beta = 1250\ \left[1/\tau_p^2\right]$, $|\delta_R| = 125\ [1/\tau_p]$.

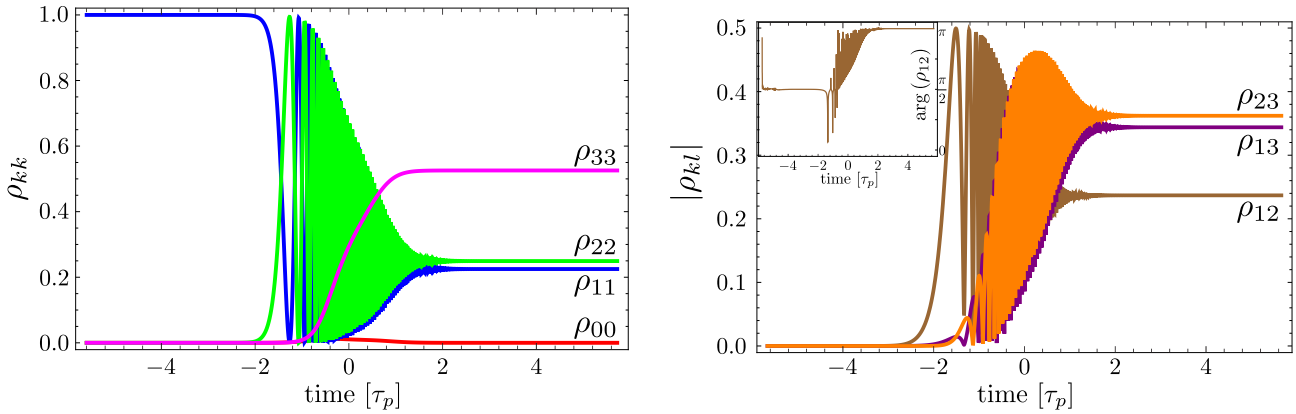

(a) Populations

(b) Coherences

Figure 2.6: Time evolution of the populations and coherenceces in case of negative Raman detuning (and positive chirp). Inset: the phase of the coherence ρ_{12}. The parameters applied are the same as in Fig. 2.5.

In the case of positive Raman detuning (with initial preparation of the atom in the state $|1\rangle$), all the three ground states are populated at the end of the interaction: the population of the "bright" state $|b_2\rangle$ is transferred into state $|3\rangle$, and the population of the "dark" superposition $|b_1\rangle$ is left intact in the ground state (see Fig. 2.6(a)). The time evolution of the atomic (bare) energy-eigenstate $|3\rangle$ corresponds to the dynamics of the single dressed state ($|a_4\rangle$). Consequently, no oscillations occur in its time evolution. In contrary, the bare states $|1\rangle$ and $|2\rangle$ can be described as a superposition of the dressed states $|a_1\rangle$ and $|a_4\rangle$ with related nonequal eigenvalues (quasi-energies) λ_1 and λ_4. Due to this superposition of the dressed states, the time evolution of populations of the bare states has an oscillatory character (see Fig. 2.6(a)). It is important to note that, in both cases, the population of the excited state is negligible (and temporary), reaching merely 1-2% of the all atomic population.

The following expressions can be obtained from Eqs. (2.17) and (2.18) for the final values of the density matrix elements corresponding to the cases of the positive ($\delta_R > 0$) and negative ($\delta_R < 0$)

Raman detuning, respectively:

$$\delta_R > 0: \quad \rho_{00}^{\text{fin}} = 0, \quad \rho_{11}^{\text{fin}} = |W_1|^2 / W_{12}^2, \quad \rho_{22}^{\text{fin}} = |W_2|^2 / W_{12}^2, \quad \rho_{33}^{\text{fin}} = 0,$$
$$\rho_{12}^{\text{fin}} = (W_1 W_2^*) / W_{12}^2, \quad \rho_{13}^{\text{fin}} = 0, \quad \rho_{23}^{\text{fin}} = 0 \tag{2.19a}$$

$$\delta_R < 0: \quad \rho_{00}^{\text{fin}} = 0, \quad \rho_{11}^{\text{fin}} = |W_2|^4 / W_{12}^4, \quad \rho_{22}^{\text{fin}} = \left(|W_1|^2 |W_2|^2\right) / W_{12}^4, \quad \rho_{33}^{\text{fin}} = |W_1|^2 / W_{12}^2,$$
$$\rho_{12}^{\text{fin}} = \left(W_1 W_2^* |W_2|^2\right) / W_{12}^4, \quad \rho_{13}^{\text{fin}} = \left(W_1 W_3^* |W_2|^2\right) / \left(W_{12}^2 |W_3|^2\right),$$
$$\rho_{23}^{\text{fin}} = \left(W_2 W_3^* |W_1|^2\right) / \left(W_{12}^2 |W_3|^2\right). \tag{2.19b}$$

Dependence of the absolute value of the final coherence on the ratio of the peak Rabi frequencies of the pulses in Raman resonance is presented in Fig. 2.7 for both cases of positive and negative Raman detuning. The results show an excellent agreement of the predictions based on the dressed states analysis (solid lines) with results of the numerical simulation of the Eqs. (2.3) for the density matrix elements (the points).

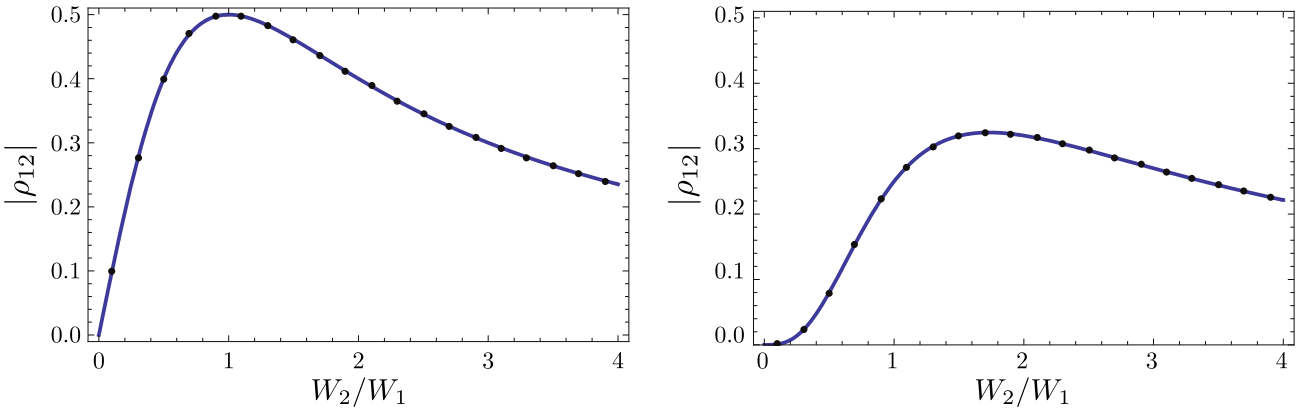

Figure 2.7: Resulting absolute values of the coherence ρ_{12} versus the ratio of the peak values of Rabi frequencies W_2/W_1 for the cases of a.) positive and b.) negative Raman detuning calculated from the dressed state analysis. The dots are the results of the numerical solution of the master equations, Eqs. (2.3), in the absence of relaxation processes. The following values of the parameters are used: $W_1 = 125\sqrt{2}\ [1/\tau_p]$, $W_3 = 137.5\sqrt{2}\ [1/\tau_p]$, $\beta = 1250\ \left[1/\tau_p^2\right]$, and W_2 is varying.

2.3.3 Creation and control of the coherent superposition states in Doppler-broadened media

The potential of schemes based on STIRAP to create coherent superposition states is limited in room temperature gases due to the Doppler-effect. We show in this subsection that using FC laser pulses in the proposed scheme allows one to create and control the coherent superposition states equally efficiently in homogeneously, as well as in Doppler- broadened media.

A Doppler-broadened medium of a gas of tripod-atoms is modeled by averaging the created coherence over distribution of the resonance frequencies of atoms in the gas at different values of temperature assuming all three FC laser pulses propagating in a same direction. Considering a gas of ^{87}Rb atoms at temperature T and assuming Maxwell-Boltzmann distribution for the velocities of the atoms, we have for the (normalized) probability distribution $P(\Delta)$ for an atom to have single-photon detuning Δ:

$$P(\Delta) = \sqrt{\frac{mc^2}{(2\pi)^3 kT\left(f_0\tau_p\right)^2}} \exp -\frac{mc^2\Delta^2}{8\pi^2 kT\left(f_0\tau_p\right)^2}, \tag{2.20}$$

where k is the Boltzmann constant, $m = 86.909$u is the mass of ^{87}Rb (u being the atomic unit) and $f_0 = 384.230\,\mathrm{THz}$ is the frequency distance between the excited and the ground states ($F = 1$ and $F' = 0$ hyperfine states in the D_2 line of ^{87}Rb), see Fig. 2.8.

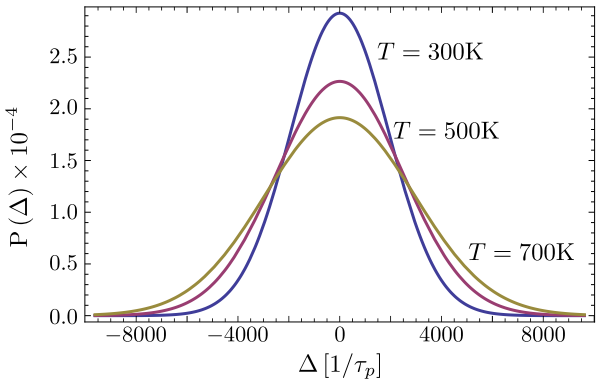

Figure 2.8: Probability distribution (normalized to unity) for atomic gas at temperatures equal to 300, 500 and 700 K.
H

The average values of the density matrix elements: populations and coherences $\langle\rho_{kl}\rangle$, $k, l \in$

$\{0, 1, 2, 3\}$ are calculated numerically. First the master equation (2.3) is solved numerically for the values of the detuning Δ corresponding to nonzero probability values (see Eq. (2.20) and Fig. 2.8) in order to obtain the density matrix elements ρ_{kl}^{fin} at the end of the interaction ($t \to \infty$). The resulting populations and induced coherences are presented in Fig. 2.9 as functions of the single-photon detuning (Doppler-shift) Δ. As it is seen from Fig.7, there is a range of values of the Doppler shift, where the final coherences (populations) are independent on Δ. This feature is due to the frequency modulation of the laser pulses: as long as the Doppler shift is smaller than the frequency range $[-5\beta\tau_p, 5\beta\tau_p]$ covered by the chirp during the interaction time (approximately equal to $5\beta\tau_p$), the velocity of motion of the atoms does not have an impact on the resulting population and coherence distribution.

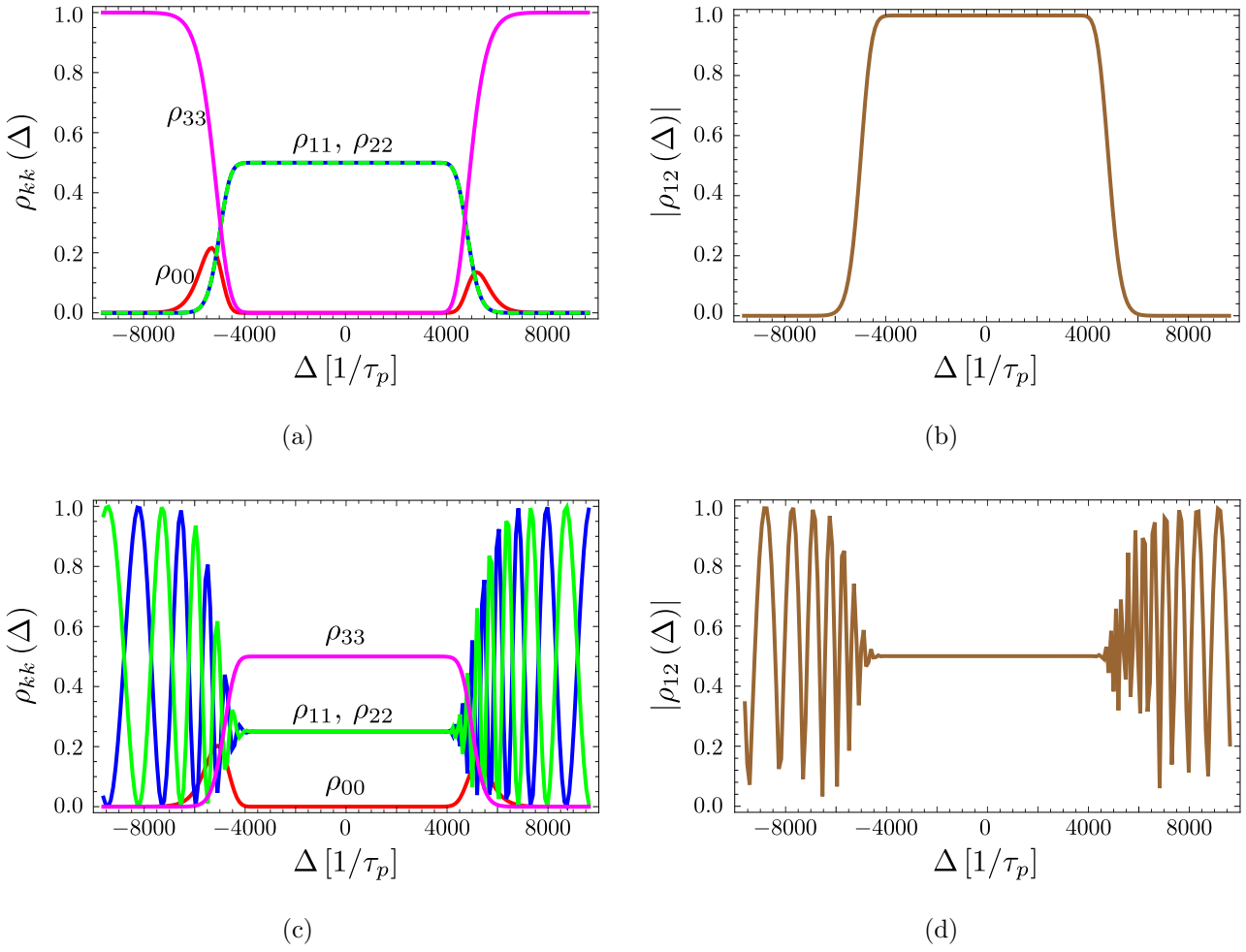

Figure 2.9: Final populations and coherences at the end of the interaction with the laser pulses as a function of the normalized single-photon detuning Δ for the cases of a.) and b.) positive Raman detuning and preparation in state $|3\rangle$ and c.) and d.) negative Raman detuning and preparation in state $|1\rangle$, respectively. The parameters used for calculation are $W_1 = W_2 = 125\sqrt{2}\ [1/\tau_p]$, $W_3 = 137.5\sqrt{2}\ [1/\tau_p]$, $\beta = 530\ [1/\tau_p^2]$, $\delta_R = 50\sqrt{2}\,[1/\tau_p]$, where $\tau_p = 1/\sqrt{2} \times 10^{-6}$s.

The averaging of the obtained solutions for the Doppler-broadened atomic gas is produced by numerically evaluating the integral

$$\langle \rho_{kl} \rangle = \int_{-\infty}^{\infty} P(\Delta)\, \rho_{kl}^{\mathrm{fin}}(\Delta)\, \mathrm{d}\Delta \tag{2.21}$$

The absolute value of the average induced coherence $|\langle \rho_{12} \rangle|$ established after the interaction with the laser field is presented in Fig. 2.10 as a function of the speed of chirp β of the laser pulses for different values of the gas temperature. As it can be seen from this figure, the average value of the induced coherence does not depend on the Doppler-broadening for sufficiently large frequency span of the pulses during the interaction time due to a sufficiently high speed of the frequency chirp.

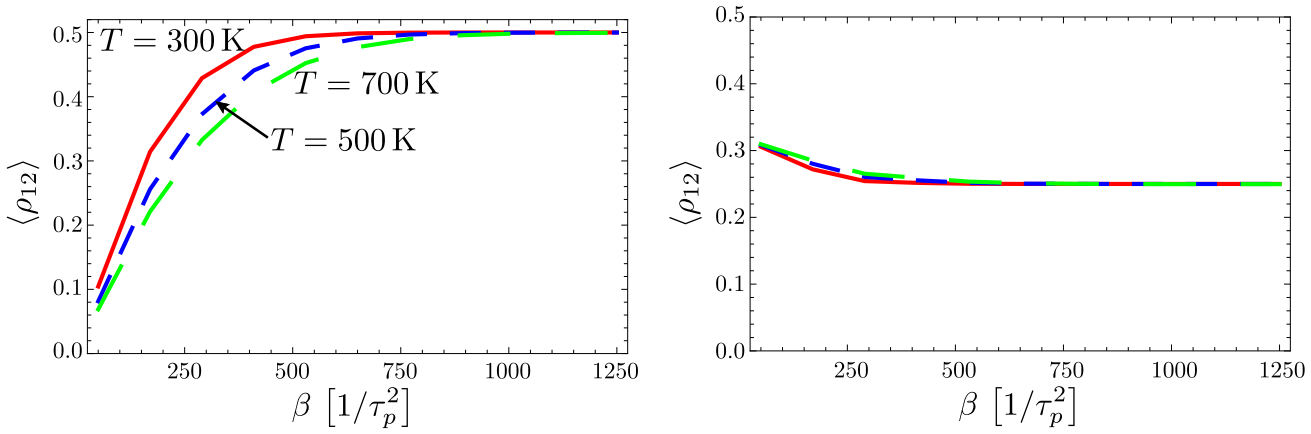

(a) (b)

Figure 2.10: Average value of the final coherence $\langle \rho_{12}^{\mathrm{fin}} \rangle$ between states $|1\rangle$ and $|2\rangle$ in the cases of a.) $\delta_R > 0$ and b.) $\delta_R < 0$ as a function of the speed of chirp for the temperatures of the gas equal to 300 (red), 500 (blue) and 700 K (green). The parameters used for calculation are the same as in Fig. 2.9

2.3.4 Effect of the relaxation processes

In this subsection, we discuss the influence of the relaxation processes on the coherent control mechanism described above. First, we analyze the effect of the spontaneous decay from the excited state. Here, we assume that the dephasing processes can be disregarded.

In Fig. 2.11, the final populations and the phase of the coherence established between states $|1\rangle$ and $|2\rangle$ after the interaction by the FC laser pulses are shown as a function of the longitudinal relaxation rate. One could anticipate a negligible influence of the spontaneous relaxation processes on the populations and coherences of the atom when no considerable excitation of the atom takes

place. However, the results of the numerical simulations show, that even for the negligible excitation of the atom, the final populations and induced coherences depend on the longitudinal relaxation rate. The reason is that the optical coherences ρ_{0k}, $k \in \{1,2,3\}$ are not negligibly small. It can be seen from Fig. 2.11 that, the larger the longitudinal relaxation rate (compared to the inverse duration of the laser pulse) is, the more the population transition process is shifted towards transferring the population into the dark superposition[1] of states $|1\rangle$ and $|2\rangle$ by the laser pulses in Raman resonance. Consequently, for larger relaxation rate, the atom ends up in the dark superposition in both cases of the positive and negative Raman detuning.

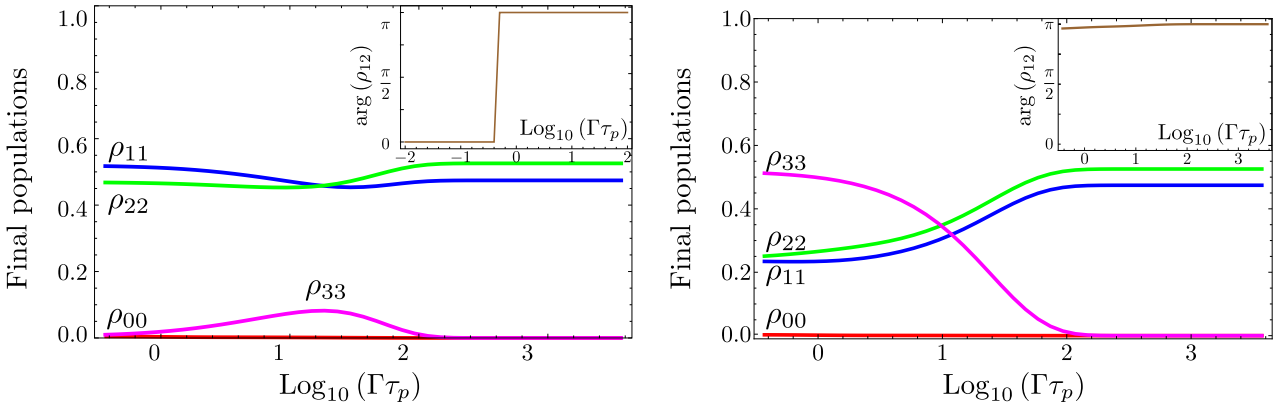

Figure 2.11: Final populations of the atomic states as a function of the product of the pulse length τ_p and the longitudinal relaxation rate Γ, in the case of a.) $\delta_R > 0$ and $\rho(t \to -\infty) = |3\rangle\langle 3|$ and b.) $\delta_R < 0$ and $\rho(t \to -\infty) = |1\rangle\langle 1|$, with neglecting the dephasing processes. Insets: the phase of the created coherence ρ_{12}, where $\arg(\rho_{12}) = 0$ corresponds to the bright, while $\arg(\rho_{12}) = \pi$ to the dark superposition of states $|1\rangle$ and $|2\rangle$. The parameters used for calculation are $W_1 = 250\sqrt{2}\ [1/\tau_p]$, $W_2 = 237.5\sqrt{2}\ [1/\tau_p]$, $W_3 = 262.5\sqrt{2}\ [1/\tau_p]$, $\beta = 1250\ \left[1/\tau_p^2\right]$ and $|\delta_R| = 125\ [1/\tau_p]$.

Since quantum interference processes are the basis for the above described coherence creation schemes, the phase relations between the probability amplitudes of the states (the values and the phases of the corresponding coherences) must play an important role in the considered processes. That is why a strong effect of the transverse relaxation (dephasing) processes may be anticipated on the creation and control of coherent superposition states as well as on the population transfer between the atomic states. The final populations of the atomic states as a function of the dephasing rate γ are presented in Fig. 2.12 as a result of numerical simulation of the master equation, Eq. (2.3). It can be seen from the behavior of the populations that the effect of the dephasing begins to be

[1]It follows from Eq. (2.5) that $\arg\rho_{12} = \pi$ corresponds to the dark, while $\arg\rho_{12} = 0$ to the bright superpositions $|b_1\rangle$ and $|b_2\rangle$, respectively.

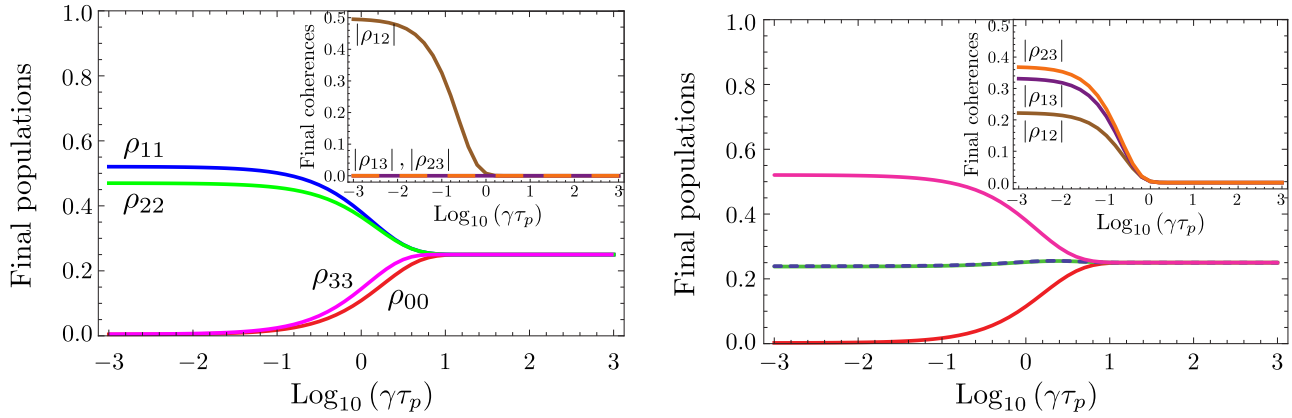

(a) (b)

Figure 2.12: Final populations of the atomic states as a function of the product of the pulse length τ_p and the transverse relaxation rate γ, in the case of a.) $\delta_R > 0$ and $\rho(t \to -\infty) = |3\rangle\langle 3|$ and b.) $\delta_R < 0$ and $\rho(t \to -\infty) = |1\rangle\langle 1|$, assuming no longitudinal relaxation. Insets: the absolute values of the coherences between the ground states. The parameters used for calculation are the same as in case of Fig. 2.11

imperative at $\tau_p\gamma = 10^{-1/2}$. This is true for both cases of positive and negative Raman detuning. If the interacting pulses are longer (compared to the inverse dephasing rate γ^{-1}), the adiabatic transfer process is destroyed by the dephasing. In this case, the interaction results in equally populated ground states without any coherence among them (see Insets in Fig. 2.12).

2.3.5 Robustness of the process

Let us now discuss robustness of the proposed scheme of creation of superposition states against variation of the main parameters of the laser radiation. As it follows from Fig. 2.7 and Eqs. (2.19a) and (2.19b), the absolute value of the created coherence $|\rho_{12}|$ depends on the ratio of the peak Rabi frequencies of the laser pulses in Raman resonance and does not depend on the phase relations between the laser pulses. In both considered cases ($\delta_R > 0$ and $\rho(t \to -\infty) = |3\rangle\langle 3|$, $\delta_R < 0$ and $\rho(t \to -\infty) = |1\rangle\langle 1|$), one can control the induced coherence for example, by varying the intensity of one of the laser pulses in Raman resonance leaving fixed the intensity of the second pulse. Note, that the induced coherence is robust against changes in the intensity of the laser pulse out of Raman resonance as long as these changes do not violate the adiabaticity conditions, (see Eq. (1.76)).

Robustness of the scheme against variations of the parameters of the pulses in Raman resonance

may be provided utilizing laser pulses from the same source. In this case, with the variation δW of the peak Rabi frequencies of the pulses, the variation of the ratio of the two peak Rabi frequencies may be estimated as

$$\delta\left(W_1/W_2\right) \approx W_1/W_2\left[1+\delta W\left(W_2-W_1\right)/\left(W_1W_2\right)\right]. \tag{2.22}$$

As it follows from this relation, the dependence of the variation $\delta\left(W_1/W_2\right)$ on the parameter δW is weak and hence, the robustness of the process is especially high in the case of close values of the peak Rabi frequencies of the pulses in Raman resonance: $W_1 \approx W_2$. In this case, the maximum value of the induced coherence $|\rho_{12}|$ equal to 0.5 is achieved for the negative Raman detuning (see Fig. 2.7). Note that the considered schemes are also extremely robust against variations of the speed of the chirp, as is usually the case for adiabatic processes.

2.4 Phase information mapping in the populations of the atomic states

In this section we suppose that the tripod-atom is initially prepared in a coherent superposition of the ground states coupled by the pulses in Raman resonance. Note that this preparation can be realized for example by applying the above described scheme with negative Raman detuning (δ_R). Our aim is to show that this scheme may be applied to map optical information into the ground states of the atom.

2.4.1 Dynamics of the populations of the atomic states

We analyze the interaction scheme in case of negative Raman detuning ($\delta_R < 0$) and we assume that the atom is prepared in a superposition of states $|1\rangle$ and $|2\rangle$, namely

$$|\psi\left(t\to-\infty\right)\rangle = \frac{\alpha_1|1\rangle+\alpha_2|2\rangle}{\sqrt{2}} = e^{-i\Delta t}\left[\frac{W_2\alpha_1+W_1\alpha_2}{W_{12}}|b_1\rangle+\frac{-W_1^*\alpha_1+W_2^*\alpha_2}{W_{12}}|b_2\rangle\right]. \tag{2.23}$$

We have seen in subsection 2.2.1 that this initial condition results in such a dynamics of the system which allows only negligible excitation, provided the condition given in Eq. (2.13) is fulfilled. This

is because, on one hand, state $|b_1\rangle$ remains unaffected by the interaction and, on the other hand, state $|b_2\rangle$ is adiabatically transferred into state $|b_3\rangle$ with an additional π phase factor, by following the time evolution of adiabatic eigenstate $|a_4\rangle$ (see Fig 2.3(b) and the successive argument). Thus, the state of the system established by the interaction is given by

$$|\psi\left(t\to-\infty\right)\rangle = e^{-i\Delta t}\left[\frac{W_2\alpha_1+W_1\alpha_2}{W_{12}}|b_1\rangle - \frac{-W_1^*\alpha_1+W_2^*\alpha_2}{W_{12}}|b_3\rangle\right]$$
$$= \frac{W_2^*\left(W_2\alpha_1+W_1^*\alpha_2\right)}{W_{12}^2}|1\rangle + \frac{W_1^*\left(W_2\alpha_1+W_1^*\alpha_2\right)}{W_{12}^2}|2\rangle + \frac{W_3\left(W_1\alpha_1-W_2^*\alpha_2\right)}{W_{12}\left|W_3\right|}|3\rangle. \quad (2.24)$$

Note that the $\delta_R<0$ case of the coherence creation problem discussed in section 2.3 is a special case the present one with $\alpha_1=1$ and $\alpha_2=0$. Accordingly, Eq. (2.18) can be obtained from Eq. (2.24) using this substitution.

From Eq. (2.24), the following expressions follow for the final populations of atomic states:

$$\rho_{00}^{fin}=0,\ \ \rho_{11}^{fin}=\frac{\left|W_2\right|^2}{W_{12}^2}Q^-,\ \ \rho_{22}^{fin}=\frac{\left|W_1\right|^2}{W_{12}^2}Q^-,\ \ \rho_{33}^{fin}=Q^+,\ \text{ where}$$
$$Q^{\pm}=\left[\left|\alpha_2\right|^2\left|W_1\right|^2+\left|\alpha_1\right|^2\left|W_2\right|^2\pm 2\left|\alpha_1\right|\left|\alpha_2\right|\left|W_1\right|\left|W_2\right|\cos\left(\varphi-\phi\right)\right]/W_{12}^2. \quad (2.25)$$

Here we introduced the relative phase $\varphi=\varphi_2^{(0)}-\varphi_1^{(0)}$ of the peak Rabi frequencies W_1 and W_2, and ϕ is the difference between the complex phases of the probability amplitudes α_1 and α_2.

In Fig. 2.13 the time evolution of the populations ρ_{kk} of the atomic states are presented for three different values of the relative phase φ, calculated numerically from the master equation (2.3), assuming the relaxation processes in the system can be disregarded. This is a good approach if the interaction time is shorter than any relaxation time including the spontaneous decay from the excited state and the coherence relaxation time. The numerical results confirm well the predictions of the adiabatic theorem: the dynamics of the populations show a significantly different behavior depending on the relative phase φ, when the other interaction parameters are the same.

We further make use of this sensitivity for designing an optical information mapping procedure. Another important feature of the interaction is that there is a negligible (and only temporary) excitation of the atom during the interaction, which is important to avoid decoherence due to spontaneous decay. We show later (in subsection 2.4.3) that the mapping process is indeed possible for moderate relaxation rates.

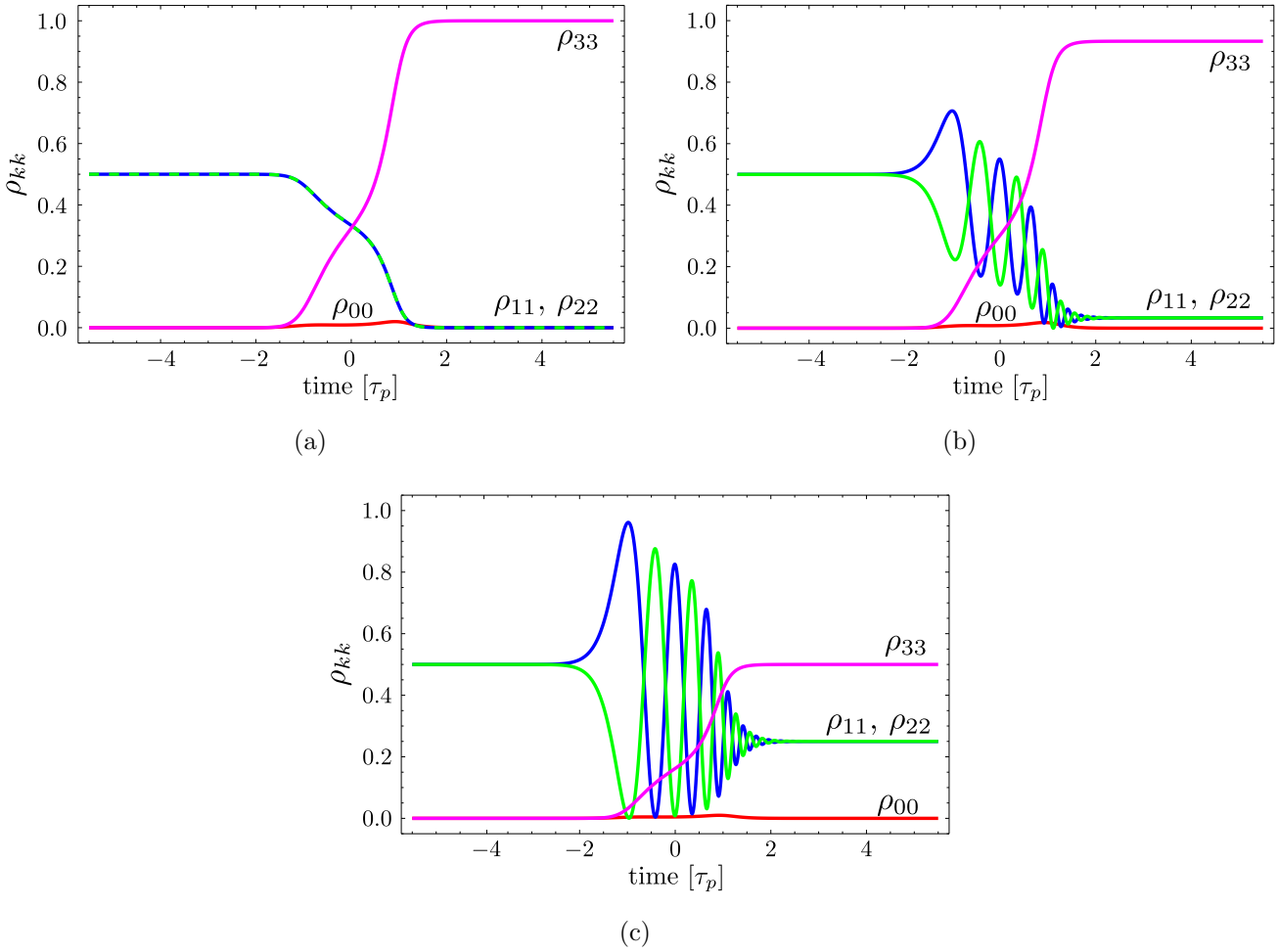

Figure 2.13: Dynamics of the atomic populations for three different values of the relative phase of the Rabi frequencies of the pulses in Raman resonance: a.) $\varphi = 0$, b.) $\varphi = \pi/6$, c.) $\varphi = \pi/2$ in the absence of relaxational processes. The following parameters were used for calculation: $|W_1| = |W_2| = 50\ [1/\tau_p]$, $W_3 = 100\ [1/\tau_p]$, $\beta = 150\ \left[1/\tau_p^2\right]$, $\Delta = 0$, $\delta_R = -25$, $\alpha_1 = \alpha_2 = 1/\sqrt{2}$.

2.4.2 Writing and storage of the phase information in the populations of the atomic states

The dependence of the final populations of the ground states on the phase difference φ of the Rabi frequencies Ω_1 and Ω_2 is presented in Fig 2.14. Here, the master equation (2.3) was numerically solved without any relaxation processes and the populations $\rho_{kk}^{\text{fin}} = \rho_{kk}\,(t \to \infty)$ established by the interaction were calculated for the relative phase φ varying between 0 and 2π in 36 steps.

We chose $\rho\,(t \to -\infty) = 1/2\,(|1\rangle + |2\rangle)\,(\langle 1| + \langle 2|)$ ($\alpha_1 = \alpha_2 = 1/\sqrt{2}$, $\phi = 0$) as initial state of the atom and $|W_1| = |W_2|$. According to the prediction of the adiabatic approximation (see (2.25)),

these conditions maximize the contrast of the phase mapping, which may be defined as

$$\mathcal{C} = \frac{\max_\varphi \rho_{33}^{\text{fin}} - \min_\varphi \rho_{33}^{\text{fin}}}{\max_\varphi \rho_{33}^{\text{fin}} + \min_\varphi \rho_{33}^{\text{fin}}}, \tag{2.26}$$

since

$$\mathcal{Q}^{\pm}(\varphi, \phi) \equiv Q^{\pm}\big|_{\alpha_1=\alpha_2=1/\sqrt{2},|W_1|=|W_2|} = \frac{1}{2}\left[1 \pm \cos(\varphi - \phi)\right] \tag{2.27}$$

changes between 0 and 1 as a function of φ, which means that $\rho_{33}^{\text{fin}}(\varphi)$ reaches its possible extreme values. Fig. 2.13 makes obvious the excellent agreement of the numerical calculations with the results

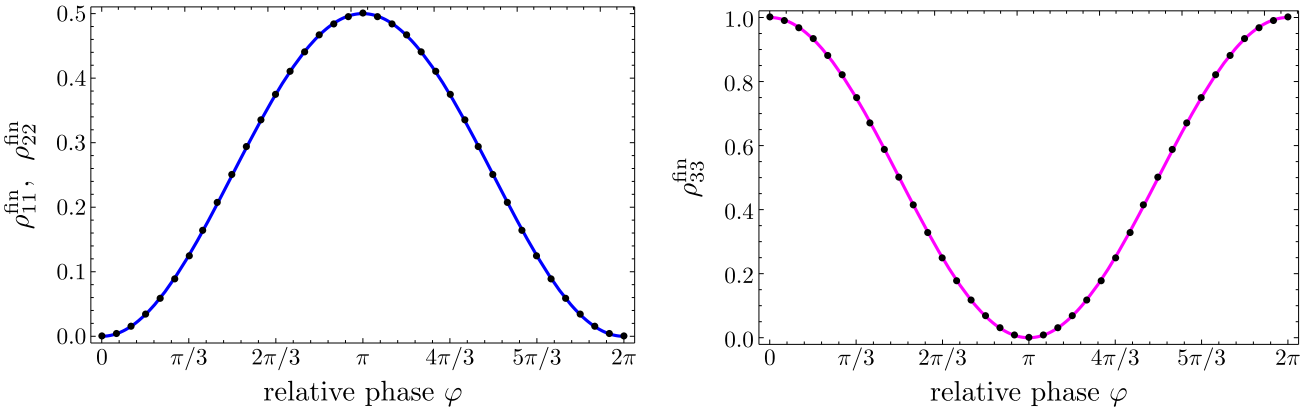

(a) (b)

Figure 2.14: Dependence of the final populations of the states (points) on the relative phase of the laser pulses in Raman resonance with fitting curve (solid line) $q^{\pm}(\varphi)$ (see (2.28)). The parameters applied for calculations are the same as in case of Fig. 2.13, the fitting parameters are a.) $A = 0.5$, $b = 0$ and b.) $A = 1$, $b = 0$.

of the investigations based on the adiabatic theorem. Namely, the fitting function

$$q^{\pm}(\varphi) = A\mathcal{Q}^{\pm} + b \tag{2.28}$$

expressing the dependence of the final populations on the relative phase, deducted from the dressed states analysis fits very well on the points resulting from numerical simulation

Because the information is written in the populations of the ground states without considerable excitation of the atom, its storage time is scaled by the lifetime of the ground states. It substantially exceeds the transverse relaxation times limiting the information storage time of EIT-based schemes.

The proposed method is applicable best to store the transverse distribution of the phase (transverse phase images). The information has to be coded in the transverse phase distribution of one of the laser beams among the two in Raman resonance with the atom. The second laser beam, in Raman resonance with the first one, has to have a homogeneous phase front.

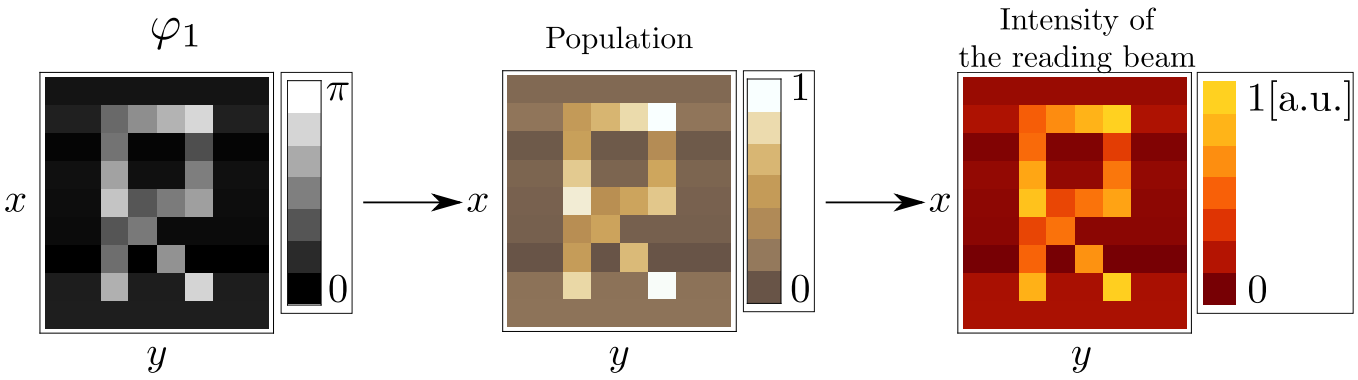

Figure 2.15: Schematic of the phase information writing in and reading out from the populations of the atomic states. The phase information mapped in the transverse distribution of the population of the metastable state $|3\rangle$ is transferred into the transverse distribution of the intensity of the reading pulse.

An additional laser pulse with homogeneous transverse distribution of the intensity will be used as a reading laser. This pulse will measure the population of a metastable state after the information writing process by transferring it to the excited state. The transverse phase information stored in the transverse distribution of the atomic state population will be transformed into the transverse distribution of the intensity of the reading pulse: The more the population of a given state of an atom at a given transverse position, the more will be the absorption of the reading beam at this transverse point, see Fig. 2.15.

To make the reading process more effective one may use a frequency chirped reading laser pulse transferring nearly all the population of the metastable state into the excited state. To store the information for further reading, one can apply another (restoring) laser pulse similar to the reading one that transfers the population of the excited state back into the metastable state previously used for the storage.

2.4.3 Impact of the relaxation processes on the information mapping process

In order to analyze the impact of the relaxation processes on the optical phase information writing, we solved the master equation (2.3) numerically with the same initial condition ($\rho(t \to -\infty) = 1/2\,(|1\rangle + |2\rangle)\,(\langle 1| + \langle 2|)$) as was used in the previous subsection. The effect of the longitudinal relaxation and dephasing processes were investigated separately. In both cases, the 36-step calculation determining the phase-dependence of the final populations was performed, for each value of the longitudinal relaxation and dephasing rate, between 10^{-3} $[1/\tau_p]$ and 10^{3} $[1/\tau_p]$ in 20 (logarithmic) steps, respectively.

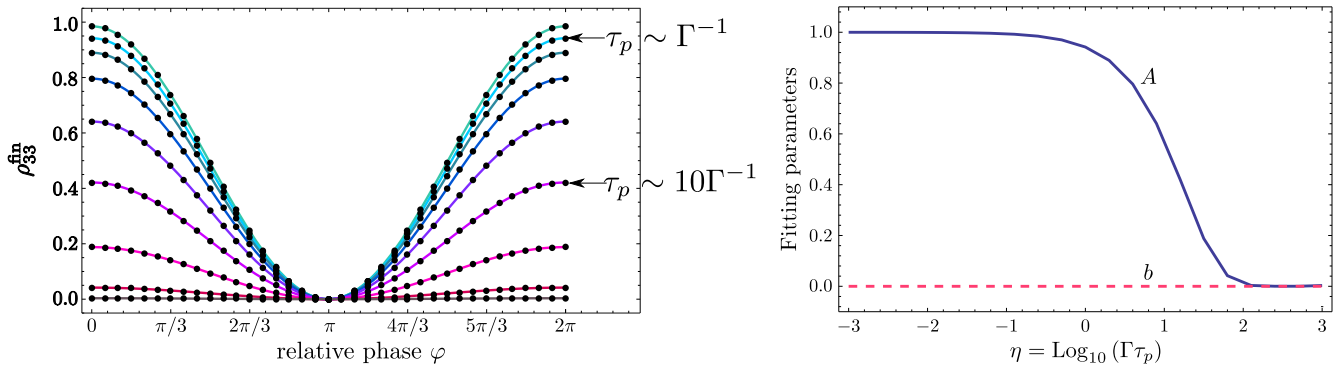

(a) (b)

Figure 2.16: a.) Dependence of the final population of state $|3\rangle$ on the relative phase φ of Ω_1 and Ω_2 for different values of the logarithm of the product of the longitudinal relaxation rate and the interaction length ($\eta = \log_{10}(\Gamma\tau_p)$). The dots are results of numerical integration of Eq. (2.3), the solid lines are fitting curves with the function $q^+(\varphi)$ given in (2.28). b.) Fitting parameters A and b for different values of η.

As Figs. 2.16 and 2.17 show, the same function $q^+(\varphi)$ (cf. Eq. (2.28)) characterizes the dependence of the final population $\rho_{33}^{\rm fin}$ on the relative phase φ as the one predicted by the adiabatic approximation. The effect of the relaxation processes (both longitudinal relaxation and dephasing) manifest themselves in the contrast (2.26) of the writing process which is a simple function of the fitting parameters A and b (see Figs. 2.16(b) and 2.17(b)):

$$\mathcal{C} = \frac{A}{A + 2b}. \tag{2.29}$$

Comparing Figs. 2.16(b) and 2.17(b) with Figs. 2.11 and 2.12, it turns out that the relaxation

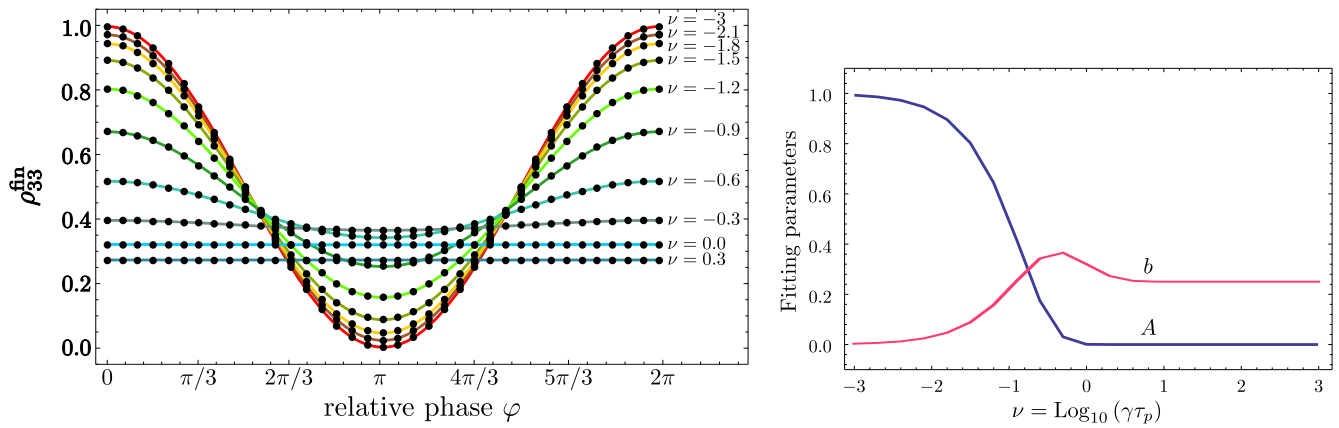

(a) (b)

Figure 2.17: a.) Dependence of the final population of state $|3\rangle$ on the relative phase φ of the pulses in Raman resonance for different values of the logarithm of the dephasing rate and the interaction length ($\nu = \log_{10}(\gamma\tau_p)$). The dots are results of numerical integration of Eq. (2.3), the solid lines are fitting curves with the function $q^{+}(\varphi)$ given in (2.28). b.) Fitting parameters A and b for different values of ν.

processes affect the coherence creation and the phase mapping mechanisms basically the same way. More specifically, the contrast of the mapping starts to significantly decrease for $\Gamma\tau_p \approx 10^{1/2}$ in case of longitudinal relaxation and for $\gamma\tau_p \approx 10^{-1/2}$ for dephasing. Consequently, the mapping has to be established faster than the typical rate of the latter processes, which is not very surprising since the basis of the mechanism is quantum interference.

On the other hand, we can see that the mapping is not too sensitive on the spontaneous decay from the excited state: even for laser pulses ten times longer than the lifetime of the excited state a noticable contrast can be achieved. Note that since the information is mapped in the ground states, the longitudinal relaxation from the excited state only affects the writing process, the storage time is only limited by the lifetime of the ground states.

2.5 Summary

In this chapter, we have analyzed the system of a tripod atom interacting with three FC laser pulses. Each atomic transition is driven by a separate pulse, two of them in Raman resonance, the third one detuned from it. By studying the adiabatic states, we have shown that both for positive and negative values of the Raman detuning, certain population redistribution processes are possible among the ground states without significant excitation of the atom. Namely, there are two eigenstates

of the interacting system which have (for suitable parameters) only a negligible projection onto the excited state. By initially preparing the atom in different states in the subspace spanned by the two mentioned states, several control tasks can be achieved. In this chapter two substantially different arrangements are presented.

First, we have presented an interaction scheme suitable for creating a superposition among two or three ground states. After being prepared in one of the ground states, the atomic population has been shown to be transferred to a coherent superposition. We have shown by studying the adiabatic eigenstates and by performing numerical calculations as well that the composition of the created superposition is controllable by the peak intensities of the laser pulses in Raman resonance. We have also analyzed the applicability of the scheme in a Doppler-broadened medium of a gas composed of tripod-atoms by averaging the induced coherence over the velocity distribution of the atoms in the gas at different temperatures. The results indicate that the scheme is effective even for relatively large widths of the Doppler-broadened transition lines if the frequency span of the laser pulses due to the chirp exceeds the width of the Doppler-broadening.

The influence of relaxation processes on the population transfer mechanism was also analyzed by numerical simulation of the master equation. Based on our results we can state that the considered scheme allows minimizing the effect of the spontaneous decay by suppression of the population of the excited state. However, even under the condition of negligible excitation of the atom, for longer laser pulses, the longitudinal relaxation may influence the induced coherences and the resulting population distribution among the ground states. For laser pulses longer that the decay time of the excited state, optical pumping of the atom by a pair of the pulses in Raman resonance results in the accumulation of the atomic population in a dark superposition of the ground states linked by the laser pulses in Raman resonance. Note that the influence of the spontaneous decay may be minimized by increasing the speed of the population transfer.

The transverse relaxation (dephasing) also forces restriction on the method: The numerical simulation of the master equation has shown that transverse relaxation processes destroy the adiabatic transfers already when the duration of the laser pulses is close to the dephasing time of the medium. At larger transverse relaxation rates or longer laser pulses, all the states are equally populated as a result of the interaction and no coherent superposition states are created. While the detrimental effect of transverse relaxation may be avoided by utilizing sufficiently short laser pulses, this effect

may also be diminished by increasing the chirp speed of the FC pulses.

In the other interaction scheme investigated in this chapter it has been assumed that the atom was initially prepared in an equal superposition of the two ground states. This initial condition may be realized, for example, by using the first interaction scheme presented here. We have shown that the population distribution established by the interaction depends on the difference of the phases of the pulses in Raman resonance. This property make this scheme suitable for phase information writing (mapping) in populations of the ground states. Measuring the population of a meta-stable state by frequency chirped laser would restore the phase information. The transverse phase image will be then transformed into the transverse intensity modulation of the reading laser beam. Note that the information reading process is analogous to measuring the created coherent superposition [120, 121].

The main advantage of the method is its long information storage time. This time scales by the lifetime of the atomic metastable states instead of the transverse relaxation time of the atomic coherences in the case of the EIT- based methods. There is a negligible temporary excitation of the atom during the information writing providing immunity of the method to the decoherence processes through decay of the excited state.

Note that both schemes considered above provide the possibility of preparing atoms in coherent superpositions of the ground states, which can be easily modified by external parameters. Thus, they may find practical applications in nonlinear optics, since the preparation of the atoms in coherent superposition states may result in extreme changes in the optical (refractive and absorption) properties of a medium composed of them via quantum interference.

Chapter 3

Coherent control using a combination of a FC and constant-frequency laser pulses

In this chapter, we analyze the population redistribution induced in a Λ-atom by two laser pulses. One of them has constant carrier frequency, while the other pulse is frequency chirped in such a way that it sweeps through two-photon resonance. We analyze this interaction in two limiting cases, resulting in substantially different passage mechanisms.

In the first case, the pulse with constant carrier frequency is exactly resonant with one of the atomic transitions, so that the FC pulse sweeps through both the one-photon and the two-photon resonances. This scheme resembles the well-known EIT-configuration (see e.g. [38] and the included references) in the sense that one of the atomic ground states is coupled to the excited state by a strong resonant field, which creates two dressed states from them [122]. This pair of dressed state has been shown to be equivalent to a pair of closely spaced lifetime-broadened resonances [123] (Autler-Townes doublet), which are superpositions of the coupled atomic states. However, the scheme analyzed here differs from the one of EIT in the point that the other dipole-allowed transition in the lambda-atom is driven by a strong frequency-chirped laser pulse instead of a weak probe wave with constant carrier frequency.

On the other hand, it has been demonstrated in [68], that in an atom having two excited states close to each other, selective population inversion can be induced by a FC pulse. Namely, the population of the atom, initially prepared in the ground state, is transferred into the excited state which the driving pulse first become resonant with.

Based on these, we anticipate that the interaction of a lambda-atom with the constant-frequency and the FC pulse may result in creation of a coherent superposition between the excited state and one of the ground states. Note that robust preparation of coherence between the ground and excited state have a great importance in high-order harmonic generation and multi-photon ionization in gases [24, 26, 28, 29, 86–89, 124].

In the second case we investigate, the carrier frequency of the non-modulated pulse is far-detuned from resonance. Namely, its detuning from the atomic resonance is much larger than the Rabi frequency of the pulse and also the frequency range covered by the other, FC pulse.

The effect of a far-detuned pulse pair (a strong coupling and a weak probe) having constant carrier frequencies close to two-photon resonance in Λ-atoms has been already investigated [125, 126]. In these works, it was proven that the probability of the excitation of the atom is negligible due to the large one-photon detuning and thus the system could be approximated by a two-state atom through eliminating the excited state. In [126], the lambda-model was shown to be well applicable for ^{85}Rb and ^{87}Rb atoms. Although, since the one-photon detuning was larger than the separation of the excited states, effective far-detuned dipole moments were needed to be introduced.

Here, we examine the possibility of using the approximation described above if we exchange the probe field having constant frequency for a stronger, frequency-modulated one. We also consider to apply this far-detuned coupling scheme for population transfer between two specific magnetic sublevels of a ground state[1] of the ^{87}Rb atom, using circularly polarized pulses. Our aim is to create coherent superposition among the ground states without significantly populating any of the excited states.

3.1 Interaction of a Λ-atom with a FC and a constant-frequency pulse

In this chapter we analyze the interaction of a single atom at a fixed location with a pair of laser pulses, one with chirped frequency and the other one having constant carrier frequency. The time

[1] $F = 1$ hyperfine level of state $5^2S_{1/2}$, see Fig. 3.5.

dependence of the electric field strength of the laser field is given as

$$\vec{E}(t) = \{\vec{\epsilon}_1 \mathcal{E}_1(t) \exp[-i(\omega_1 t + \varphi(t))] + \vec{\epsilon}_2 \mathcal{E}_2(t) \exp[-i\omega_2 t]\} + \text{c.c.}, \tag{3.1}$$

where $\vec{\epsilon}_k$ is the polarization, ω_k is the central frequency, $\mathcal{E}_k(t)$ is the slowly varying envelope function of the k^{th} laser pulse (having a constant complex phase) and $\varphi(t)$ is the time dependent phase due to the frequency modulation.

These laser pulses act on an atom having Λ-type linkages: each of them couples a (meta-stable) ground state $|g_k\rangle$ to the excited state(s) of the atom. We consider two limiting cases with respect to the frequencies of the interacting pulses compared to the atomic transition frequencies. In the first one (Fig 3.1(a)), the laser pulse having constant frequency ω_2 is on resonance with the transition from one of the ground states to one of the excited state ($|e\rangle$). Meanwhile, the frequency of the other pulse is swept through two-photon resonance. The frequency-range covered by the frequency-modulation is small enough that the FC pulse stays far from being resonant with any other atomic transitions. Therefore, it is enough to take into account only one excited state (for more detailed discussion, see subsec. 1.1.1). In the second case, however, the constant frequency pulse is tuned

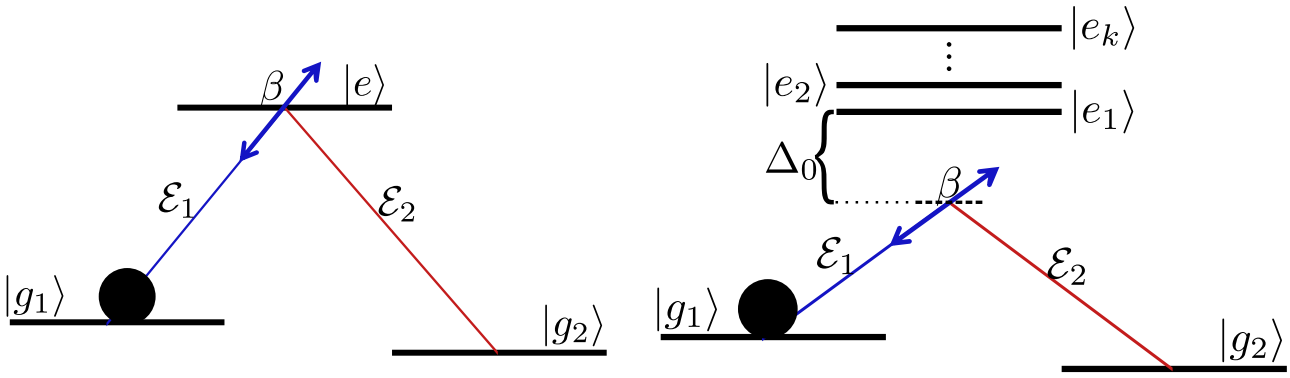

Figure 3.1: Interaction schemes including a pair of laser pulses having chirped and a constant carrier frequencies in case of a.) resonant b.) far-detuned coupling

significantly below the atomic transitions ("far-detuned" case, Fig 3.1(b)) and the frequency of the other pulse is chirped in such a way that it becomes two-photon resonant, but remains far from one-photon resonance during the interaction time. Since there is not one excited state selected by resonant driving, several excited states have to be taken into account in the coupling scheme.

In both cases, we assume that the atom is initially prepared in the ground state coupled by the frequency-modulated pulse ($|g_1\rangle$ with the notations of Fig. 3.1). It is also assumed in both situations that the atom-laser interaction takes place in a timescale which is significantly shorter than the lifetimes of the states. Thus, we disregard the decay processes and we describe the time evolution of the system by the Schrödinger-equation.

3.2 Coherence creation between the excited and one of the ground states (case of resonant driving)

In this section, we investigate the interaction of the atom with the laser pulses for the case when the pulse with constant carrier frequency ω_2 is in resonance with the transition $|g_2\rangle \rightarrow |e\rangle$.

3.2.1 Mathematical formalism

For describing the atomic states, we use the rotational basis introduced in Eq. (1.23), which incorporates the time-dependent phases

$$\varphi_1\left(\vec{x}_0, t\right) = \beta t^2/2 \qquad \varphi_2\left(\vec{x}_0, t\right) = 0, \tag{3.2}$$

where $\vec{x}_0$ is the location of the atom, assumed to be an arbitrary, fixed value. We assume here a linear chirp with a rate of β. Using this rotational basis, the interaction Hamiltonian is given by

$$\hat{\mathcal{H}}_{\mathrm{res}} = -\hbar \left\{ -\beta t |g_1\rangle\langle g_1| + \frac{1}{2}\left[|e\rangle\left(\Omega_1\langle g_1| + \Omega_2\langle g_2|\right) + \mathrm{H.c.}\right] \right\}. \tag{3.3}$$

Here $\Omega_k = \vartheta_k \exp\left(-i\varphi_k^{(0)}\right)$ is the Rabi frequency belonging to the k^{th} pulse (cf. Eq. (1.28)), with slowly changing absolute value and constant complex phase.

Coordinate transformation: symmetric-antisymmetric basis

It is convenient for our considerations to introduce the following set of basis states which contains a symmetric and an antisymmetric superposition of the excited state $|e\rangle$ and the ground state $|g_2\rangle$,

which is coupled to the excited state by the constant-frequency laser field:

$$\{|b_1\rangle, |b_s\rangle, |b_a\rangle\} = \left\{ e^{-i\varphi_1^{(0)}}|g_1\rangle, \frac{|e\rangle + e^{-i\varphi_2^{(0)}}|g_2\rangle}{\sqrt{2}}, \frac{|e\rangle - e^{-i\varphi_2^{(0)}}|g_2\rangle}{\sqrt{2}} \right\}, \tag{3.4}$$

where $-\varphi_k^0$ is the complex phase of the Rabi frequency Ω_k. The Hamiltonian $\hat{\mathcal{H}}_{\text{res}}$ in this coordinate system reads as

$$\hat{\mathcal{H}}_{\text{res}}^{sa} = -\hbar \left\{ -\beta t|b_1\rangle\langle b_1| + \frac{|\Omega_2|}{2}\left(|b_s\rangle\langle b_s| - |b_a\rangle\langle b_a|\right) + \frac{1}{2}\left[\frac{|\Omega_1|}{\sqrt{2}}\left(|b_s\rangle + |b_a\rangle\right)\langle b_1|\right] + \text{H.c.} \right\}. \tag{3.5}$$

3.2.2 The results of the numerical calculations

We proceed with numerical solution of the Schrödinger equation

$$i\hbar\partial_t|\psi\rangle = \hat{\mathcal{H}}_{\text{res}}|\psi\rangle \tag{3.6}$$

for the state vector $|\psi\rangle = c_0|e\rangle + c_1|g_1\rangle + c_2|g_2\rangle$ with the Hamiltonian $\hat{\mathcal{H}}_{\text{res}}$ given in Eq. (3.3). We assume the same Gaussian envelopes of the laser pulses:

$$\Omega_{1,2}(t) = \Omega_{1,2}^{(0)} f(t) \quad \text{with} \quad f(t) = \exp\left[-t^2/2\right], \tag{3.7}$$

where the time is measured in the units of $\tau_p = \tau_L/\left(2\sqrt{\ln 2}\right)$ with τ_L being the full width at half maximum and $\Omega_{12}^{(0)}$ being the peak amplitudes of the pulses. The population of the bare states of the atom and the absolute value of the created coherence in the field of the pair of the laser pulses is presented in Fig. 3.2. As it is seen from Fig. 3.2(b), a maximum value of coherence of 0.5 is created as a result of the interaction.

In Fig. 3.3, the final absolute value of the coherence between the initially empty ground state $|g_2\rangle$ and excited state $|e\rangle$ is shown by a color map versus the chirp rate and the proportion of the peak Rabi frequencies. As it can be seen from this Figure, the value of the created coherence is extremely robust against variation of these parameters. Note that both of these parameters are given in logarithmic scale.

For efficient coherent enhancement of processes such as multi-photon ionization or high-order

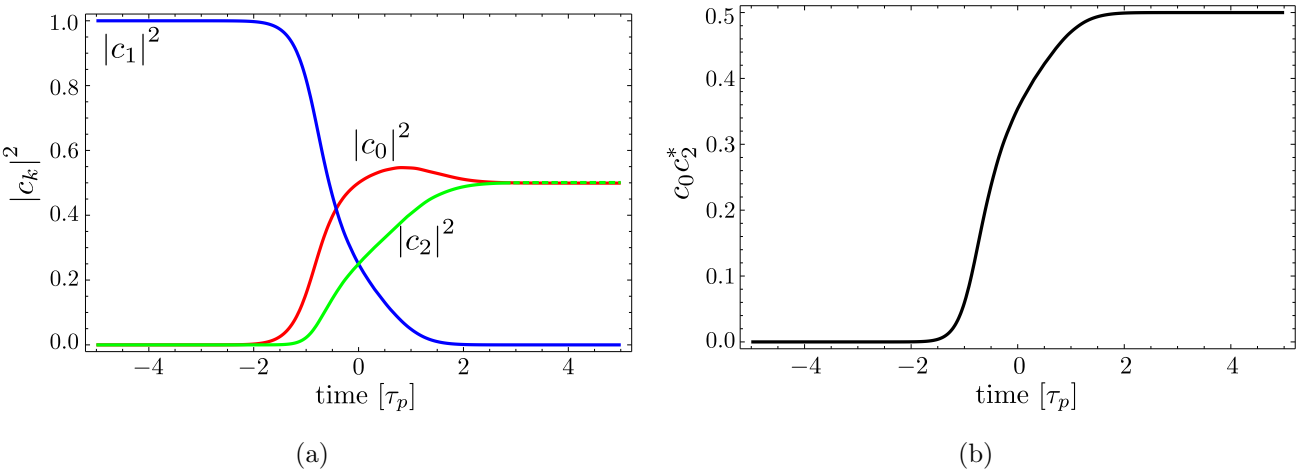

(a) (b)

Figure 3.2: a.) Dynamics of the states' populations in the laser field and b.) absolute value of the coherence created between the states $|e\rangle$ and $|g_2\rangle$. Parameters applied are: the peak Rabi frequencies $\Omega_1^{(0)} = \Omega_2^{(0)} = 30\,[1/\tau_p]$, linear chirp rate $\beta = 20\,[1/\tau_p^2]$, and duration of the pulses $\tau_p = 1.5\,\mathrm{ns}$.

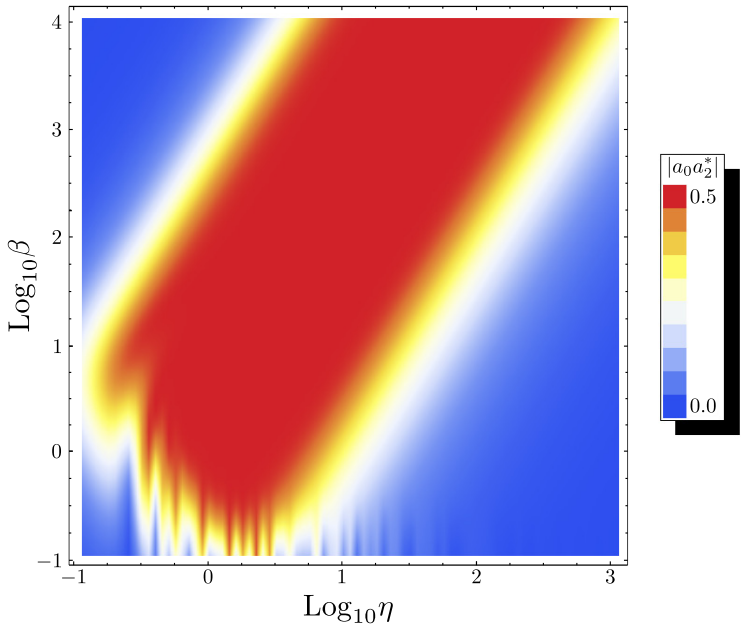

Figure 3.3: Color plot of the absolute value of the created coherence versus the speed of the chirp β and the peak Rabi frequency $\Omega_2^{(0)}$ of the laser pulse with constant carrier frequency (in logarithmic scale): $\Omega_2^{(0)} = \eta\Omega_1^{(0)}$ with a fixed value of the peak Rabi frequency of the chirped laser pulse $\Omega_1^{(0)} = 45\,[1/\tau_p]$. Other parameters applied are: $\tau_p = 3\,\mathrm{ns}$.

harmonic generation, one has to create coherent superpositional states with the same (arbitrary) phase of the coherence in all atoms of the ensemble. Provided that the interaction takes place in the adiabatic regime (cf. Sec. 1.3), the scheme under consideration allows robust creation of coherence with a phase that does not depend on the shape, duration and intensity of the laser pulses or the speed of the chirp. At the same time, the phase may be controlled by the sign of the frequency

chirp: for a positive frequency chirp the created coherence has a phase equals 0 radians; while it equals π radians for the opposite direction of the chirp (negative chirp), Fig. 3.4. In the analysis

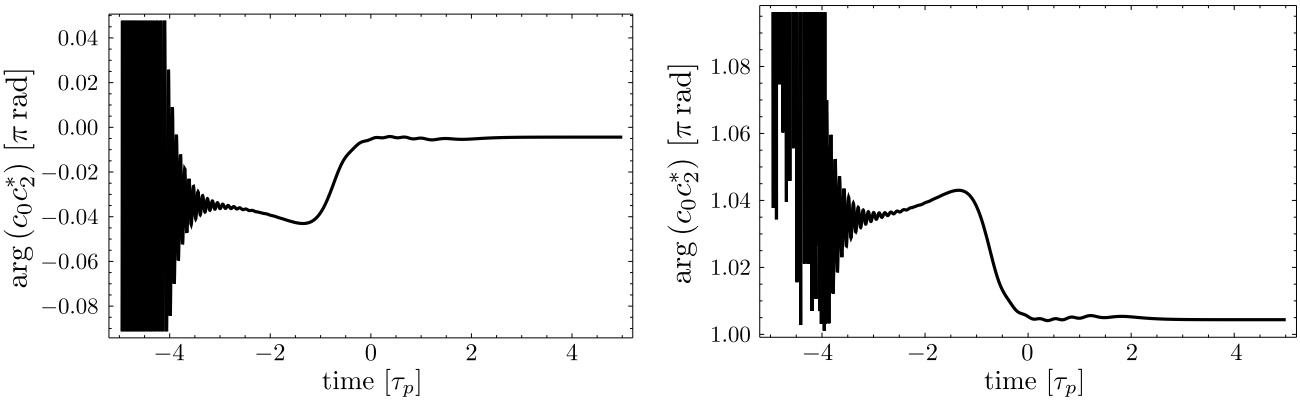

(a) (b)

Figure 3.4: The phase of the coherence between the initially empty ground and excited states in π radians a.) in the case of positive chirp $\beta = 20\left[1/\tau_p^2\right]$, and b.) in the case of negative chirp $\beta = 20\left[1/\tau_p^2\right]$. Other parameters applied are the same as in Fig. 3.2.

above, the constant phases φ_1^0 and φ_2^0 of the Rabi frequencies Ω_1 and Ω_2, respectively, are assumed to be the same. This allowed us to calculate with real-valued peak Rabi frequencies $\Omega_1^{(0)}$ and $\Omega_2^{(0)}$. In the case when the relative phase $\Delta\Phi_L = \varphi_1^0 - \varphi_2^0 \neq 0$, the phase of the created coherence will be $\Delta\Phi_L$ for positive frequency chirp, and $\pi - \Delta\Phi_L$ for the negative chirp. It means that the phase of the created coherence can be controlled by the sign of the frequency chirp and, additionally, by the initial relative phase of the two laser pulses.

Such a behavior of the phase may be explained as follows. The population of the initially populated ground state is transferred to one of the superpositional states, either the symmetric state with the coherence having phase of 0 radians, or the anti-symmetric one having coherence with phase equals π radians.

3.3 Creation of coherence between the Zeeman sublevels in ^{87}Rb (the case of far-detuned driving)

In this section, we proceed with the second limiting case of the problem at hand. Here, we wish to describe the interaction of the atom with two pulses which are significantly detuned from the possible transitions from the ground states. As it was mentioned above, we need to take into account several

atomic excited states. That is, it is the level scheme of the atom for which we wish to apply the interaction scheme that determines which atomic levels are needed to be included into our model.

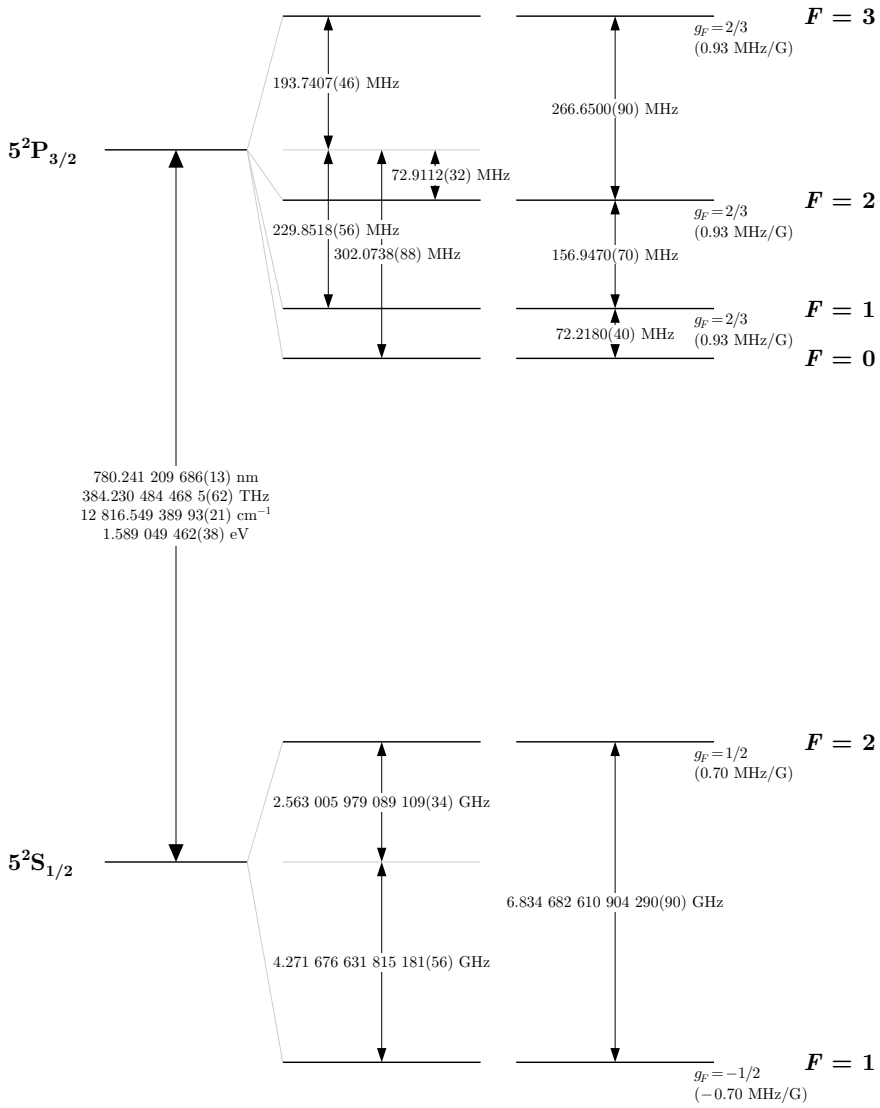

Figure 3.5: The scheme of the hyperfine level structure of the $5^2S_{1/2} - 5^2P_{3/2}$ transition ($D2$ line) of ^{87}Rb

Here, we choose the magnetic sublevels $|m = -1\rangle$ and $|m = +1\rangle$ of the $F = 1$ hyperfine level of the $5^2S_{1/2}$ state of ^{87}Rb to be the ground states $|g_1\rangle$ and $|g_2\rangle$ (see Fig. 3.5 for the scheme of the hyperfine level structure of the $5^2S_{1/2} - 5^2P_{3/2}$ transition ($D2$ line) of ^{87}Rb [127]). Our aim is to investigate the two-photon transitions between these two states through the excited state $5^2P_{3/2}$ by using a pair of laser beams: One with σ^- circular polarization and constant carrier frequency and another one with σ^+ polarization with frequency swept through the Raman resonance with two-photon transition between the states $|g_1\rangle$ and $|g_2\rangle$. Here the atomic quantization axis is aligned with

the light propagation direction. However, both of the central frequencies ω_1 and ω_2 are tuned below resonance so that their detuning from the transition frequency between states $|F = 1\rangle$ and $|F' = 0\rangle$ is larger than the energy difference between the hyperfine states of the excited state. Fig. 3.6 shows the possible dipole-allowed transitions induced by this pair of laser pulses, taking into account the selection rules [111]

$$\begin{aligned} F' = F \quad &\text{or} \quad F' = F \pm 1 \\ m'_F = m_f \quad &\text{or} \quad m'_F = m_F \pm 1 \\ F' \neq F \quad &\text{if} \quad m'_F = m_F = 0 \end{aligned} \tag{3.8}$$

for the hyperfine transition $|F\, m_F\rangle \rightarrow |F'\, m'_F\rangle$ and also the law of angular momentum conservation which implies that the $m'_F = m_F + 1$ and $m'_F = m_F - 1$ transitions can be coupled by positively (σ^+) and negatively (σ^-) circularly polarized light, respectively. We assume for simplicity that there

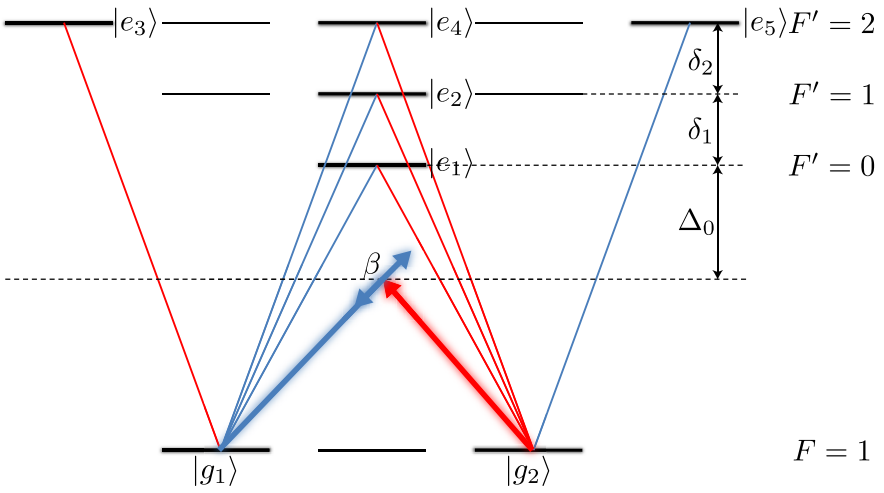

Figure 3.6: Diagram of the manifold of the $F = 1 \rightarrow F'$ transition in ^{87}Rb (D_2 line) with all possible transitions marked by red and blue arrows. One of the laser pulses (red, thick) has a constant carrier

is at most a very weak magnetic field present, therefore the Zeeman-sublevels have the same energy. However, the considerations above also holds in the presence of nonzero Zeeman-shifts with a small modification.

3.3.1 Mathematical formalism

The interaction of the atom with the laser pulses is described in RWA approximation (cf. subsec. 1.1.3) by the Hamiltonian

$$\begin{aligned}\hat{H}_{\mathrm{Rb}} = -\frac{1}{2}\big\{&\mathcal{E}_1 d_{11} e^{i[\Delta_0 t-\varphi(t)]}|e_1\rangle\langle g_1| + \mathcal{E}_1 d_{21} e^{i[(\Delta_0+\delta_1)t-\varphi(t)]}|e_2\rangle\langle g_1| + \mathcal{E}_2 d_{31} e^{i(\Delta_0+\delta_1+\delta_2)t}|e_3\rangle\langle g_1| \\ &+ \mathcal{E}_1 d_{41} e^{i[(\Delta_0+\delta_1+\delta_2)t-\varphi(t)]}|e_4\rangle\langle g_1| + \mathcal{E}_2 d_{12} e^{i\Delta_0 t}|e_1\rangle\langle g_2| + \mathcal{E}_2 d_{22} e^{i(\Delta_0+\delta_1)t}|e_2\rangle\langle g_2| + \\ &\mathcal{E}_2 d_{42} e^{i(\Delta_0+\delta_1+\delta_2)t}|e_4\rangle\langle g_2| + \mathcal{E}_1 d_{52} e^{i[(\Delta_0+\delta_1+\delta_2)t-\varphi(t)]}|e_5\rangle\langle g_2| + \mathrm{H.c.}\big\}. \quad (3.9)\end{aligned}$$

Here $d_{kl} = \langle e_k \mid \hat{d} \mid g_l\rangle$ is the matrix element of the electric dipole moment operator $\hat{d}$ between the excited state $|e_k\rangle$ and the ground state $|g_l\rangle$. $\Delta_0 = \omega_{F=1,F'=0} - \omega_2$ is the frequency difference between the frequency of the $F = 1 \to F' = 0$ transition and the constant carrier frequency of the laser pulse with σ^- polarization, δ_1 and δ_2 are the frequency separations between the hyperfine levels $|F' = 0\rangle$, $|F' = 1\rangle$ and $|F' = 2\rangle$, respectively. $\phi(t)$ is the time-dependent phase of the laser pulse with σ^+ polarization due to frequency chirp.

Rotating basis

It is more convenient in further analysis to describe the interaction in a basis which incorporates the time-dependent complex phases into the rotation of the states:

$$\begin{aligned}\big\{&|\tilde{g}_1\rangle \equiv e^{i\varphi(t)}|g_1\rangle,\ |\tilde{g}_2\rangle \equiv |g_2\rangle,\ |\tilde{e}_1\rangle \equiv e^{i\Delta_0 t}|e_1\rangle,\ |\tilde{e}_2\rangle \equiv e^{i(\Delta_0+\delta_1)t}|e_2\rangle, \quad (3.10)\\ &|\tilde{e}_3\rangle \equiv e^{[i(\Delta_0+\delta_1+\delta_2)t+\varphi(t)]}|e_3\rangle,\ |\tilde{e}_4\rangle \equiv e^{i(\Delta_0+\delta_1+\delta_2)t}|e_4\rangle,\ |\tilde{e}_5\rangle \equiv e^{[i(\Delta_0+\delta_1+\delta_2)t-\varphi(t)]}|e_5\rangle\big\},\end{aligned}$$

which leads to the Hamiltonian

$$\hat{\mathcal{H}}_{\mathrm{Rb}} = \hbar\left\{\dot{\varphi}(t)\,|g_1\rangle\langle g_1| + \sum_{l=1}^{5}\left[\Delta^l(t)\,|e_k\rangle\langle e_k| + \frac{1}{2}\left(\Omega_1^l|e_l\rangle\langle g_1| + \Omega_2^l|e_l\rangle\langle g_2| + \mathrm{H.c.}\right)\right]\right\}, \quad (3.11)$$

where the couplings (Ω_1^l and Ω_2^l) and the detunings $\Delta^l(t)$ may be represented as components of the following "Rabi frequency vectors" and "detuning vector":

$$\vec{\Omega_1} = \frac{1}{\hbar}\left[d_{11}\mathcal{E}_1 \quad d_{21}\mathcal{E}_1 \quad d_{31}\mathcal{E}_2 \quad d_{41}\mathcal{E}_1 \quad 0\ \right] \tag{3.12a}$$

$$\vec{\Omega_2} = \frac{1}{\hbar}\left[d_{12}\mathcal{E}_2 \quad d_{22}\mathcal{E}_2 \quad 0 \quad d_{42}\mathcal{E}_2 \quad d_{52}\mathcal{E}_1\right] \tag{3.12b}$$

$$\vec{\Delta}(t) = \left[\Delta_0 \quad \Delta_0+\delta_1 \quad \Delta_0+\delta_1+\delta_2+\dot{\varphi}(t) \quad \Delta_0+\delta_1+\delta_2 \quad \Delta_0+\delta_1+\delta_2-\dot{\varphi}(t)\right], \tag{3.12c}$$

where dot denotes the partial differentiation with respect to time t.

3.3.2 Analytical consideration

The dynamics of the atomic state

$$|\psi\rangle_{\mathrm{Rb}} = \sum_{k=1}^{2} a_k(t)\,|g_k\rangle + \sum_{l=1}^{5} b_l(t)\,|e_5\rangle \tag{3.13}$$

is given by the Schrödinger equation $i\hbar\partial_t|\psi\rangle_{\mathrm{Rb}} = \hat{\mathcal{H}}_{\mathrm{Rb}}|\psi\rangle_{\mathrm{Rb}}$ which may be rewritten in the form

$$\dot{a_1}(t) + i\dot{\varphi}(t)\,a_1(t) = \frac{i}{2}\sum_{l=1}^{5}\Omega_1^{l*}b_l(t) \tag{3.14a}$$

$$\dot{a_2}(t) = \frac{i}{2}\sum_{l=1}^{5}\Omega_2^{l*}b_l(t) \tag{3.14b}$$

$$\dot{b_l}(t) + i\Delta^l(t)\,b_l(t) = \frac{i}{2}\left(\Omega_1^l a_1(t) + \Omega_2^l a_2(t)\right), \quad \forall l \in \{1,\ldots,5\}, \tag{3.14c}$$

where the "vectors" defined in Eq. (3.12c) for the Rabi frequencies and the detunings were used. Here we take into the account the assumption that the laser pulses are "far detuned" from one-photon resonance, that is

$$\Omega_{1,2} \ll \Delta_0, \quad \delta_{1,2} \ll \Delta_0, \quad \dot{\varphi}(t) \ll \Delta_0 \ \ \forall t \in [-\tau_p, \tau_p], \tag{3.15}$$

with τ_p being the duration of the laser pulses (equal for both of them). Therefore, the time derivatives $\dot{b_l}(t)$ may be neglected in Eq. (3.14c), to obtain the expressions

$$b_l \approx \frac{\Omega_1^l a_1(t) + \Omega_2^l a_2(t)}{\Delta_0}, \ \forall l \in \{1, \ldots, 5\} \tag{3.16}$$

for the amplitudes of the excited states, where $\Delta_l(t) \approx \Delta_0$ was also assumed. Substituting the relations given in Eq. (3.15) into Eqs. (3.14a) and (3.14b), we can formulate the relation for the phase-shifted probability amplitudes $\tilde{a}_{1,2}(t) = a_{1,2}(t) \exp\left[-i|\vec{\Omega}_1|^2/(2\Delta_0)\right]$ of the ground states as

$$\dot{\tilde{a}}_1(t) + i\dot{\varphi}(t) = \frac{i}{2}\Omega_{\text{eff}}^* \tilde{a}_2(t) \tag{3.17a}$$

$$\dot{\tilde{a}}_2(t) + i\Delta_{\text{eff}} = \frac{i}{2}\Omega_{\text{eff}} \tilde{a}_1(t), \tag{3.17b}$$

with the effective Rabi frequency and detuning

$$\Omega_{\text{eff}} = \vec{\Omega}_1 \cdot \vec{\Omega}_2^*/\Delta_0 \ \text{ and } \ \Delta_{\text{eff}} = \left(|\vec{\Omega}_1|^2 - |\vec{\Omega}_2|^2\right)/(2\Delta_0). \tag{3.18}$$

As it follows from Eq. (3.17), in the proposed scheme the interaction of the pair of laser pulses with a multilevel atomic system may be represented as an interaction of a laser pulse with the effective Rabi frequency with a two-level system consisting of the two meta-stable states $|g_1\rangle$ and $|g_2\rangle$. The influence of the remaining levels is reduced to additional ac-Stark shifts of the transitions described by the effective detuning given in Eq. (3.18). These Stark shifts compensate each other when $\Delta_{\text{eff}} = 0$, so that the behavior of the multilevel system under consideration becomes completely equivalent to that of a corresponding two-level system. This similarity to a two-level atom is useful for interpretation of the results of the numerical analysis given below.

3.3.3 Results of the numerical simulations

We first consider the laser pulses with the same temporal Gaussian shape, $f_1(t) = \exp[-t^2/2]$, with the time measured in the units of the pulse length $\tau_p = \tau_L/\left(2\sqrt{\ln 2}\right)$, where τ_L is the full width at half maximum. In this case we assume a linear modulation in the carrier frequency of the pulse having positive circular polarization, so that $\dot{\varphi}_1(t) = \beta t$, with β being the speed of chirp. In such a

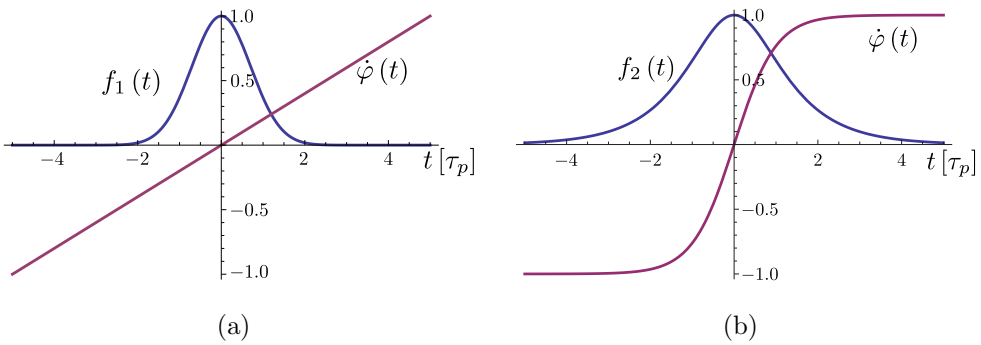

Figure 3.7: Shapes (blue curve) and frequencies of a.) Gaussian and b.) bell-like laser pulses used in the simulations presented as functions of time

case, we analyze the amplitude of the coherence $\rho_{g_1 g_2}$ between the two meta-stable states $|g_1\rangle$ and $|g_2\rangle$, where $\rho_{g_1 g_2} = a_1 a_2^*$. Next, we study the dependence of the coherence amplitude on the pulse shape, as well as on the frequency chirp dynamics. For this purpose, simulations with bell-shaped laser pulses, $f_2(t) = \cosh^{-1}(t)$, and the time variation of the carrier frequency given by $\dot{\varphi}_2(t) = \beta \tanh(t)$ (see Fig. 3.7), are performed.

To have the numerical analysis adequately describing the experiment, some constraints must be imposed on the parameters of the applied laser pulses. First of all, we assume that only sublevels of the $F = 1$ hyperfine level are involved in the interaction. This means that both the width of the Fourier spectrum of the envelope of the laser pulses and the frequency chirp span are smaller than the frequency distance Δ_{F12} ($\Delta_{F12} \approx 6.83\,\mathrm{GHz}$) between the two meta-stable (ground) hyperfine levels $F = 1$ and $F = 2$ of ^{87}Rb (see Fig. 3.5). For laser pulses with duration τ_p, the condition for eliminating the $F = 2$ hyperfine level from the interaction is: $1/\tau_p, \beta\tau_p \ll \Delta_{F12}$. Another constraint has to be put on the duration of the laser pulses and the speed of the chirp. Namely, at any time during the interaction, the frequency of the pulses must remain far from the single-photon resonance, so the conditions given in Eq. (3.15) along with $\Delta\omega_p \approx 1/\tau_p \ll \Delta_0$ need to be fulfilled, with $\Delta\omega_p$ being the width of the Fourier spectrum of the pulse envelopes. At the same time the condition $\Delta_0 \gg \Gamma$ has to be granted, where Γ is the natural line-width of the excited states in the case of motionless atoms (for moving atoms, the role of Γ is played by the Doppler width of the relevant transition). Since we use an adiabatic sweep of the laser frequency through the Raman resonance and assume that the resonance takes place in the center of the pulses (t=0), the detunings ($\mp\beta\tau_p$) from the Raman resonance at the leading and rear fronts of the pulse must be large: $|\beta| > 1/\tau_p$.

All these restrictions on the parameters were taken into account in the numerical simulations. The Rabi frequencies for the allowed transitions from magnetic sublevels of the $F = 1$ level to the excited states of the $5^2S_{1/2} \rightarrow 5^2P_{3/2}$ transition in ^{87}Rb were calculated using the values of dipole moments for the corresponding transitions. In the simulations the following "reduced" Rabi frequencies were used: $W_1 = \left(\mathcal{E}_1^{(0)} C_{JJ}\right)/\hbar$ and $W_2 = \left(\mathcal{E}_2^{(0)} C_{JJ}\right)/\hbar$, where $\mathcal{E}_{1,2}^{(0)}$ are the peak amplitudes of the σ^+ and σ^--polarized laser pulses, respectively, while $C_{JJ} = \langle J = 1/2 \,||er||\, J' = 1/2\rangle$ is the reduced matrix element (see, e.g. [111]). The dynamics of the populations of states $|g_1\rangle$ and $|g_2\rangle$ along with the

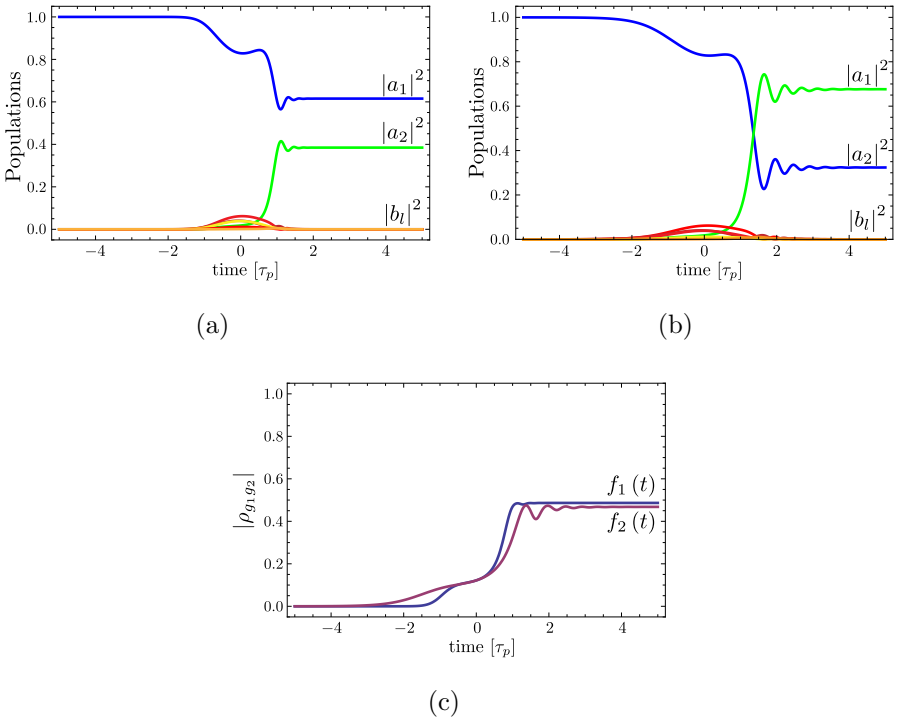

Figure 3.8: Dynamics of the populations of the working levels labeled as in Fig. 3.6. $|a_1|^2$ and $|a_2|^2$ are the populations of the metastable states and $|b_l|^2$ are populations of the excited states in the case of a.) linear and b.) nonlinear chirp. c.) The amplitude of the coherence ρ_{g1g2} created between the states $|g_1\rangle$ and $|g_2\rangle$ in the cases of the linear and nonlinear chirp. The simulations were performed with the parameters $W_1 = 1565\ [1/\tau_p]$, $W_2 = 1329\ [1/\tau_p]$, $\Delta_0 = 1500\sqrt{2}\ [1/\tau_p]$, and $\beta = 30\ \left[1/\tau_p^2\right]$. The durations of the laser pulses are $\tau_p = \sqrt{2}\,\mu s$.

populations of the excited states in the field of the laser pulses are shown in Figs. 3.8(a) and 3.8(b) for Gaussian shaped pulses and linear chirp of the frequency chirped laser pulse, and for the bell-shaped laser pulse with the corresponding nonlinear chirp function, with initial preparation of the atom in state $|g_1\rangle$. The corresponding amplitudes of the created coherence $|\rho_{g_1g_2}|$ are shown in Fig. 3.8(c). As it can be seen in Fig. 3.8, the proposed scheme offers negligible atomic excitation and generates maximum coherence. It is also worth noting that the dynamics of the induced coherence

does not significantly depend on the exact laser pulse shape and frequency chirp behavior. The

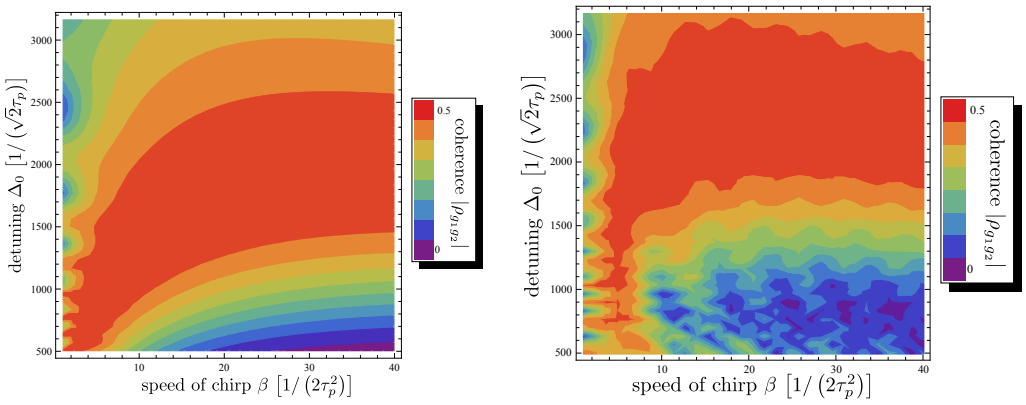

Figure 3.9: Dependence of the absolute value of the created coherence $|\rho_{g_1g_2}|$ on the single-photon detuning Δ_0 and the speed of the chirp β at $t = 0$ in the case of: a.) linear ($\dot{\varphi}_1(t)$), and b.) nonlinear ($\dot{\varphi}_2(t)$) chirp. The parameters applied are: $W_1 = 1442\ [1/\tau_p]$, $W_1 = 1280\ [1/\tau_p]$, $\Delta_0 = 1500\sqrt{2}\ [1/\tau_p]$ and $\tau_p = \sqrt{2}\,\mu s$.

maximum value 0.5 for the created coherence may be achieved for some range of values for the parameters of the laser radiation. Color maps showing the amplitude of the created coherence are presented in Fig. 3.9 as a function of the single-photon detuning Δ_0 and the chirp rate β for the two types of the laser pulse shapes and frequency chirp behavior (see Fig. 3.7). It can be observed that there are regions of values of Δ_0 and β for which the coherence $\rho_{g_1g_2}$ reaches its maximum value. In order to examine how the regions of the maximum coherence depend on the peak intensities (Rabi frequencies) of the applied laser pulses, the coherence is calculated as a function of the Rabi frequency of the laser pulses with fixed values for the other parameters corresponding to the region of maximum coherence on the color maps in Fig. 3.9. This dependence is presented in Fig. 3.10 as a function of the peak amplitude of the pulse with constant carrier frequency assuming a fixed product of the peak intensities of the two pulses. The results of simulations for both Gaussian-shaped laser pulses with a linear chirp and for bell-shaped pulses with the corresponding chirp function are presented in Figs. 3.10(a) and 3.10(b). The results show weak dependence on the shape of the pulses and their chirp functions. As it can be seen from both figures, the maximum value of the coherence is reached at two different values of the laser peak intensity, nearly symmetrically located around the value at which the Rabi frequencies of the laser pulses are equal to each other and no coherence is generated. This result is in agreement with the previous analysis, (see Eq. (3.17) showing equivalence of the

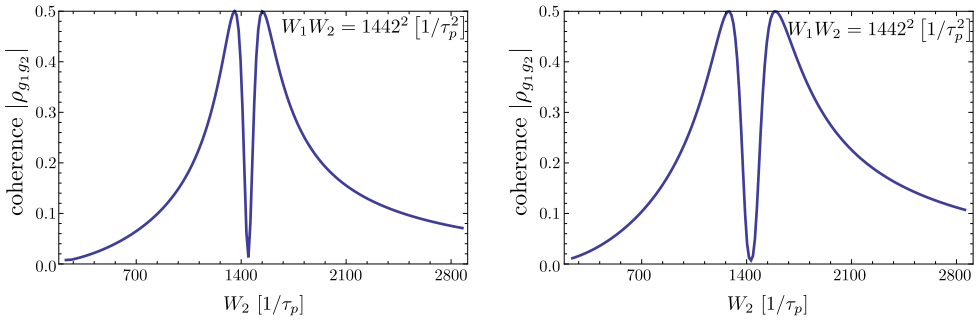

(a) (b)

Figure 3.10: Dependence of the ground-state coherence amplitude on the Rabi frequency of one of the laser pulses with $W_1 \cdot W_2 = \text{const}$. The calculations are performed for the Gaussian-shaped pulse with a.) linear chirp and b.) the bell-like pulse with chirp function $\dot{\varphi}_2(t) = \beta \tanh(t)$. The parameters applied in the simulations are $\Delta_0 = 1500\sqrt{2}\ [1/\tau_p]$, $\beta = 30\ \left[1/\tau_p^2\right]$, $W_1 \cdot W_2 = 1442^2\ \left[1/\tau_p^2\right]$, and $\tau_p = \sqrt{2}\,\mu s$.

multi-state system with a two-level atom) according to which a complete population is transferred from one meta-stable state to the other one and no coherence between the two states is established. Thus, the points of zero coherence in Figs. 3.10(a) and 3.10(b) represent the complete population transfer between $|g_1\rangle$ and $|g_2\rangle$ which may be of interest for many applications.

3.4 Summary

Coherent coupling by a FC and a constant-frequency laser pulse has been analyzed in this chapter, in two limiting cases. In both cases we regarded Λ-type configurations, where each pulses couple a corresponding ground state to the excited state(s). The frequency of the chirped pulses is swept through two-photon resonance. The difference between the two cases is made by the one-photon detuning of the constant frequency pulse. In the first case we have assumed that it is exactly resonant with an allowed transition of the atom, and thus during the interaction, one- and two-photon resonance occurs in the same moment. On the other hand, in the second case we have regarded the pulses are far detuned from the frequencies of transitions to any possible excited states.

We have seen that the two limits of one-photon detuning result in substantially different population transfer mechanisms. First, when it comes for applying the scheme to real atoms, the resonance condition makes it possible to use the simple atom model. In contrary, if the one-photon detuning exceeds the splitting between the excited states of actual atomic level structure, several excited states

are needed to be taken into account. On the other hand, the two cases also differ strongly in the point of populating the excited state.

As our results show, the *resonant* limit of coupling results in creation of maximum coherence between the excited state and the ground state driven by the constant-frequency pulse. It is demonstrated that the scheme is robust against relatively large variations of the parameters of the laser pulses. While the absolute value of the coherence does not depend on the phase relations between the laser pulses and the chirp of the frequency modulated laser pulse, the phase of the coherence may be controlled by the (constant) relative initial phase of the laser pulses and by the direction of the frequency chirp. The underlying physics of the process can by explained by introducing symmetric and anti-symmetric superpositional states.

The extreme robustness of the proposed scheme makes possible an effective generation of the same (maximum) coherence between the ground and excited states in an atomic gas with approximately the same value of the coherence across the laser beams even if the beams are tightly focused. This is especially important when the prepared atomic medium is used for generation of high-order harmonics requiring tight focusing of laser radiation for achieving ultra-high light intensities. In addition, since robust control of the phase of the created coherence is possible simultaneously for all atoms in an ensemble, the proposed scheme may also be applicable in other processes of coherent nonlinear optics including nonlinear wave mixing and anti-Stokes or hyper-Raman scattering.

In the case of the *far-detuned* limit, in accordance with our anticipation, the majority of the population remains in the ground states. Since the population of the excited states is negligible during the whole interaction process, the system can be approximated by a two-level atom, with an effective Rabi frequency. For a simple model atom including only one excited state, complete population transfer is induced between the two states (which coincide with the original ground states), via rapid adiabatic passage.

However, this simple model has to be reconsidered when we wish to describe the population dynamics induced by the far detuned, circularly polarized pulses among the Zeeman-sublevels of a real atom. In this case, we need to add an extra time-dependent term in the description, which modifies the population redistribution process between the two states. Our result indicates that as a result of the interaction, a superposition between the ground states is established, which depends on the proportion of the peak amplitudes of the interacting laser pulses. We have shown that by

properly choosing the parameters, maximum Zeeman-coherence is possible to create. Note that the presented method allows coherent control of the Zeeman-sublevels without significant excitation of the atom. Thus, it allows avoiding the decoherence due to the spontaneous emission from the excited state.

Chapter 4

Coherence creation in optically thick medium

In the previous chapters, we concentrated on adiabatic control (AC) in single atoms and we regarded the laser pulses as given control tools. However, when AC is performed in an optically thick medium [90–93], the back-action of the atoms on the laser fields and other effects, such as interaction of the laser pulses with each other become important. Therefore, these effects are needed to be taken into account and thus the laser fields turn to be regarded as dynamical variables from parameters.

In case of the interaction of an optically thick medium with a couple of quasi-resonant electromagnetically fields, two, interconnected problems emerge. The questions to be addressed are, in one hand, that how the radiation field is affected by the medium while propagating in it and, on the other hand, in which state the medium is driven by the propagating laser radiation.

Preparation of the atoms of a medium in coherent superposition of the quantum states may significantly modify its optical properties leading to very interesting and important propagation effects, like electromagnetically induced transparency (EIT). In the EIT-based schemes (see [36, 37, 94] and references therein), an intense laser-pulse (of constant carrier frequency) renders the whole medium transparent for a weak probe pulse in Raman resonance with the intense one. In this scheme, there is no substantial population redistribution.

Nearly lossless propagation was demonstrated in the case of constant frequency pulses having identical [128] and complementary pulse envelopes [129], and also for a *single* FC laser pulse in optically thick media consisting of lambda-atoms(see Fig. 1.2(a)) [91]. In the above mentioned

schemes, the lossless propagation of the electromagnetic field(s) was ensured by initially preparing the medium to a dark superposition of the ground states. This means that no excitation occurs in the atoms during the interaction, which significantly reduces the back-action of the atoms on the laser field. As a result, basically the same population-control mechanism was established in the atoms of the extended medium even for significant propagation distances.

On the other hand, it has been shown in [96] that for a sufficiently intense laser pulse pair having constant frequencies in Raman resonance, lossless propagation is possible in a medium of Λ-atoms even if the initial preparation of the atoms does not coincide with the dark state. The explanation is that the laser pulses become distorted by the interaction with the medium in such a way that the initial preparation of the atoms corresponds to a dark state for the pulse-pair after propagating some distance. In this sense, the interacting laser pulses become *matched* to each other through the interaction with the atoms of the medium. This *matched-pulse* case obviously differs from the previous ones in the point that, in this case, the population-distribution process inside the medium is significantly changed compared to the one at the boundary.

In earlier works of our group [75] and [77], several interaction schemes including single lambda-atoms and FC pulses were considered. Comparing these schemes we may conclude that the population transition process induced among the states of the lambda-atom depends on whether the coupling of the two ground states are in Raman resonance. It was shown in [77] that a nearly excitation-free population transfer may be established among the ground states with a single FC pulse which can couple both of the transitions, provided that there is an energy difference between them (i.e. there is a Raman detuning between the couplings). In [91], it was demonstrated that this scheme is possible to be applied in optically thick medium for inducing a population transfer between the ground states of the lambda-atoms which built up the medium.

In contrast, the action of a pair of strong Raman-resonant FC pulses on a single atom results in adiabatic excitation of the bright component of the superposition of the ground states leaving intact the dark component of this superposition [75]. As a result, a coherent superposition of the ground states is robustly created along with excitation of the atom. This excitation, however, is detrimental for the created coherence: One has to transfer the population of the excited state to another ground state to preserve the created coherence from the destructive effect of the spontaneous decay.

In this chapter, we examine the possibility of applying this interaction scheme containing a

Raman-resonant pulse pair in optically thick medium of lambda-atoms. We investigate whether the Raman-resonant pulse pair is able to propagate in the medium despite of the fact that, unlike the Raman-detuned case, it causes a significant excitation in the atoms at the boundary. Based on the similarities of our case to the one analyzed in [96], we anticipate that there is a *matching effect* for frequency-modulated laser-pulse pairs as well.

We are also interested in the population transfer mechanism which is induced by the potentially propagating laser pulses inside the medium, which may differ strongly from the one at the boundary of the medium because of the distortion in the laser pulses caused by the macroscopic polarization. Our aim is to find a mechanism which is suitable for preparing the majority of the atoms in the medium in a controllable superposition of their the ground states.

4.1 Propagation of a Raman-resonant FC pulse pair in an optically thick medium consisting of lambda-atoms

4.1.1 Mathematical formalism

We use the semiclassical approach introduced in Section 1.2 for studying the propagation of the FC pulses in a medium consisting of Λ-atoms in one given direction. The internal electronic state of the atoms is treated in the frame of quantum mechanics, while the laser pulses are described by the classical electric field

$$\vec{E}\,(x,t) = \sum_{i=1}^{2} \vec{\epsilon}_i \left[\mathcal{E}_i\,(x,t) \cdot e^{-i(\omega_i t - k_i x)} + c.c.\right], \tag{4.1}$$

and their propagation is described by the by the Maxwell equation. Here we have used the same notations as in(1.7), i.e. $\mathcal{E}_i\,(x,t)$, ω_i and k_i denote the envelope function, the central frequency and the wave vector of the i^{th} pulse ($i \in \{1,2\}$), respectively. The medium in which this classical pulse pair propagates is modeled by identical, noninteracting and motionless λ-atoms, which are initially prepared in one of their ground state (for example, in $|2\rangle$).

We assume that the requirements for the time scales and the couplings given in subsection 1.1.7 are fulfilled. Namely, the both dipole-allowed transitions of the lambda-atoms are separately coupled

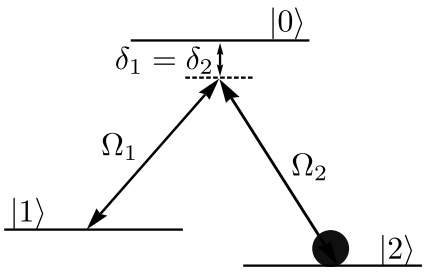

Figure 4.1: Level scheme of the lambda-atom. The dipole-allowed transitions (between the excited state $|0\rangle$ and the lower metastable states $|1\rangle$ and $|2\rangle$, respectively) are each coupled by a frequency modulated (FC) laser pulse. In this chapter, we consider Raman-resonant coupling, i.e. $\delta_1 = \delta_2 = 0$. The atoms are initially prepared in state $|2\rangle$.

by a laser pulse having an envelope slowly varying in space and time. In accordance with this assumption, we describe the system in the frame of the rotating wave and the slowly varying envelope approximations (see subsecs. 1.1.3 and 1.2.2). The interaction of an arbitrary atom localized in the region $[x, x+\delta x]$ with the laser pulses is described by the interaction Hamiltonian (cf. Eq. (1.22))

$$\hat{H}(x,t) = -\hbar \sum_{k=1}^{2} \left[-\delta |k\rangle\langle k| + \left(\frac{1}{2} \Omega_k(x,t) |0\rangle\langle k| + \text{H.c.} \right) \right], \tag{4.2}$$

where $\Omega_k(x,t) = |\Omega_k| \cdot e^{-i\phi_k(x,t)}$, $k \in \{1,2\}$ is the Rabi frequency (see Eq. (1.17)) of the k^{th} laser pulse, with the change of the frequency included in the phase $\phi_k(x,t)$. In the considered case, the propagating pulse pair is in Raman resonance, which means that their central frequencies (ω_1 and ω_2) are detuned from the corresponding transition frequencies by the same amount of δ. For the sake of simplicity, we now set this common detuning to be zero.

For later convenience it is worth introducing

$$\xi = x/\xi_0 \tag{4.3a}$$

$$\tau = (t - x/c)/\tau_\sigma \tag{4.3b}$$

dimensionless, retarded space and time coordinates. The time is measured in the unit of τ_σ, which characterizes the duration of the pulses. For the normalization of the space coordinates we introduce the absorption length of a laser pulse of constant frequency ω_L in a medium consisting of resonant

two-level atoms with a density of $\mathcal{N}$, which is given by [39]

$$\xi_0 = \frac{\varepsilon_0 \hbar c}{\mathcal{N}\omega_L \left|d_A\right|^2 T}, \tag{4.4}$$

where T is the natural lifetime of the excited state and d_A is the dipole moment of the coupled atomic transition. Although there are two atomic transitions in the present case, it is consistent with our previous approximations to regard a common absorption length for both coupling pulses by setting $|d_{01}| = |d_{02}| = d_A$, $\omega_L = (\omega_1 + \omega_2)/2$ and $T = 2/\Gamma_1 = 2/\Gamma_2 = 2/\Gamma$, where Γ_i is the longitudinal relaxation rate from the excited state $|0\rangle$ to the metastable state $|i\rangle$, $i \in \{1, 2\}$.

We describe the response of the atoms for the ingoing laser radiation inside a certain space-interval by the master equation

$$\begin{aligned}\partial_\tau \hat{\rho}(\xi,\tau) = \frac{1}{i\hbar}\left[\hat{H}(\xi,\tau), \hat{\rho}(\xi,\tau)\right] - 2\Gamma|0\rangle\langle 0|\rho_{00}(\xi,\tau) + \sum_{k=1}^{2}\left[\Gamma\rho_{00}(\xi,\tau)\,|k\rangle\langle k|\right. \\ \left. - \left(\Gamma\rho_{0k}(\xi,\tau)\,|0\rangle\langle k| + \text{H.c.}\right)\right],\end{aligned} \tag{4.5}$$

where $\rho_{kl} = \langle k|\hat{\rho}|l\rangle$ and $\hat{\rho}(\xi,\tau)$ is the average density matrix defined in Eq. (1.43). Since the change in the electromagnetic field is neglected inside a small segment, the Hamiltonian $\hat{H}(\xi,\tau)$ which drives the evolution of the average density operator is formally the same as in Eq. (4.2).

The atoms of the medium may affect the propagating laser pulses by means of basically two mechanisms: by spontaneous emission from the excited state and by dipole-radiation [96]. In the present case, we regard a weakly decaying regime: we assume that the lifetime of the excited state is about an order of magnitude longer than the pulse duration. The action of the atomic dipoles on the laser radiation propagating in the field can be taken into account by the macroscopic polarization of the medium. This polarization, induced by the laser fields at a certain space segment $[\xi, \xi + \delta\xi]$ (see Eq. (1.42)) is proportional to the average of coherences ρ_{01} and ρ_{02} between the ground states $|1\rangle$ and $|2\rangle$ and the excited state $|0\rangle$ of the atoms located there. Pursuing the deduction presented in sec. 1.2, we have the following equation for the Ω_k Rabi frequency of the k^{th} laser pulse:

$$\frac{\partial}{\partial\xi}\Omega_k(\xi,\tau) = i\alpha\rho_{0k}(\xi,\tau), \quad k \in \{1,2\}. \tag{4.6}$$

Note that this differential equation system is analogous with Eq. (1.50), although it has a simpler form in the retarded coordinates given by Eq. (4.3). We assume that the coupling strength between both laser modes and the corresponding dipole transitions are the same and described by $\alpha = \tau_\sigma / (2T)$. This assumption is valid for example for two laser pulses having σ^+ and σ^- polarizations, interacting with a $F = 1 \to F' = 0$ transition of an atom.

In order to study the behavior of the propagating FC pulses and the atomic transitions induced by the laser field, we solve the system of differential equations formed by Eqs. (4.5)) and (4.6) numerically. We use the following boundary conditions of two Gaussian, linearly chirped pulses entering the medium at $\xi = 0$ (see Fig 4.2(a)):

$$\begin{bmatrix} \Omega_1(\xi = 0, \tau) \\ \Omega_2(\xi = 0, \tau) \end{bmatrix} = \begin{bmatrix} \vartheta_1 \\ \vartheta_2 \end{bmatrix} e^{-\tau^2\left(\frac{1}{2} + i\beta\right)}, \quad \vartheta_k \in \mathbb{R} \ \ \forall k \in \{1, 2\} \tag{4.7a}$$

$$\hat{\rho}(\xi, \tau \to -\infty) = |2\rangle\langle 2|, \tag{4.7b}$$

where ϑ_1 and ϑ_2 are the peak amplitudes of the laser pulses at the entrance of the medium. The parameters $\{\vartheta_1, \vartheta_2, \beta, \tau_\sigma\}$ in what follows are chosen in such a way that the conditions of adiabaticity (see subsec. 1.3) are fulfilled.

Symmetric-antisymmetric basis

For further investigation of the population dynamics in arbitrary segments of the medium, it is useful to introduce a basis transformation on the atomic states adapted to the boundary conditions given in Eq. (4.7), which leads us to the following symmetric-antisymmetric basis:

$$\{|0\rangle, |s\rangle, |a\rangle\} = \left\{ |0\rangle, \frac{\vartheta_1|1\rangle + \vartheta_2|2\rangle}{\vartheta} \frac{\vartheta_2|1\rangle - \vartheta_1|2\rangle}{\vartheta} \right\}, \text{where} \quad \vartheta = \sqrt{\vartheta_1^2 + \vartheta_2^2}. \tag{4.8}$$

The Hamiltonian in this new basis becomes

$$\hat{H}_{sa}(\xi, \tau) = -\hbar \sum_{j \in s,a} \left[\Omega_j(\xi, \tau) |0\rangle\langle j| + \text{H.c.} \right], \tag{4.9}$$

where we have defined the effective Rabi frequencies as

$$\begin{bmatrix}\Omega_s\\ \Omega_a\end{bmatrix} = \begin{bmatrix}\left(\vartheta_1\Omega_1 + \vartheta_2\Omega_2\right)/\vartheta\\ \left(\vartheta_2\Omega_1 - \vartheta_1\Omega_2\right)/\vartheta\end{bmatrix} \tag{4.10}$$

for the couplings between the excited state $|0\rangle$ and the symmetric and antisymmetric superpositional states $|s\rangle$ and $|a\rangle$, respectively. The spatial dependence of the coupling obeys formally the same differential equation as the original Rabi frequencies:

$$\partial_\xi \Omega_j = -i\alpha\rho_{j0}, \quad j \in \{s,a\}\,, \rho_{j0} = \langle j \mid \hat{\rho} \mid 0\rangle \tag{4.11}$$

where $\vartheta_k \in \mathbb{R} \;\; \forall k \in \{1,2\}$ was utilized. Transforming the boundary conditions according to Eq. (4.10)

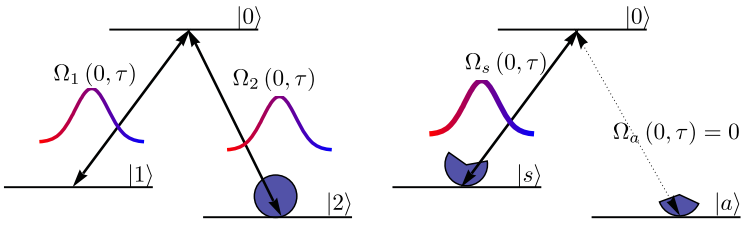

(a) (b)

Figure 4.2: Boundary conditions given in a.) the original atomic basis b.) the symmetric-asymmetric basis. All the atoms in the medium are initially prepared in the metastable state $|2\rangle$, which corresponds to a coherent superposition in the symmetric-antisymmetric basis given by the peak amplitudes ϑ_1 and ϑ_2 of the ingoing laser pulses.

yields a set of boundary conditions which is more convenient for our purposes, as it only contains one ingoing laser mode (see Fig 4.2(b)):

$$\begin{bmatrix}\Omega_s\left(\xi=0,\tau\right)\\ \Omega_a\left(\xi=0,\tau\right)\end{bmatrix} = \begin{bmatrix}\vartheta\\ 0\end{bmatrix} e^{-\tau^2\left(\frac{1}{2}+i\beta\right)}, \tag{4.12a}$$

$$\hat{\rho}\left(\xi,\tau\to-\infty\right) = \frac{1}{\vartheta^2}\left(\vartheta_2|s\rangle - \vartheta_1|a\rangle\right)\left(\vartheta_2\langle s| - \vartheta_1\langle a|\right). \tag{4.12b}$$

Rotating basis for the adiabatic approximation

In order to use the adiabatic approximation for the dynamics of the state of the atoms in a certain space segment, we need to describe their interaction with the laser radiation using an interaction

picture in which the interaction Hamiltonian only contains slowly varying matrix elements (in the scale of the interaction time). It follows from the form of the boundary conditions (4.12) that the Rabi frequencies $\Omega_j,\ \ j \in \{a, s\}$ (as well as $\Omega_k,\ \ k \in \{1, 2\}$) contain a time-dependent phase, which may prevent us from applying the adiabatic approximation for the eigenstates of the Hamiltonian (4.2). Instead, we have to describe the atomic dynamics in each segment by using the following rotating basis vectors which suits to the phase dependence of the coupling (cf. (1.23)):

$$\{|0\rangle, |\tilde{s}\rangle, |\tilde{a}\rangle\} \equiv \left\{|0\rangle, |s\rangle\, e^{-i\phi_s(\xi,\tau)}, |a\rangle\, e^{-i\phi_a(\xi,\tau)}\right\}. \tag{4.13}$$

Very similarly to Eq. (1.28), the interaction Hamiltonian in the rotating basis reads as

$$\hat{\mathcal{H}}_{sa} = -\hbar \sum_{j\in\{s,a\}} \left[\partial_\tau \phi_j\left(\xi,\tau\right) |\tilde{j}\rangle\langle\tilde{j}| + \frac{1}{2}\left(|\Omega_j\left(\xi,\tau\right)|\, |0\rangle\langle\tilde{j}| + \text{H.c.}\right)\right],$$

$\phi_j,\ \ j \in \{s, a\}$ being the phase of the Rabi frequency $\Omega_j,\ \ j \in \{s, a\}$ (c.f. Eq.(1.17)). Note that this transformation does not change the absolute values of the coefficients in the system's state vector.

4.1.2 Atom-laser interaction near the boundary of the medium

We first describe the interaction of the atoms with the Raman-resonant FC pulse pair at the boundary of the medium in the symmetric-antisymmetric basis. (The results are also valid approximately for an optically dilute medium). It is easy to see from Eqs. (4.14a) and (4.12) that the antisymmetric state $|\tilde{a}\rangle$ is an eigenstate of the Hamiltonian $\hat{\mathcal{H}}_{sa}\left(\xi = 0, \tau\right)$ since the coupling Ω_a is 0 for $\xi = 0$. Thus, it remains unchanged during the interaction. The other metastable state $|\tilde{s}\rangle$ and the excited state $|0\rangle$ form a two-state atom coupled by a FC pulse. As we have discussed in subsec. 1.3.3, the FC pulse drives a rapid adiabatic passage from state $|\tilde{s}\rangle$ to the excited state $|0\rangle$, [41] (see Fig. 4.3). Since the antisymmetric state is decoupled from the excited state, it represents a dark state for the Raman-resonant FC pulses. Similarly to the original case of constant frequency matched pulses propagating in media of Λ-atoms [95, 96], the initial preparation of the atoms given in Eq. (4.12) does not coincide with the "dark" state. Based on the above considerations in the frame of the adiabatic approximation, the atoms at the boundary are expected to be transferred from a superposition of the ground states $|\tilde{s}\rangle$ and $|\tilde{a}\rangle$ to a superposition of states $|\tilde{s}\rangle$ and the excited state $|0\rangle$. This result is

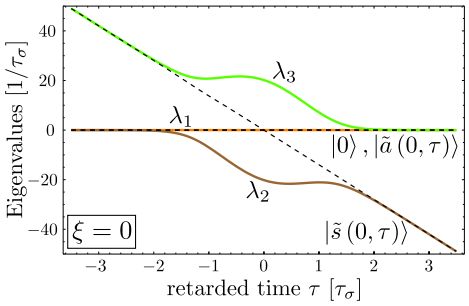

Figure 4.3: Eigenvalues of the Hamiltonian $\hat{\mathcal{H}}_{sa}$ (Eq. (4.14a)) which describes the atom-laser system at the boundary of the medium ($\xi = 0$). The eigenvalues belonging to the diabatic states are plotted with dashed lines which correspond to states $|0\rangle$, $|\tilde{s}\rangle$ and $|\tilde{a}\rangle$, respectively. The eigenvalues of the adiabatic states are plotted with solid lines. The antisymmetric state $|\tilde{a}\rangle$ is an eigenstate of the Hamiltonian $\hat{\mathcal{H}}_{sa}$ with an eigenvalue of $\lambda_1 = 0$. The eigenstate belonging to λ_2 evolves from the excited state $|0\rangle$ to the symmetric state $|\tilde{s}\rangle$, while the other eigenstate belonging to λ_3 follows the inverse path ($|\tilde{s}\rangle \rightarrow |0\rangle$).

in perfect agreement with the numerical solution of the master Eq. (4.5) at $\xi = 0$, which is depicted in Fig. 4.4.

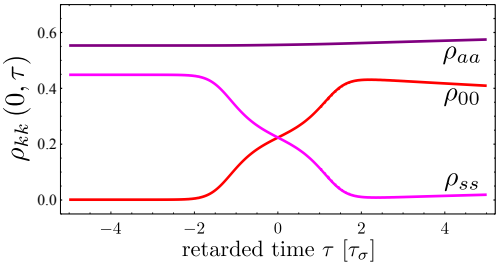

Figure 4.4: Dynamics of the atomic populations in the symmetric-asymmetric basis at the boundary of the medium. The parameters used for calculation are $\vartheta_1 = 30\,[1/\tau_\sigma]$, $\vartheta_2 = 27\,[1/\tau_\sigma]$, $\beta = 7\,[1/\tau_\sigma^2]$.

In order to understand the laser propagation, it is important to analyze the time evolution of the coherences ρ_{0a} and ρ_{0s}. The behavior of the absolute values of the coherences (see Fig. 4.5(a)) are easily understood from the predictions of the adiabatic approximation. Since there is a complete population transfer between states $|s\rangle$ and $|0\rangle$, the absolute value of the coherence between them is 0 in the beginning and at the end of the interaction, and only differs from zero during the population transfer with a maximum value of $\vartheta_2^2/(2\vartheta^2)$. The time evolution of $|\rho_{0a}|$ is determined by the change of the population of the excited state $|0\rangle$ in time, since the population of state $|a\rangle$ remains unattached, as it is a dark eigenstate of the dressed atoms at the boundary of the medium.

In parallel with the excitation of the atom, a coherence $\rho_{0a} = \vartheta_1\vartheta_2/\vartheta^2$ is established as a result of the interaction. The time evolution of the phase of ρ_{0s} is determined by the phase of the coupling

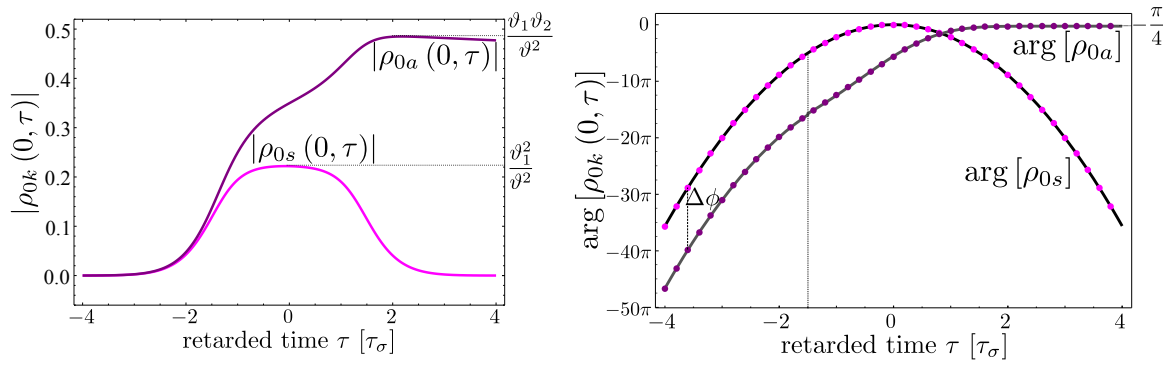

(a) (b)

Figure 4.5: Time evolution of a.) the absolute value and b.) the phase of the atomic coherences at the boundary of the medium. For the absolute values of the coherences, the solid lines show the result of the numerical solution of the master equation for $\xi = 0$ using the same parameters that are given in Fig. 4.4. In the case of the phase of the coherences, the dots represent the result of the numerical solution, and the solid lines are the fitted functions: The function $\beta_0 + \beta_1\tau^2$ is fitted on the values of $\rho_{0s}(\xi = 0, \tau)$ and on $\rho_{0a}(\xi = 0, \tau < -1.5\tau_\sigma)$ with the fitting parameters of $\{\beta_1^s = -6.99, \beta_0^s = 0.04\}$ and $\{\beta_1^a = -7.01, \beta_0^a = -34.35\}$, with $\beta_0^s - \beta_0^a = \Delta\phi = 10\pi + 0.95\pi$. A different function determines the time evolution of $\rho_{0a}(\xi = 0, \tau > -1.5\tau_\sigma)$: the function $\alpha_0 + \alpha_1 \exp(-\pi \exp[\alpha_2\tau]/2)$ is fitted on the values, with the parameters $\{\alpha_0^{a0} = -0.78, \alpha_1^{a0} = -80.12, \alpha_2^{a0} = 0.76\}$

pulse Ω_s, which is set to be linearly chirped. Indeed, it is clearly seen from Fig 4.5(b) that the quadratic function $\beta_0 + \beta_1\tau^2$ accurately fits the numerically calculated results of $\arg(\rho_{0s})$. The behavior of the phase of the coherence between the excited and the asymmetric ground state ρ_{0a} is more complicated. Its time function starts as the same quadratic one as for ρ_{0s}, but the evolution changes approximately at $\tau = -1.5\tau_\sigma$, and it tends to a constant value as $\alpha_0 + \alpha_1 \exp(-\pi \exp[\alpha_2\tau]/2)$. Note that the complex phase functions can be tuned by $n \times 2\pi$, $n \in \mathbb{Z}$, thus the fitting parameters β_0 and α_0 are undetermined up to a free constant times 2π.

4.1.3 Dynamics of the atoms inside the medium

Let us now consider the time and space evolution of the effective Rabi frequencies Ω_s and Ω_a. In the symmetric-antisymmetric basis, only one strong coupling field (Ω_s) enters the medium of Λ-atoms, which are prepared in a superposition of states $|a\rangle$ and $|s\rangle$ (c.f. Eq. (4.12)). In the course of the coherent transition process between the atomic states induced by Ω_s, a coherence is established between the asymmetric and the excited state of the atoms close to the boundary, with a time function of its phase described in the previous subsection (c.f. Fig 4.5). This coherence generates the laser field Ω_a, which strongly influences the transition process between the atomic states in the

further part of the medium (see Fig. 4.6). Namely, the majority of the population is transferred into the asymmetric state $|a\rangle$, and the excitation of the atom is drastically reduced (it does not exceed 5% during the whole interaction). Thus, although complete population trapping is not established as in the case of the constant frequency matched pulses [96], a quasi-dark state is created by the two modes Ω_s and Ω_a. The absolute values of the atomic coherences ρ_{0a} and ρ_{0s} become smaller for

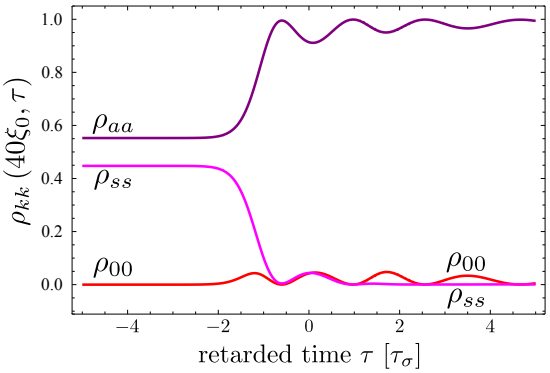

Figure 4.6: Dynamics of the populations of the atomic states inside the medium ($\xi = 40\xi_0$) in the symmetric-asymmetric basis. The parameters used for the calculation are the same as given in Fig. 4.4.

atoms at larger propagation distance ξ, and the time function of their phases has the same character at any propagation length (see Fig. 4.7). An important difference can be observed compared with the case of $\xi = 0$: at the time points where $|\rho_{0a}| = 0$, there is a jump of π in the phase $\arg(\rho_{0a})$. This jump occurs because the sign of the coherence changes at these points, which indicates an oscillating behavior of the populations and coherences induced by the interaction with the pulse pair of Ω_s and Ω_a. The time evolution of the absolute values and phases of the effective Rabi frequencies Ω_a and Ω_s at a given space point of the medium ($\xi = 40\xi_0$) is presented in Fig. 4.8. The coupling field Ω_s is only slightly modified during the propagation. The pulse envelope remains Gaussian with a good approximation after a propagation of multiple times of the absorption length ξ_0. The change in the envelope of the effective Rabi frequency Ω_s is presented in the inset of Fig. 4.8(a). It can be observed that after $40\xi_0$ of propagation, the distortion from the boundary condition is less than 4% of the pulse area. The phase function with respect to time inside the medium also has the same character as at the boundary: the same quadratic function $\beta_0 + \beta_1\tau^2$ fits the data in Fig. 4.8(a), so the frequency of this effective field changes linearly in time. Thus, the incoming laser mode Ω_s preserves its initial properties during the propagation in the medium, with only a small loss in the pulse envelope. It is worth noticing that the presence of this loss is crucial for this quasi-lossless propagation mechanism,

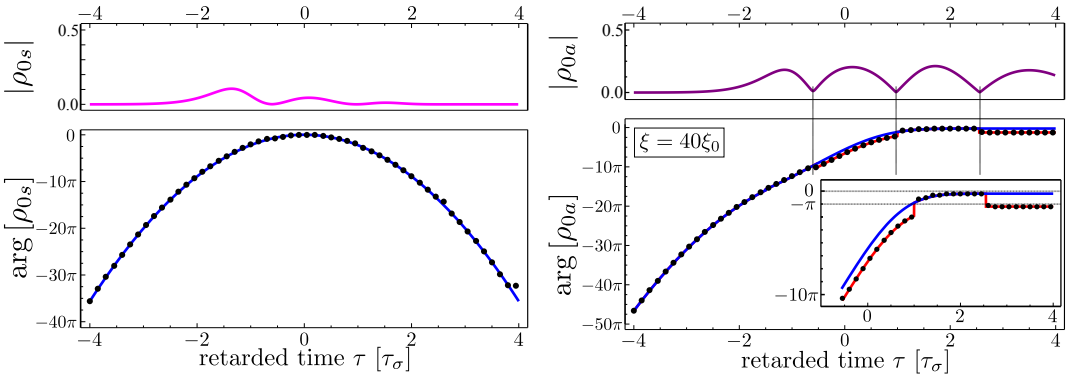

(a) (b)

Figure 4.7: Time evolution of the absolute values and phases of the atomic coherences ρ_{0s} (a.) and ρ_{0a} (b.) inside the medium ($\xi = 40\xi_0$). (Inset: Magnification of the plot showing the time evolution of the phases between $\tau = -1$ and $\tau = 4$.) The solid lines in case of the absolute values and the dots in case of the phases are results of numerical calculation with the same parameters as in Fig. 4.4. The solid lines that connect the dots are functions fitted on the points. The same fitting functions were used as in case of the coherences at the boundary (see Fig. 4.5) and the fitting parameters also proved to be the same. The only exception is β_0 which needs to be shifted by π at the point where there is a jump in the data.

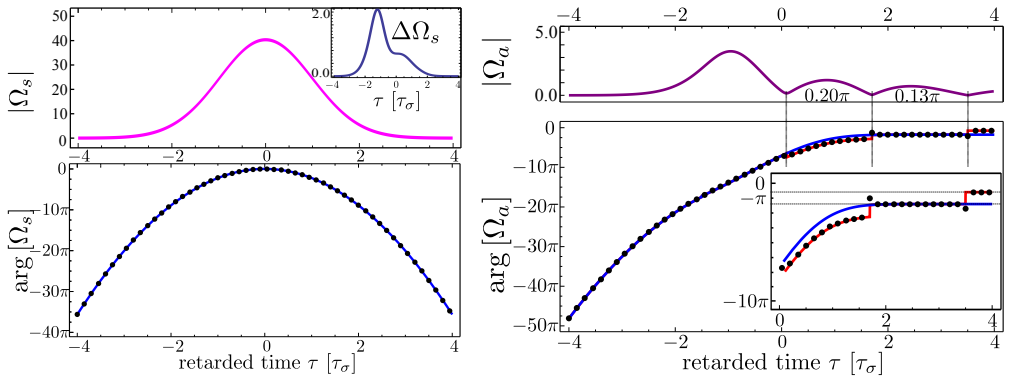

(a) (b)

Figure 4.8: Absolute values and phases of the effective Rabi frequencies Ω_s (a.) and Ω_a (b.) as a function of the retarded time at a fixed space point inside the medium ($\xi = 40\xi_0$). (Inset: Magnification of the plot showing the time evolution of the phases between $\tau = -1$ and $\tau = 4$.) The parameters used for the calculation are the same as given in Fig. 4.4. The solid lines in case of the absolute values and the dots in case of the phases are results of the numerical calculation. The solid lines that connect the dots are functions fitted on the points. The same fitting function was used as in case of the coherences, except for the constants, which are shifted by $3\pi/2$ (see Fig. 4.5)

because the generated field Ω_a gains its energy from it. Since the source of this field in the Maxwell equation is proportional to the coherence between the excited and the asymmetric ground state $|a\rangle$, it is plausible that the phase evolution of both the Rabi frequency Ω_a and the coherence ρ_{0a} possess a very similar character (c.f. Figs 4.7(b) and 4.8(b)). As it is demonstrated in Fig. 4.8(b), the same

curve fits the numerical values of Ω_a as in the case of the coherence ρ_{0a} at the boundary as well as inside the medium, with almost the same fitting parameters. The only difference is a shift of $-3\pi/2$ in the constant parameters α_0 and β_0. Similarly to the coherence ρ_{a0}, the induced Rabi frequency Ω_a shows an oscillatory behavior, and there is a phase-jump of π in the phase at every retarded time point where $\Omega_a = 0$. The time evolution of its phase is close to constant for approximately $\tau > 1.5\tau_\sigma$. This means that the excited and the asymmetric ground states $|0\rangle$ and $|a\rangle$ are coupled by a train of small resonant pulses having nearly constant frequency, with a phase difference of π between the adjoining pulses. The pulse areas of these small pulses are much less than π, thus as a result of the interaction with one pulse, a small part of a Rabi-cycle proceeds between states $|0\rangle$ and $|a\rangle$. After this interaction, the process is reversed because of the next pulse which has an opposite sign (π phase-shift). Once this oscillation appears in the coherence ρ_{0a}, it affects the formation of the field Ω_a, that is why the further this pulse propagates the smaller pulses appear (see Fig. 4.9).

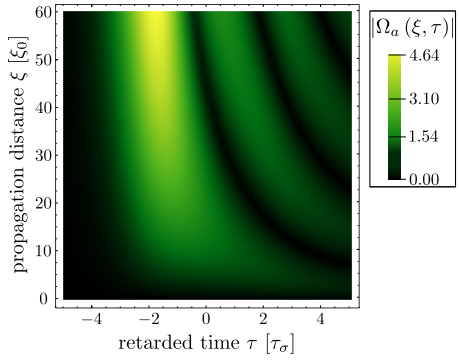

Figure 4.9: Absolute value of the effective Rabi frequency Ω_a as a function of the retarded time coordinate and the propagation distance. The parameters used for the calculation are the same as in Fig. 4.4.

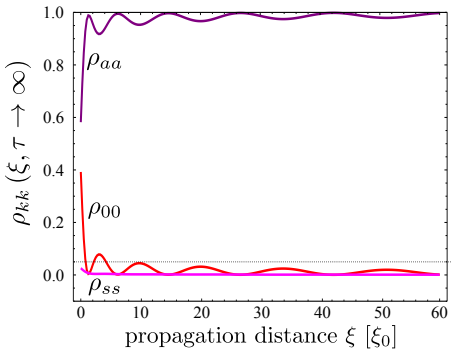

Figure 4.10: Final populations of the atoms at different space points ξ in the symmetric-antisymmetric basis. The same parameters were used for the calculation as in Fig. 4.4.

Our calculations show that the population control process induced by the laser pulse pair changes in the course of their propagation in the medium. At the boundary and within one absorption length ξ_0, a significant part of the population is transferred into the excited state. After a few absorption lengths, the excitation of the atom decreases, and although shows an oscillatory behavior, it is always below 5% for atoms that are located at space positions $\xi > 6\xi_0$ (see Fig. 4.10).

Notice that from a small distance away from the boundary, the final population of the symmetric state $|s\rangle$ is zero (up to the precision of the calculation). It is an important feature, because it means that the final population distribution among the atomic ground states is exactly determined by the

antisymmetric superposition $|a\rangle$. This property is different compared to the case of the matched pulses with constant frequency [96], where a small amount of population is always transferred into the symmetric state. From the temporal behavior of the eigenvalues of the interaction Hamiltonian $\hat{\mathcal{H}}_{sa}$ (see Fig. 4.11) one can see that frequency modulation is the cause of the difference. It is known from the literature (see e.g. [130] and references within) that in the constant-frequency case, the transparency occurs through a STIRAP-like mechanism. Namely, as a result of the action of the atoms of the medium, one of the coupling pulses is shifted in time so that population trapping is established, and the excited state is decoupled from the system. The final distribution of the population among the ground states is determined by the intensities of trailing edges of laser pulses [92], which may significantly vary at different locations.

On the other hand, the frequency modulation of the incoming laser mode Ω_s defines a different transfer process in the atoms of the medium. We have already seen that at $\xi = 0$ there is an avoided crossing between two eigenvalues (λ_2 and λ_3) with a gap between them. This gap is large enough to restrain the mixing of the populations initially set into the eigenstates belonging to the two eigenvalues (let us denote them by $\vec{v}_2$ and $\vec{v}_3$, respectively), that is why it is possible to use the adiabatic approximation. If we regard the eigenvalues of the interaction Hamiltonian which describes the dynamics inside the medium ($\xi \gg \xi_0$), we notice that a practically same gap characterizes the spectrum, so the subspace spanned by $\vec{v}_2$ is separated just like for the Hamiltonian at $\xi = 0$. The difference between the eigenvalues typical for $\xi = 0$ and $\xi \gg \xi_0$ is caused by the appearence of the coupling field Ω_a, which is generated by the back-action of the atoms of the medium. In the presence

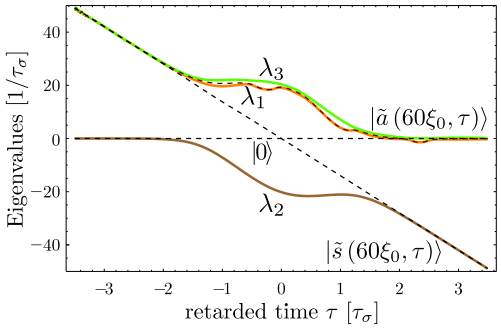

Figure 4.11: Eigenvalues of the Hamiltonian $\hat{\mathcal{H}}_{sa}$ (Eq. (4.14a)) which describes the atom-laser system far from the boundary of the medium ($\xi = 40\xi_0$). The notations are the same as in Fig. 4.3

of the coupling Ω_a, the space of states is divided to a temporarily degenerate subspace spanned by the eigenstates $\vec{v}_1$ and $\vec{v}_3$ belonging to the eigenvalues λ_1 and λ_3, and to the subspace of $\vec{v}_2$. As the

atoms are prepared in the superposition of $|a\rangle$ and $|s\rangle$, the whole process takes place in the former subspace, which indicates that the population of the symmetric state $|s\rangle$ becomes 0 at the end of the interaction. (However, because of the degeneracy, the suppression of the excitation cannot be explained in the frame of this adiabatic picture.)

4.1.4 Description of the system in the original basis

From the point of view of possible applications it is useful to "translate" our results into the symmetric-asymmetric basis and with the effective couplings Ω_a and Ω_s to the original atomic basis. In Fig. 4.12 the population transfer process is presented in the original atomic basis at the boundary and at a given propagation length inside the medium ($\xi = 40\xi_0$). At the boundary, the Raman-resonant pulse pair induces a coherent population transfer which distributes the population initially prepared in state $|2\rangle$ into a superposition of the three atomic states. The population of the excited state as a result of the interaction with the pulse pair is $\rho_{00} = \vartheta_2^2/\vartheta^2$ coinciding with the population of state $|s\rangle$ at the beginning of the interaction, while the populations that remain in the ground states after the population transition process are $\rho_{11} = \left(\vartheta_1^2\vartheta_2^2\right)/\vartheta^2$ and $\rho_{22} = \vartheta_1^4/\vartheta^2$, respectively (which coincides with the initial population of the asymmetric state $|a\rangle$).

Note that the requirement of Raman resonance between the couplings plays an important role in the whole process. That is, a substantially different population evolution is induced by Raman-detuned couplings of the two allowed transitions [77], which leads to population transfer between the ground states, along with negligible excitation of the atom. Thus, in the Raman-detuned case, the initial preparation of the atoms (Eq. (4.7)) coincide with the dark state, and, as it was shown in [91], results in a quasi-lossless propagation of the coupling FC pulse in the medium accompanied by the same induced population transfer mechanism inside as at the boundary. In contrast, in the present case including Raman-resonant coupling, both the pulse envelopes and the time function of the phases of the pulses are modified by the interaction with the medium after a short propagation length. The modification takes place in such a way that instead of exciting the atom, the pulses drive the main part of the population into the $\left(\vartheta_2|1\rangle - \vartheta_1|2\rangle\right)/\vartheta$ superposition of the ground states, which is the asymmetric state $|a\rangle$ (see Fig. 4.14).

Note that, similarly to the constant frequency case [96], not all the population is transferred to

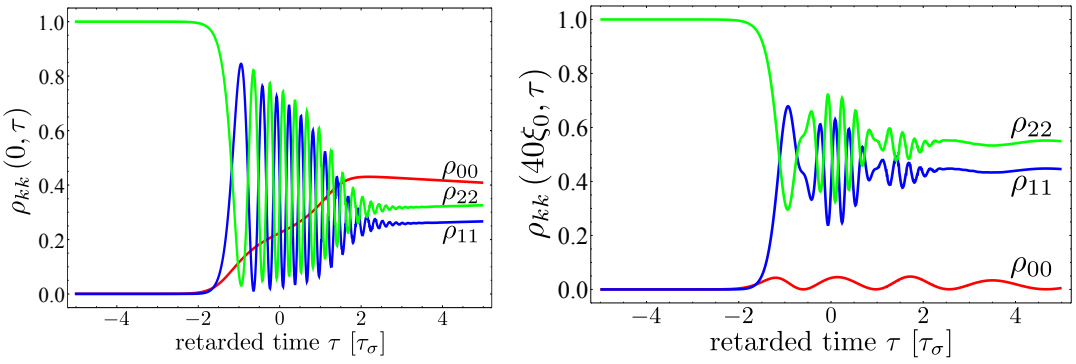

(a) (b)

Figure 4.12: Evolution of the populations as a function of the retarded time τ a.) at the boundary and b.) at a typical propagation length inside the medium ($\xi = 40\xi_0$). The parameters used for the numerical calculations are the same as in Fig.4.4.

the asymmetric superposition. In case of the FC pulse pair it is the excited state which is slightly populated but in the weakly decaying regime under consideration this does not disturb significantly the preparation of the medium into a well-defined superpositional state controlled by the peak Rabi frequencies of the ingoing pulses, as is shown in Fig. 4.13(a). Fig. 4.13(b) demonstrates the advantage of the frequency modulation of the laser pulses. Since the matched pulses having constant frequency transfer a varying (though small) amount of population into the symmetric superposition $|s\rangle$ in case of atoms at different space points ξ, the induced population distribution among the atomic states changes significantly as a function of ξ (see Fig. 4.13(b)). The Rabi frequencies can be expressed

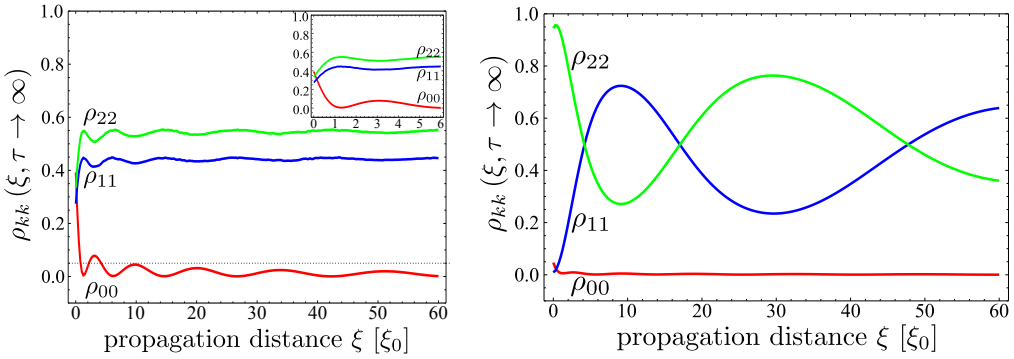

(a) (b)

Figure 4.13: Final populations of the atoms at different space points ξ in case of a.) frequency-chirped b.) constant frequency pulse pair. Inset: Final populations close to the boundary ($\xi \leq 6\xi_0$) for a FC pulse pair. After a few absorption length ξ_0 of propagation, the FC pulse pair transfers the majority of the atomic population to the antisymmetric superposition of the ground states, while in case of the matched pulses having constant frequency, the final state strongly varies with ξ. The parameters used for calculations are: $\vartheta_1 = 30\,[1/\tau_\sigma]$, $\vartheta_2 = 27\,[1/\tau_\sigma]$, $\beta = 7\,[1/\tau_\sigma^2]$ and $\beta = 0$, respectively.

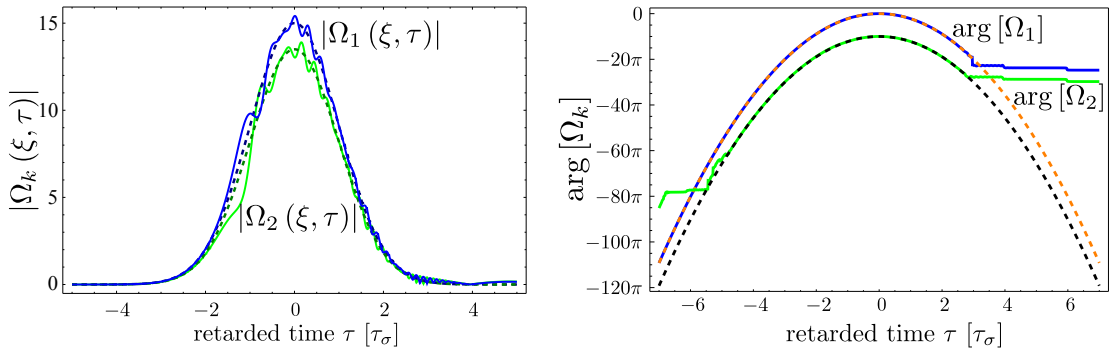

(a) (b)

Figure 4.14: a.) Envelope functions of the pulses at the boundary (dashed lines) and at $\xi = 40\xi_0$ (solid lines) b.) The phases of the Rabi frequencies as a function of the retarded time τ at the boundary (dashed lines) and inside the medium (solid lines). The same parameters were used for numerical calculation as given in the caption of Fig.4.4.

by the symmetric and asymmetric Rabi frequencies as

$$\Omega_1 = \frac{\vartheta_1}{\vartheta}\Omega_s + \frac{\vartheta_2}{\vartheta}\Omega_a \tag{4.14a}$$

$$\Omega_2 = \frac{\vartheta_2}{\vartheta}\Omega_s - \frac{\vartheta_1}{\vartheta}\Omega_a. \tag{4.14b}$$

As the pulses propagate in the medium, energy is transferred from Ω_2 (which couples the transition where the atoms are prepared) to Ω_1. Since Ω_a is one order of magnitude weaker than Ω_s, even after propagation length of many times ξ_0 (c.f. 4.8), the distortion is small. In this sense it can be stated that the FC pulse pair propagates quasi-transparently and that it can prepare a well-defined coherent superposition of the ground states in an extended medium of great optical depth.

4.1.5 Summary

We have analyzed the propagation of a pair of Raman-resonant, linearly frequency modulated strong laser pulses in an optically thick medium, which is modeled as a motionless and noninteracting ensemble of Λ-atoms. We have demonstrated that quasi-lossless propagation of FC pulses is possible not only when the medium is initially prepared in a quasi-dark state [91], but through a *matching* effect between the two pulses. Namely, although the Raman-resonant pulse pair causes a significant excitation in the atoms close to the boundary of the medium, the excitation of the atoms becomes negligible in the medium at larger propagation length. Excitation of the atoms near the boundary

of the medium, however, plays an important role in generation of a macroscopic polarization, which interaction with the FC pulses results in the matched quasi-lossless propagation of the pulses in the optically thick medium.

By analyzing the dressed states of the atoms, we have demonstrated that the FC pulse pair induces a population transfer mechanism substantially different from the transfer process typical for the matched pulses having constant carrier frequency. The FC pulse pair, in the course of its propagation transfers the majority of the atoms of the medium into approximately the same coherent superposition of their ground states. In contrary, the population distribution among the ground states induced by the constant frequency pulse pair may change significantly at different locations in the medium.

We have shown that the composition of the coherent superposition, established by the propagating FC pulse pair, depends on the peak amplitudes of the these laser pulses at the boundary of the medium. Therefore, the magnitude of the coherence created by the interaction may be tuned by parameters which are easily controllable experimentally.

The obtained results, especially those concerning the robust creation of coherence between atomic metastable (ground) states in a spatially extended, optically thick medium may find important applications in schemes of frequency conversion through nonlinear optical mixing processes, as well as in other nonlinear processes where the initial preparation of an extended medium in a coherent superposition state is needed.

Summary

Control of atoms or atomic ensembles by laser radiation is an important and quickly developing field of quantum optics, which serves as a basic tool in numerous significant fields of modern physics, such as trapping and cooling of atoms and molecules [10–13], nonlinear optics[24–38], processing of optical information [17, 21–23], quantum computation [14–20] and many others.

One of the main tasks to achieve is coherent preparation of the atomic inner state, that is, the state of the valence electron of the atom, for which a large variety of techniques exists. A laser pulse, resonant with an atomic transition, induces Rabi oscillation occurs between the population of the atomic states. The population distribution established by the laser depends on the area of the Rabi-frequency. Complete population inversion may be established for example, if this area equals $(2k+1)\,\pi, k \in \mathbb{N}$. However the sensitivity of this scheme to variations of the pulse area and the resonance conditions results in difficulties in experimental realization [39].

More robust control of the atomic states are allowed by adiabatic control(AC) schemes[40–42] which are based on gradually tuning one of the interaction parameters in time in order to drive the atomic populations along the adiabatic states of the system.

One of the most-used AC schemes is Stimulated Raman Adiabatic Passage (STIRAP) [40, 41, 45–52], where the control of the states of a Λ-atom is achieved by two, constant-frequency laser pulses, time-delayed in the counter-intuitive order. Being sensitive to the two-photon resonance conditions, this scheme allows complete population transfer between the ground states, without excitation of the atom. With some extensions to the STIRAP scheme [53–59], coherence creation among the atomic states is also possible.

Another, widely applied AC method is rapid adiabatic passage (RAP), which is based on varying the detuning between the frequency of the interacting laser fields and the atomic transitions in time [60]. One possibility is using laser fields with constant carrier frequency and shifting the energy

level of the atomic excited state, as it happens in case of Stark chirped rapid adiabatic passage (SCRAP)[61–66] by making use of the Stark-effect. This method is not sensitive to the resonance conditions, but the population transfer occurs along with temporary excitation of the atom.

An alternative method for preforming ARP is the application of frequency-modulated (chirped) laser pulses in the atom-laser interaction [67–80]. Several arrangements were proven useful[12, 70, 73–78, 81–85] for various control problems by using FC pulses. A group of these works concentrated on coherent population using one FC pulse transfer between ground states of Λ [74, 77]- and tripod-atoms [78], with the priority of avoiding the excitation of the atom, in optically dilute and, for Λ-atoms [91], optically thick medium. On the other hand, it was also shown that by using more than one laser modes, a greater freedom is achievable in controlling the induced population distributions in Λ-atoms [73, 75]. Altough this scheme has the drawback of populating the atomic excited state it was proposed to be applied for optical information mapping.

Objectives

Motivated by these results, this dissertation concentrated, on one hand, on upgrading the previous control schemes using FC pulses in order to unify their advantages. That is, one of our objectives was to develop a control scheme using a limited number of FC pulses which possesses the following characteristics. It is suitable for creating coherent superposition of the ground state of the atom, which can be adjusted by easily controllable parameters of the interacting laser pulses such as the peak intensities or constant phase difference. In order to avoid decoherence effects due to the finite lifetime of the excited state, we put emphases on avoiding the excitation of the atom.

Another goal was to widen the range of possible applicability of FC pulses by combining them with constant-frequency pulse. We aimed to consider control schemes in Λ-atoms which incorporate instantaneous Raman-resonance and to prove them useful in applications.

In optically thick medium, the coherent control processes may be modified by the back-action of the medium on the interacting pulses and other propagation effects. For nonlinear optical applications it is necessary to take these effects into consideration. In our work, we would also like to discover an interaction scheme using FC pulses which is applicable for preparing the majority of the atoms in a coherent superposition of their ground states, in an externally adjustable way if possible.

We have already given a detailed summary on our results at the end of each chapter. Here, let us formulate our achievements in theses.

Theses of the dissertation

1. We have proposed a new interaction scheme for creating coherent superposition among the metastable ('ground') states of an atom having tripod-structure as working levels ('tripod-atom'), along with negligible excitation. The method is based on adiabatic control of the atomic states by three laser pulses with the same (linear) modulation ('chirp') in their carrier frequencies, each of them separately coupling one dipole allowed transition of the atom. We have shown by analyzing the time evolution of the adiabatic states that if two pulses are in Raman resonance with the corresponding atomic transitions and the third one is Raman-detuned, two different population-redistribution mechanism may be achieved by changing the sign of the Raman detuning, without significant population appearing in the excited state during the interaction.

   By numerically solving the master-equation of the system, we have demonstrated that the scheme can be used even if the lifetime of the excited state is a tenth of the interaction time. We have found that coherence can also be created between the ground states in the presence of stronger spontaneous decay from the excited state, with a π phase factor of difference compared to the non-decaying case.

   We have demonstrated that the presented scheme may be applicable in (optically dilute) atomic gas of room temperature in case of fast enough frequency modulation and copropagating pulses, since the chirp is capable to compensate for the Doppler-effect. [I, II]

2. We have proposed a method for robust writing and storage of optical phase information into the populations of the ground states of a tripod atom using three frequency-chirped laser pulses, two in Raman resonance and the third Raman-detuned from the corresponding atomic transition (the same arrangement as in thesis 1). The scheme is based on the fact that after preparing the atom in a coherent superposition of the two ground states coupled by two pulses in Raman resonance, the population of the third ground state established by the interacting pulses is a cosine-function of the phase difference of the pulses in Raman resonance. Since the

information is mapped into the population of the atomic ground states, the proposed method provides much longer storage times compared with the schemes based on the collective atomic spin coherences, being only restricted by the lifetime of the ground states.

We have shown that the presence of weak longitudinal and transverse relaxation affects the contrast of the mapping process: 50% of contrast can be achieved if the duration of the interaction is smaller than a tenth of the coherence lifetime and 10 times of the lifetime of the excited state, respectively [III].

3. We have demonstrated that a pair of laser pulses, one with constant and the other with monotonicly modulated carrier frequency establishes a maximum coherence between a ground and the excited state of a λ-atom. The initially unpopulated ground state is resonantly coupled by a constant-frequency laser pulse to the excited state, forming an Autler-Townes doublet, while the other pulse having a frequency sweeping through one-photon and two photon resonance adiabatically transfers the population from the ground state to that member of the doublet with which it first becomes resonant with. We have shown that this mechanism, provided that the resonance condition of the constant-frequency pulse is fulfilled, is extremely robust against the parameters of the laser pulses such as the Rabi-frequencies or the chirp rate [IV].

4. We have proposed a novel scheme for creating coherent superposition between two magnetic sublevels of the $F = 1$ hyperfine ground state of ^{87}Rb atoms. It is based on the interaction of the atom with a frequency-modulated (chirped) laser pulse having σ^+ and a pulse of a constant carrier-frequency having σ^- circular polarization, both far detuned from one-photon resonance but the chirped pulse sweeping through two-photon resonance. Taking into account all the possible atomic transitions allowed by the selection rules, we have shown numerically that the scheme yields a maximum possible degree of coherence of superposed states with negligible atomic excitation, which eliminates decoherence by spontaneous emission [V].

5. We have demonstrated a matching effect for a pair of frequency-modulated (chirped) Raman-resonant laser pulses that simultaneously propagate in an optically thick medium of lambda-structured atoms. That is, the laser pulses become distorted by the interaction with the medium in such a way that it no longer causes excitation in the atoms, reducing the back-

action of the atoms on the pulses and allowing a quasi-lossless propagation. By introducing a coordinate transformation, we separated a symmetric and an antisymmetric coupled modes of the lasers and the amplitudes of the atomic states, with the antisymmetric laser mode being zero at the boundary of the medium. We have shown that due to the excitation of the atoms at the boundary, the antisymmetric laser mode is generated, changing the population transfer mechanism in a way that the majority of the population is transferred into the same coherent superposition of the atomic ground states all throughout the medium. We have also shown that the composition of this coherent superposition can be controlled by the peak amplitudes of the laser pulses at the boundary of the medium [VI,VII].

List of publications

Publications related to the theses:

[I] N. Sandor, J. S. Bakos, Zs. Sörlei, and G. P. Djotyan,Creation of coherent superposition states in inhomogeneously broadened media with relaxation. J. Opt. Soc. Am. B, 28:2785-2796, (2011).

[II] N. Sandor, J. S. Bakos, Zs. Sörlei, and G. P. Djotyan. Creation of coherent superpositions between metastable atomic states in doppler-broadened media. J. Phys. - Conf. Ser., 350:012002, (2012).

[III] G. P. Djotyan, N. Sandor, J. S. Bakos, and Zs. Sorlei. Optical phase information writing and storage in populations of metastable quantum states. J. Opt. Soc. Am. B., 26:1959-1966, (2009).

[IV] G. P. Djotyan, N. Sandor, J. S. Bakos, and Zs. Sörlei. An extremely robust strong-field control of atomic coherence. Opt. Exp., 19:17493-17499, (2011).

[V] G. P. Djotyan, N. Sandor, J. S. Bakos, Zs. Sörlei, W. Gawlik, A. Wojciechowski, J. Zachorowski, S. Pustelny, G. Yu. Kryuchkyan. Creation and measurement of coherent superposition states in multilevel atoms. Proc. SPIE 01/2011; 7998:79981A- 1. (2011).

[VI] N. Sandor, G. P. Djotyan. Propagation of Raman-resonant frequency chirped laser pulses in a medium of lambda-atoms. Proc. SPIE 8773; 87730Z (2013).

[VII] N. Sandor, G. Demeter, D. Dzsotjan, G. P. Djotyan. Matched propagation of Raman-resonant frequency chirped laser pulses. Under publication in Phys. Rev. A, arXiv:1302.7266 [quant-ph]

Other publications:

[VIII] G. P. Djotyan, J. S. Bakos, Zs. Sörlei, G. Demeter, N Sandor, D. Dzsotjan, M. A. Kedves, B. Raczkevi, P. N. Ignacz, and J. Szigeti. Modern Optics and Photonics - Atoms and Structured Media, chapter Frequency chirped laser pulses in atomic physics: Coherent control of inner and translational quantum states, pages 77-91. Singapore: World Scientific, (2010).

[IX] G. P. Djotyan, N. Sandor, J. S. Bakos, and Zs. Sörlei. Optical storage in quantized media. Proc. SPIE, 8414: 84140X, (2011).

[X] G. P. Djotyan, J. S. Bakos, Zs. Sörlei, G. Demeter, N. Sandor, D. Dzsotjan, M. A. Kedves, and B. Raczkevi. Atom physics with frequency chirped laser pulses. In Proceedings of the International Conference LASER-PHYSICS-2009, p. 21-24, Astharak, Armenia, (2009).

[XI] G. P. Djotyan, N Sandor, J. S. Bakos, and Zs. Sörlei. Optical phase information writing and storage in populations of metastable quantum states. In A Papoyan, E Sharoyan, R Kostanyan, G Grigoryan, editor, Proceedings of the Conference on Laser Physics-2008, p. 166-169, Astharak, Armenia, (2009).

[XII] G. P. Djotyan, N. Sandor, J. S. Bakos, Zs. Sörlei, and D. Dzsotjan Robust optical information writing in populations of metastable quantum states. In Laser Physics 2008. 40th National Conference Ashtarak, Astharak, Armenia, (2008).

[XIII] G. P. Djotyan, J. S. Bakos, Zs. Sörlei, D. Dzsotjan, N. Sandor, A. P. Jotyan, and A. A. Avetisyan All-optical writing and storage of images using multilevel quantum systems and frequency-chirped laser pulses. In Proceedings of Conference on Laser Physics, Astharak, Armenia, (2007).

Acknowledgment

I would like to thank my supervisior, Gagik Djotyan for his guidance throughout my years at the Wigner Research Center for Physics. Without his professional and personal support this work could not have been completed. Besides the knowledge that he gave me I am grateful for his optimism and patience.

I would also like to express my gratitude towards every member of the "Cold plasma and atomic physics" group for creating a friendly and supportive atmosphere. In particular, I would like to thank Zsuzsa Sörlei and József Bakos for sharing their experience about Physics and scientific life, David Dzsotjan for his personal encouragement and Gábor Demeter for carefully reading the manuscript and adding his indispensable comments and suggestions to it.

I would like to express my gratitude towards all members of the Department of quantum optics and quantum information in the SZFI for very entertaining group seminars and for many interesting and enthusiastic discussions about various subjects.

Last, but not least, I would like to thank my husband, my parents, my sister, my brother and my friends for believing in me, encouraging me and providing their loving understanding and generous support.

Appendix

A.1 Basis transformation

Let us assume that we wish to perform a time-dependent unitary basis-transformation on the system:

$$\hat{\mathcal{V}}(t) : \{|a_0\rangle, |a_1\rangle, \dots |a_N\rangle\} \to \{|b_0\rangle, |b_1\rangle, \dots |b_N\rangle\}\,. \tag{A.15}$$

Then, as it is well-known from basic linear algebra, the coefficient vector of state $|\psi\rangle$ and the coefficient matrix of an operator, for example the density operator $[\hat{\rho}]$ is transformed as

$$[\psi]_b = \left[\mathcal{V}^\dagger\right] \cdot [\psi]_a\,, \tag{A.16a}$$

$$[\rho]_b = \left[\mathcal{V}^\dagger\right] \cdot [\rho]_a \cdot [\mathcal{V}]\,, \tag{A.16b}$$

where [.] denotes the coefficient matrix of any vector or operator. However, because of the time dependence of the transformation operator, the coefficient matrix of the Hamiltonian does not follow the transformation rule given in Eq. (A.16b). Now we develop the transformation rule for the Hamiltonian from the Schrödinger and the von Neumann equations.

The Schrödinger equation in the basis $\{|a_j\rangle \mid j \in \{1, 2, \dots n\}\}$ basis reads as

$$i\hbar\partial_t [\psi]_a = [H]_a \cdot [\psi]_a\,, \tag{A.17}$$

where the coefficient matrix of the Hamiltonian given in the "a" basis is denoted by $[H]_a$. After

substituting Eq.(A.16a) into Eq. (A.17), we obtain the followings

$$
\begin{aligned}
&i\hbar\left([\mathcal{V}]\cdot\partial_t[\psi]_b+\partial_t[\mathcal{V}]\cdot[\psi]_b\right)=[H]_a\cdot[\mathcal{V}][\psi]_b \qquad /\left[\mathcal{V}^\dagger\right]\cdot\\
&i\hbar\partial_t[\psi]_b=\left(\left[\mathcal{V}^\dagger\right]\cdot[H]_a\cdot[\mathcal{V}]-i\hbar\left[\mathcal{V}^\dagger\right]\partial_t[\mathcal{V}]\right)[\psi]_b,
\end{aligned}
$$

so the Hamiltonian in the "b" basis reads as

$$
[H]_b=\left[\mathcal{V}^\dagger\right]\cdot[H]_a\cdot[\mathcal{V}]-i\hbar\left[\mathcal{V}^\dagger\right]\partial_t[\mathcal{V}]. \tag{A.18}
$$

Now let us show that the transformation rules given in Eqs. (A.16b) and (A.18) are consistent with the von Neumann equation for pure states. The generalization for mixed states is straightforward. The von Neumann equation given in the "a" basis reads as

$$
i\hbar\frac{\partial[\rho]_a}{\partial t}=[[H]_a,[\rho]_a]. \tag{A.19}
$$

Substituting Eq. (A.16b) into Eq. (A.19), we get

$$
\begin{aligned}
&i\hbar\left(\partial_t[\mathcal{V}]\cdot[\rho]_b\left[\mathcal{V}^\dagger\right]+[\mathcal{V}][\rho]_b\cdot\partial_t\left[\mathcal{V}^\dagger\right]+[\mathcal{V}]\left(\partial_t[\rho]_b\right)\left[\mathcal{V}^\dagger\right]\right)=[H]_a[\mathcal{V}][\rho]_b\left[\mathcal{V}^\dagger\right]-[\mathcal{V}][\rho]_b\left[\mathcal{V}^\dagger\right][H]_a\\
&i\hbar\frac{\partial[\rho]_b}{\partial t}=-i\hbar\left(\left[\mathcal{V}^\dagger\right]\partial_t[\mathcal{V}]\cdot[\rho]_b+[\rho]_b\cdot\underbrace{\partial_t\left[\mathcal{V}^\dagger\right][\mathcal{V}]}_{-\left[\mathcal{V}^\dagger\right]\partial_t[V]}\right)+\left[\mathcal{V}^\dagger\right][H]_a[\mathcal{V}]\cdot[\rho]_b-[\rho_b]\cdot\left[\mathcal{V}^\dagger\right][H]_a[V]\\
&i\hbar\frac{\partial[\rho]_b}{\partial t}=\left[\left(\left[\mathcal{V}^\dagger\right][H]_a[V]-i\hbar\left[\mathcal{V}^\dagger\right]\partial_t[V]\right),[\rho]_b\right]\quad\Rightarrow\quad[H]_b=\left[\mathcal{V}^\dagger\right][H]_a[V]-i\hbar\left[\mathcal{V}^\dagger\right]\partial_t[V],
\end{aligned} \tag{A.20}
$$

which is exactly the same as in Eq. (A.18).

A.1.1 Application: phase transformation on the atomic bare states

Let us consider the basis consisting of the atomic eigenstates $\{|k\rangle, k\in\{1,2,\dots n\}\}$ as the basis "a", and we wish to perform the basis transformation given in Eq. (1.20):

$$
\hat{\mathcal{V}}=\sum_{k=1}^{N}e^{i(\delta_k t-k_k x)}|k\rangle\langle k|+|0\rangle\langle 0|. \tag{A.21}
$$

Using the transformation rule given in Eq. (A.18), the Hamiltonian in the new basis is the following:

$$
\begin{aligned}
\left[\hat{H}\right]_{\mathcal{V}} &= \left[\hat{\mathcal{V}}^{\dagger}\right] \cdot \left[\hat{H}_{\mathrm{RWA}}\right] \cdot \left[\hat{\mathcal{V}}\right] - i\hbar \left[\mathcal{V}^{\dagger}\right] \partial_t \left[\mathcal{V}\right] \\
&= -\hbar \begin{pmatrix} 1 & 0 & 0 & \cdots \\ 0 & e^{-i(\delta_1 - k_1 x)} & 0 & \cdots \\ 0 & 0 & e^{-i(\delta_2 - k_2 x)} & \cdots \\ \vdots & \vdots & \vdots & \ddots \end{pmatrix} \begin{pmatrix} 0 & \Omega_1 e^{-i(\delta_1 - k_1 x)} & \Omega_2 e^{-i(\delta_2 - k_2 x)} & \cdots \\ \Omega_1^* e^{i(\delta_1 - k_1 x)} & 0 & 0 & \cdots \\ \Omega_2^* e^{i(\delta_2 - k_2 x)} & 0 & 0 & \cdots \\ \vdots & \vdots & \vdots & \ddots \end{pmatrix} \begin{pmatrix} 1 & 0 & 0 & \cdots \\ 0 & e^{i(\delta_1 - k_1 x)} & 0 & \cdots \\ 0 & 0 & e^{i(\delta_2 - k_2 x)} & \cdots \\ \vdots & \vdots & \vdots & \ddots \end{pmatrix} \\
&- i\hbar \begin{pmatrix} 1 & 0 & 0 & \cdots \\ 0 & e^{-i(\delta_1 - k_1 x)} & 0 & \cdots \\ 0 & 0 & e^{-i(\delta_2 - k_2 x)} & \cdots \\ \vdots & \vdots & \vdots & \ddots \end{pmatrix} \begin{pmatrix} 0 & 0 & 0 & \cdots \\ 0 & i\delta_1 e^{i(\delta_1 - k_1 x)} & 0 & \cdots \\ 0 & 0 & i\delta_2 e^{i(\delta_2 - k_2 x)} & \cdots \\ \vdots & \vdots & \vdots & \ddots \end{pmatrix} \\
&= -\hbar \begin{pmatrix} 0 & \Omega_1 & \Omega_2 & \cdots \\ \Omega_1^* & -\delta_1 & 0 & \cdots \\ \Omega_2^* & 0 & -\delta_2 & \cdots \\ \vdots & \vdots & \vdots & \ddots \end{pmatrix} \Rightarrow \hat{H}_{\mathcal{V}} = -\hbar \left[\sum_{k=1}^{N} -\delta_k |k\rangle_{\mathcal{V}} \langle k|_{\mathcal{V}} + (\Omega_k |0\rangle \langle k|_{\mathcal{V}} + H.c.) \right].
\end{aligned} \tag{A.22}
$$

Bibliography

[1] W. S. Warren, H. Rabitz, and M. Dahleh, "Coherent control of quantum dynamics - the dream is alive," Science **259** (1993)

[2] J. Janszky, P. Adam, A. V. Vinogradov, and T. Kobayashi, "Vibrational-state shaping for selective laser chemistry," Chem. Phys. Letts. **213** (1993)

[3] R. J. Gordon, L. C. Zhu, and T. Seideman, "Coherent control of chemical reactions," Accounts Chem. Res. **32** (1999)

[4] V. I. Prokhorenko, A. M. Nagy, S. A. Waschuk, L. S. Brown, R. R. Birge, and R. J. D. Miller, "Coherent control of retinal isomerization in bacteriorhodopsin," Science **313** (2006)

[5] D. Budker, D. F. Kimball, S. M. Rochester, and V. V. Yashchuk, "Nonlinear magneto-optics and reduced group velocity of light in atomic vapor with slow ground state relaxation," Phys. Rev. Lett. **83** (1999)

[6] D. Budker, W. Gawlik, D. F. Kimball, S. M. Rochester, V. V. Yashchuk, and A. Weis, "Resonant nonlinear magneto-optical effects in atoms," Rev. Mod. Phys. **74** (2002)

[7] V. Acosta, M. P. Ledbetter, S. M. Rochester, D. Budker, D. F. Jackson Kimball, D. C. Hovde, W. Gawlik, S. Pustelny, J. Zachorowski, and V. V. Yashchuk, "Nonlinear magneto-optical rotation with frequency-modulated light in the geophysical field range," Phys. Rev. A **73** (2006)

[8] A. Wojciechowski, E. Corsini, J. Zachorowski, and W. Gawlik, "Nonlinear faraday rotation and detection of superposition states in cold atoms," Phys. Rev. A **81** (2010)

[9] G. P. Djotyan, N. Sandor, J. S. Bakos, Z. Sörlei, W. Gawlik, A. Wojciechowski, J. Zachorowski, S. Pustelny, and G. Y. Kryuchkyan, "Creation and measurement of coherent superposition states in multilevel atoms," in *Society of Photo-Optical Instrumentation Engineers (SPIE) Conference Series* (2010)

[10] T. Hansch and A. Schawlow, "Cooling of gases by laser radiation," Opt. Comm. **13** (1975)

[11] A. Aspect, E. Arimondo, R. Kaiser, N. Vansteenkiste, and C. Cohentannoudji, "Laser cooling below the one-photon recoil energy by velocity-selective coherent population trapping," Phys. Rev. Lett. **61** (1988)

[12] J. S. Bakos, G. P. Djotyan, G Demeter, and Z. Sörlei, "Transient laser cooling of two-level quantum systems with narrow natural line widths," Phys. Rev. A **53** (1996)

[13] M. Viteau, A. Chotia, M. Allegrini, N. Bouloufa, O. Dulieu, D. Comparat, and P. Pillet, "Optical pumping and vibrational cooling of molecules," Science **321** (2008)

[14] C. Monroe, "Quantum information processing with atoms and photons," Nature **416** (2002)

[15] M. Fleischhauer, S.F. Yelin, and M. D. Lukin, "How to trap photons? storing single-photon quantum states in collective atomic excitations," Opt. Commun. **179**, 395–410 (2000)

[16] Z. Kis and F. Renzoni, "Qubit rotation by stimulated raman adiabatic passage," Phys. Rev. A **65** (2002)

[17] P. K. Vudyasetu, R. M. Camacho, and J. C. Howell, "Storage and retrieval of multimode transverse images in hot atomic rubidium vapor," Phys. Rev. Lett. **100** (2008)

[18] G.-J. Yang, T. Qiu, K. Wang, and M. Xie, "Reversible storage of a weak light pulse in a thermal atomic medium," Phys. Rev. A **81** (2010)

[19] K. Hammerer, A. S. Sorensen, and E. S. Polzik, "Quantum interface between light and atomic ensembles," Rev. Mod. Phys. **82** (2010)

[20] C. P. Williams, *Explorations in Quantum Computing* (Springer, 2011)

[21] R. M. Camacho, C. J. Broadbent, I. Ali-Khan, and J. C. Howell, "All-optical delay of images using slow light rid b-1841-2010 rid d-5097-2009," Phys. Rev. Lett. **98** (2007)

[22] R. Pugatch, M. Shuker, O. Firstenberg, A. Ron, and N. Davidson, "Topological stability of stored optical vortices," Phys. Rev. Lett. **98**, 203601 (2007)

[23] A. Mair, J. Hager, D. F. Phillips, R. L. Walsworth, and M. D. Lukin, "Phase coherence and control of stored photonic information," Phys. Rev. A **65**, 031802 (2002)

[24] J. B. Watson, A. Sanpera, X. Chen, and K. Burnett, "Harmonic generation from a coherent superposition of states," Phys. Rev. A **53** (1996)

[25] T. Rickes, J. P. Marangos, and T. Halfmann, "Enhancement of third-harmonic generation by stark-chirped rapid adiabatic passage," Opt. Comm. **227** (2003)

[26] D. B. Milosevic, "Theoretical analysis of high-order harmonic generation from a coherent superposition of states," J. Opt. Soc. Am. B **23** (2006)

[27] G. H. C. New, "Nonlinear optics: the first 50 years," *Contemporary Physics*, Contemporary Physics **52** (2011)

[28] R. R. Jones, "Multiphoton ionization enhancement using two phase-coherent laser pulses," Phys. Rev. Lett. **75**, 1491–1494 (1995)

[29] R. R. Jones, "Interference effects in the multiphoton ionization of sodium," Phys. Rev. Lett. **74** (1995)

[30] M. Stellpflug, M. Johnsson, I. D. Petrov, and T. Halfmann, "Investigation of auto-ionizing states in xenon by resonantly enhanced multi-photon ionization," Eur. Phys. J. D **23**, 35–42 (2003)

[31] M. Jain, H. Xia, G. Y. Yin, A. J. Merriam, and S. E. Harris, "Efficient nonlinear frequency conversion with maximal atomic coherence," Phys. Rev. Lett. **77** (1996)

[32] L. Deng, M. G. Payne, and W. R. Garrett, "Nonlinear frequency conversion with short laser pulses and maximum atomic coherence," Phys. Rev. A **58** (1998)

[33] Z. Kis and E. Paspalakis, "Enhancing nonlinear frequency conversion using spatially dependent coherence," Phys. Rev. A **68** (2003)

[34] A. Eilam and A. D. Wilson-Gordon, "Enhanced frequency conversion of nonadiabatic resonant pulses in coherently prepared lambda systems," Phys. Rev. A **73** (2006)

[35] S. E. Harris, J. E. Field, and A. Imamoglu, "Nonlinear optical processes using electromagnetically induced transparency," Phys. Rev. Lett. **64** (1990)

[36] J. P. Marangos, "Topical review electromagnetically induced transparency," J. Mod. Opt. **45** (1998)

[37] J. Wang, L. B. Kong, X. H. Tu, K. J. Jiang, K. Li, H. W. Xiong, Y. F. Zhu, and M. S. Zhan, "Electromagnetically induced transparency in multi-level cascade scheme of cold rubidium atoms," Phys. Letts. A **328** (2004)

[38] M. Fleischhauer, A. Imamoglu, and J. P. Marangos, "Electromagnetically induced transparency: Optics in coherent media," Reviews of modern physics **77** (2005)

[39] L. Allen and J. H. Eberly, *Optical Resonance and Two-Level Atoms* (Dover: New York, 1987)

[40] K. Bergmann, H. Theuer, and B. W. Shore, "Coherent population transfer among quantum states of atoms and molecules," Rev. Mod. Phys. **70** (1998)

[41] N. V. Vitanov, T. Halfmann, B. W. Shore, and K. Bergmann, "Laser-induced population transfer by adiabatic passage techniques," Ann. Rev. Phys. Chem. **52** (2001)

[42] P. Kral, I. Thanopulos, and M. Shapiro, "Colloquium: Coherently controlled adiabatic passage," Rev. Mod. Phys. **79**, 53–77 (2007)

[43] J. Oreg, F. T. Hioe, and J. H. Eberly, "Adiabatic following in multilevel systems," Phys. Rev. A **29**, 690–697 (1984)

[44] D. Grischkowsky, "Coherent excitation, incoherent excitation, and adiabatic states," Phys. Rev. A **14** (1976)

[45] U. Gaubatz, P. Rudecki, S. Schiemann, and K. Bergmann, "Population transfer between molecular vibrational levels by stimulated raman scattering with partially overlapping laser fields. a new concept and experimental results.." J. Chem. Phys. **92** (1990)

[46] B. W Shore, K. Bergmann, J. Oreg, and S. Rosenwaks, "Multilevel adiabatic population transfer," Phys. Rev. A **44** (1991)

[47] C. E. Carroll and F. T. Hioe, "Coherent population transfer via the continuum," Phys. Rev. Lett. **68** (1992)

[48] P. Pillet, C. Valentin, R. Yuan, and J. Yu, "Adiabatic population transfer in a multilevel system," Phys. Rev. A **48** (1993)

[49] P. Marte, P. Zoller, and J. Hall, "Coherent atomic mirrors and beam-splitters by adiabatic passage in multilevel systems," Phys. Rev. A **44** (1991)

[50] R. G. Unanyan, B. W. Shore, and K. Bergmann, "Preparation of an n-component maximal coherent superposition state using the stimulated raman adiabatic passage method," Phys. Rev. A **63** (2001)

[51] P. A. Ivanov, N. V. Vitanov, and K. Bergmann, "Effect of dephasing on stimulated raman adiabatic passage," Phys. Rev. A **70** (2004)

[52] Q. Shi and E. Geva, "Stimulated raman adiabatic passage in the presence of dephasing," The Journal of Chemical Physics **119** (2003)

[53] Lei Wang, Xiao-Li Song, Ai-Jun Li, Hai-Hua Wang, Xiao-Gang Wei, Zhi-Hui Kang, Yun Jiang, and Jin-Yue Gao, "Coherence transfer between atomic ground states by the technique of stimulated raman adiabatic passage," Opt. Letts. **33** (2008)

[54] F. Beil, J. Klein, and T. Halfmann, "Optically driven atomic coherences in a pr_3+:y_2sio_5 crystal," Phot. Nano. Fund. Appl. **7** (2009)

[55] N. V. Vitanov, K.-A. Suominen, and B. W. Shore, "Creation of coherent atomic superpositions by fractional stimulated raman adiabatic passage," Journal of Physics B: Atomic, Molecular and Optical Physics **32** (1999)

[56] R. Unanyan, M. Fleischhauer, B. W. Shore, and K. Bergmann, "Robust creation and phase-sensitive probing of superposition states via stimulated raman adiabatic passage (stirap) with degenerate dark states," Optics Communications **155** (1998)

[57] R. G. Unanyan, B. W. Shore, and K. Bergmann, "Laser-driven population transfer in four-level atoms: Consequences of non-abelian geometrical adiabatic phase factors," Phys. Rev. A **59** (1999)

[58] H. Theuer, R. G. Unanyan, C. Habscheid, K. Klein, and K. Bergmann, "Novel laser controlled variable matter wave beamsplitter," Optics Express **4**, 77 (1999)

[59] C. Lazarou and N. V. Vitanov, "Dephasing effects on stimulated raman adiabatic passage in tripod configurations," Phys. Rev. A **82** (2010)

[60] M. M. T. Loy, "Observation of population inversion by optical adiabatic rapid passage," Phys. Rev. Lett. **32** (1974)

[61] L. P. Yatsenko, B. W. Shore, T. Halfmann, K. Bergmann, and A. Vardi, "Source of metastable h($2s$) atoms using the stark chirped rapid-adiabatic-passage technique," Phys. Rev. A **60** (1999)

[62] L. P. Yatsenko, N. V. Vitanov, B. W. Shore, T. Rickes, and K Bergmann, "Creation of coherent superpositions using stark-chirped rapid adiabatic passage," Opt. Comm. **204** (2002)

[63] A. A. Rangelov, N. V. Vitanov, L. P. Yatsenko, B. W. Shore, T. Halfmann, and K. Bergmann, "Stark-shift-chirped rapid-adiabatic-passage technique among three states," Phys. Rev. A **72**, 053403 (2005)

[64] N. Sangouard, L. P. Yatsenko, B. W. Shore, and T. Halfmann, "Preparation of nondegenerate coherent superpositions in a three-state ladder system assisted by stark shifts," Phys. Rev. A **73** (2006)

[65] M. Oberst, H. Munch, and T. Halfmann, "Efficient coherent population transfer among three states in no molecules by stark-chirped rapid adiabatic passage," Phys. Rev. Lett. **99** (2007)

[66] M. Radonjic and B. M. Jelenkovic, "Stark-chirped rapid adiabatic passage among degenerate-level manifolds," Phys. Rev. A **80** (2009)

[67] E. B. Treacy, "Adiabatic inversion with light pulses," Phys. Letts. A **27** (1968)

[68] J. S. Melinger, Suketu R. Gandhi, A. Hariharan, J. X. Tull, and W. S. Warren, "Generation of narrowband inversion with broadband laser pulses," Phys. Rev. Lett. **68** (1992)

[69] B. Broers, H. B. van Linden van den Heuvell, and L. D. Noordam, "Efficient population transfer in a three-level ladder system by frequency-swept ultrashort laser pulses," Phys. Rev. Lett. **69** (1992)

[70] G. P. Djotyan, J. S. Bakos, G. Demeter, and Zs. Sörlei, "Theory of the adiabatic passage in two-level quantum systems with superpositional initial states," J. Mod. Opt. **44** (1997)

[71] I. R. Sola, V. S. Malinovsky, B. Y. Chang, J. Santamaria, and K. Bergmann, "Coherent population transfer in three-level lambda systems by chirped laser pulses: Minimization of the intermediate-level population," Phys. Rev. A **59** (1999)

[72] V. S. Malinovsky and J. L. Krause, "Efficiency and robustness of coherent population transfer with intense, chirped laser pulses," Phys. Rev. A **63**, 043415 (2001)

[73] G. P. Djotyan, J. S. Bakos, and Z Sörlei, "Coherent writing and reading of information using frequency-chirped short bichromatic laser pulses," Opt. Exp. **4** (1999)

[74] G. P. Djotyan, J. S. Bakos, G. Demeter, and Z. Sorlei, "Population transfer in three-level lambda atoms with doppler-broadened transition lines by a single frequency-chirped short laser pulse," J. Opt. Soc. Am. B **17** (2000)

[75] G. P. Djotyan, J. S. Bakos, and Zs. Sörlei, "Three-level lambda atom in the field of frequency-chirped bichromatic laser pulses: Writing and storage of optical phase information," Phys. Rev. A **64** (2001)

[76] G. P. Djotyan, J. S. Bakos, G. Demeter, P. N. Ignácz, M. Á. Kedves, Zs. Sörlei, J. Szigeti, and Z. L. Tóth, "Coherent population transfer in rb atoms by frequency-chirped laser pulses," Phys. Rev. A **68** (2003)

[77] G. P. Djotyan, J. S. Bakos, Zs. Sörlei, and J. Szigeti, "Coherent control of atomic quantum states by single frequency-chirped laser pulses," Phys. Rev. A **70** (2004)

[78] G. P. Djotyan, J. S. Bakos, G. Demeter, Zs. Sorlei, J. Szigeti, and D. Dzsotjan, "Creation of a coherent superposition of quantum states by a single frequency-chirped short laser pulse," J. Opt. Soc. Am. B **25** (2008)

[79] S. A. Malinovskaya, "Optimal coherence via adiabatic following," Opt. Comm. **282**, 3527–3529 (2009)

[80] L. Deng, Y. P. Niu, Y. Xiang, S. Q. Jin, and S. Q. Gong, "Creation of an arbitrary coherent superposition state with chirped delayed pulses," J Phys. B **43** (2010)

[81] J. S. Bakos, G. P. Djotyan, P. N. Ignácz, M. Á. Kedves, M. Serényi, Zs. Sörlei, J. Szigeti, and Z. Tóth, "Interaction of frequency modulated light pulses with rubidium atoms in a magneto-optical trap," The European Physical Journal D - Atomic, Molecular, Optical and Plasma Physics **39**, 59–66 (2006)

[82] J. S. Bakos, G. P. Djotyan, P. N. Ignácz, M. Á. Kedves, M. Serényi, Zs. Sörlei, J. Szigeti, and Z. Tóth, "Acceleration of cold rb atoms by frequency modulated light pulses," The European Physical Journal D **44**, 141–149 (2007)

[83] G. P. Djotyan, J. S. Bakos, G. Demeter, and Zs. Sörlei, "Manipulation of two-level quantum systems with narrow transition lines by short linearly polarized frequency-chirped laser pulses," J. Opt. Soc. Am. B **13** (1996)

[84] G. Demeter, G. P. Djotyan, and J. S. Bakos, "Deflection and splitting of atomic beams with counterpropagating, short, chirped laser pulses," J. Opt. Soc. Am. B **15** (1998)

[85] G. Demeter, G. P. Djotyan, Zs. Sörlei, and J. S. Bakos, "Mechanical effect of retroreflected frequency-chirped laser pulses on two-level atoms," Phys. Rev. A **74** (2006)

[86] F. I. Gauthey, C. H. Keitel, P. L. Knight, and A. Maquet, "Role of initial coherence in the generation of harmonics and sidebands from a strongly driven two-level atom," Phys. Rev. A **52** (1995)

[87] A. K. Gupta and D. Neuhauser, "Control of harmonic generation by initial-state preparation," Chemical Physics Letters **290** (1998)

[88] Jun Bao, Wenbo Chen, Zengxiu Zhao, and Jianmin Yuan, "High-order harmonic generation from coherently excited molecules," Journal of Physics B: Atomic, Molecular and Optical Physics **44** (2011)

[89] L. Feng and T. Chu, "Intensity improvement in the attosecond pulse generation with the coherent superposition initial state," Physics Letters A **376** (2012)

[90] M. Fleischhauer, "Electromagnetically induced transparency and coherent-state preparation in optically thick media," Opt. Exp. **4**, 107–112 (1999)

[91] G. Demeter, D. Dzsotjan, and G.P. Djotyan, "Propagation of frequency-chirped laser pulses in a medium of atoms with a λ-level scheme," Phys. Rev. A **76**, 023827 (2007)

[92] V. V. Kozlov and E. B. Kozlova, "Adiabatic and nonadiabatic preparation of a ground-state coherence in an optically thick lambda medium," Opt. Comm. **282** (2009)

[93] P. A. Siddons, C. S. Adams, and I. G. Hughes, "Optical preparation and measurement of atomic coherence at gigahertz bandwidth," J. of Phys. B **45** (2012)

[94] M. Fleischhauer and M. D. Lukin, "Dark-state polaritons in electromagnetically induced transparency," Phys. Rev. Lett. **84**, 5094–5097 (2000)

[95] S. E. Harris, "Normal-modes for electromagnetically induced transparency," Phys. Rev. Lett. **72** (1994)

[96] S. E. Harris and Z. F. Luo, "Preparation energy for electromagnetically induced transparency," Phys. Rev. A **52** (1995)

[97] Q-H. Park and H. J. Shin, "Matched pulse propagation in a three-level system," Phys. Rev. A **57** (1998)

[98] V. Boyer, C. F. McCormick, E. Arimondo, and P. D. Lett, "Ultraslow propagation of matched pulses by four-wave mixing in an atomic vapor," Phys. Rev. Lett. **99** (2007)

[99] J. Okuma, N. Hayashi, A. Fujisawa, and M. Mitsunaga, "Ultraslow matched-pulse propagation in sodium vapor," Opt. Letts. **34** (2009)

[100] W. P. Schleich, *Quantum Optics in Phase Space* (Wiley-VCH Verlag Berlin, 2001)

[101] M. Frasca, "A modern review of the two-level approximation," Annals of Physics **306** (2003)

[102] D. A. Steck, "Rubidium 85 d line data," (2012)

[103] I. I. Rabi, "Space quantization in a gyrating magnetic field," Phys. Rev. **51** (1937)

[104] C. Gerry and P. Knight, *Introductory Quantum Optics* (Cambridge University Press, 2005)

[105] E. Paspalakis and Z. Kis, "Pulse propagation in a coherently prepared multilevel medium," Phys. Rev. A **66** (2002)

[106] L. E. Ballentine, *Quantum Mechanics: A Modern Development* (World Scientific, 1998)

[107] A. Messiah, *Quantum mechanics* (Dover Publications, 1999)

[108] G. P. Djotyan P. N. Ignácz M. Á. Kedves B. Ráczkevi Zs. Sörlei J. S. Bakos, G. Demeter and J. Szigeti, "Advances in laser and optics research," (Nova Science Publishers, Inc., 2009) Chap. 5

[109] V. S. Malinovsky and J. L. Krause, "General theory of population transfer by adiabatic rapid passage with intense, chirped laser pulses," Eur. Phys. J. D **14** (2001)

[110] I. Nebenzahl and A. Szoke, "Deflection of atomic beams by resonance radiation using stimulated emission," Applied Physics Letters **25** (1974)

[111] D. A. Steck, "Quantum and atom optics," (2012)

[112] C. E. Rogers III, J. L. Carini, J. A. Pechkis, and P. L. Gould, "Characterization and compensation of the residual chirp in a mach-zehnder-type electro-optical intensity modulator," Opt. Express **18** (2010)

[113] M. D. Lukin, "*Colloquium*: Trapping and manipulating photon states in atomic ensembles," Rev. Mod. Phys. **75** (2003)

[114] M. Shuker, O. Firstenberg, R. Pugatch, A. Ben-Kish, A. Ron, and N. Davidson, "Angular dependence of dicke-narrowed electromagnetically induced transparency resonances," Phys. Rev. A **76** (2007)

[115] A. Kasapi, M. Jain, G. Y. Yin, and S. E. Harris, "Electromagnetically induced transparency: Propagation dynamics," Phys. Rev. Lett. **74** (1995)

[116] A. E. Kozhekin, K. Mølmer, and E. Polzik, "Quantum memory for light," Phys. Rev. A **62** (2000)

[117] M. Fleischhauer and M. D. Lukin, "Quantum memory for photons: Dark-state polaritons," Phys. Rev. A **65** (2002)

[118] E. Kuznetsova, O. Kocharovskaya, P. Hemmer, and M. O. Scully, "Atomic interference phenomena in solids with a long-lived spin coherence," Phys. Rev. A **66** (2002)

[119] M. Johnsson and K. Mølmer, "Storing quantum information in a solid using dark-state polaritons," Phys. Rev. A **70** (2004)

[120] N. V. Vitanov, B. W. Shore, R. G. Unanyan, and K. Bergmann, "Measuring a coherent superposition," Optics Communications **179** (2000)

[121] N. V. Vitanov, "Measuring a coherent superposition of multiple states," Journal of Physics B: Atomic, Molecular and Optical Physics **33** (2000)

[122] K.-J. Boller, A. Imamolu, and S. E. Harris, "Observation of electromagnetically induced transparency," Phys. Rev. Lett. **66** (1991)

[123] A. Imamoğlu and S. E. Harris, "Lasers without inversion: interference of dressed lifetime-broadened states," Opt. Lett. **14** (1989)

[124] Carlos Trallero-Herrero, J. L. Cohen, and Thomas Weinacht, "Strong-field atomic phase matching," Phys. Rev. Lett. **96** (2006)

[125] D. D. Yavuz, "Refractive index enhancement in a far-off resonant atomic system," Phys. Rev. Lett. **95** (2005)

[126] Chris O'Brien, Petr M. Anisimov, Yuri Rostovtsev, and Olga Kocharovskaya, "Coherent control of refractive index in far-detuned λ systems," Phys. Rev. A **84** (2011)

[127] D. A. Steck, "Rubidium 87 d line data," (2010)

[128] S. E. Harris, "Electromagnetically induced transparency with matched pulses," Phys. Rev. Lett. **70** (1993)

[129] F. T. Hioe R. Grobe and J. H. Eberly, "Formation of shape-preserving pulses in a nonlinear adiabatically integrable system," Phys. Rev. Lett. **73** (1994)

[130] S. E. Harris, "Electromagnetically induced transparency," Physics Today **50** (1997)